

Continuum Diffusion Modeling Using the SMOL Package

—— Finite Element Method Application

Yuhui Cheng

ycheng@mccammon.ucsd.edu

NBCR Summer Institute

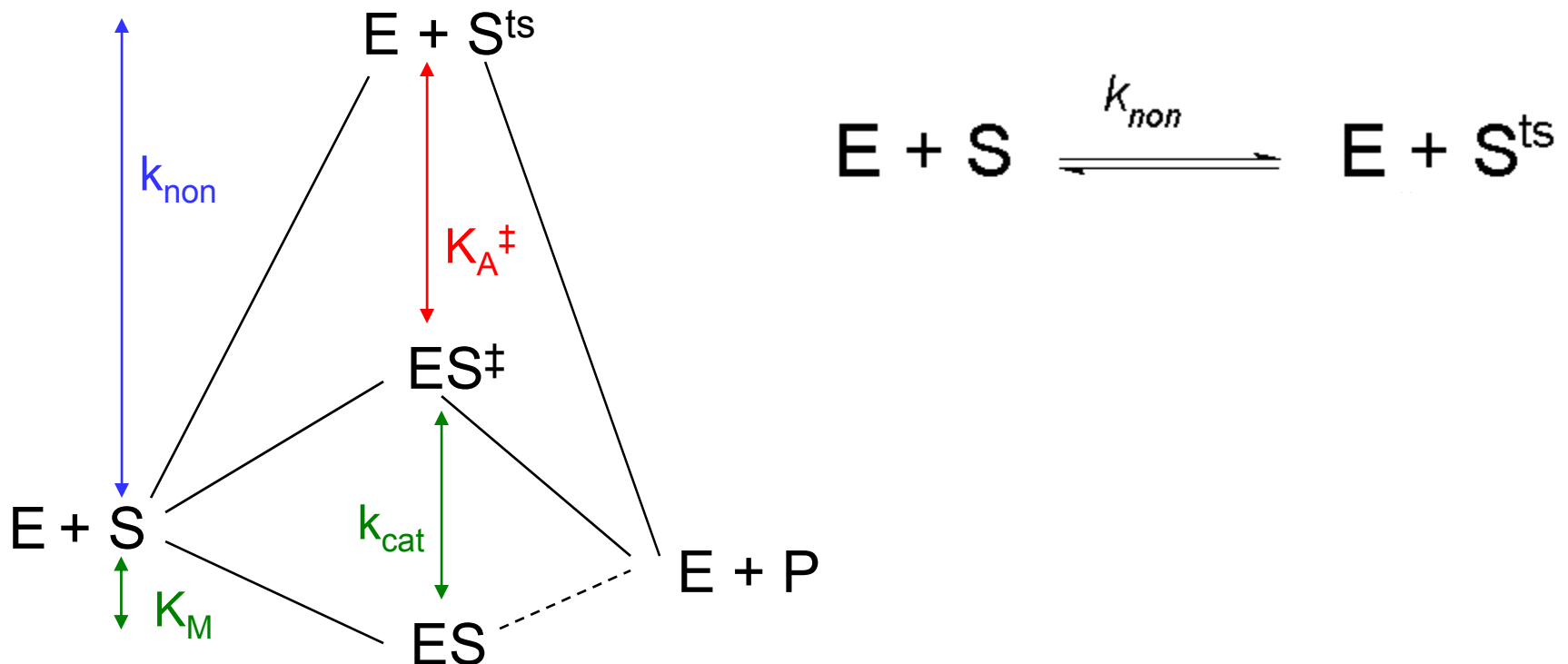
Aug. 6, 2008

<http://mccammon.ucsd.edu/smol/doc/lectures/nbcr080608.pdf>

Outline

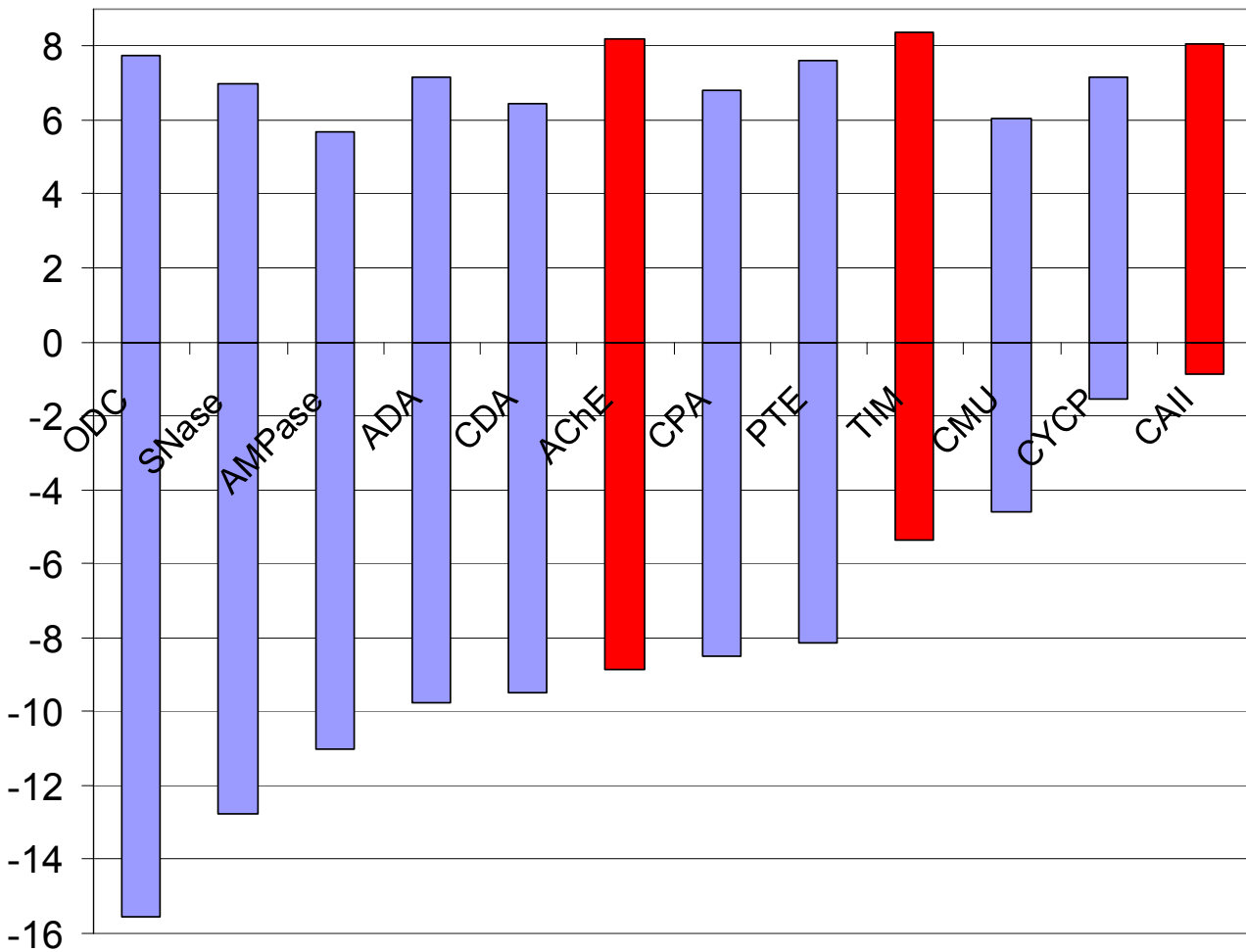
- To introduce diffusion-controlled diffusion reactions.
- To introduce the biological applications of the finite element tool kit (FEtk).
- To introduce the basic math background in solving diffusion problems.
- Examples to solve steady-state and time-dependent diffusion equations and preliminary visualization.
 - Analytical tests
 - mAChE case
 - Neuromuscular Junction
 - Substrate channeling in sulfate activating complexes
- Finite element Poisson-Nernst-Planck solvers and future possible projects.

Enzyme catalysis: mathematics



$$k_{cat}/K_M = k_{non} * K_A^{\ddagger}$$

Enzymes exert remarkable control over k_{cat}/K_M relative to the variation of k_{non}



$\updownarrow k_{cat}/K_M: 10^{2.5}$
variation

$\updownarrow k_{non}: 10^{14}$
variation

Radzicka, A. and Wolfenden, G. (1995). *Science* **267** (5194), 90-93.

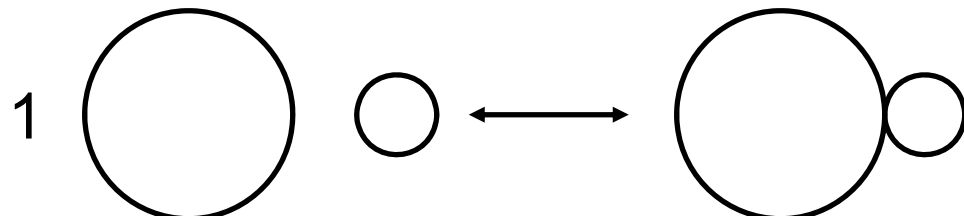
Diffusion-controlled enzymes

Molecular encounter limits k_{cat}/K_M if
 k_2 is high

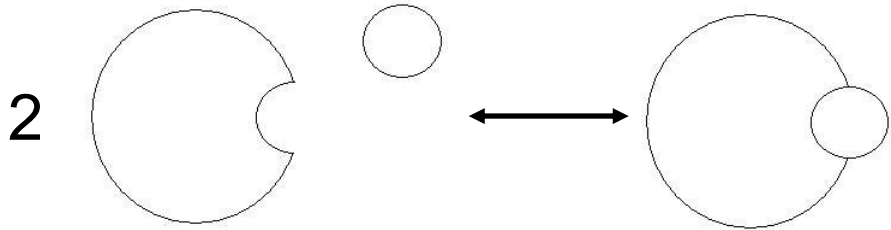


What is the limit of the molecular encounter rate?

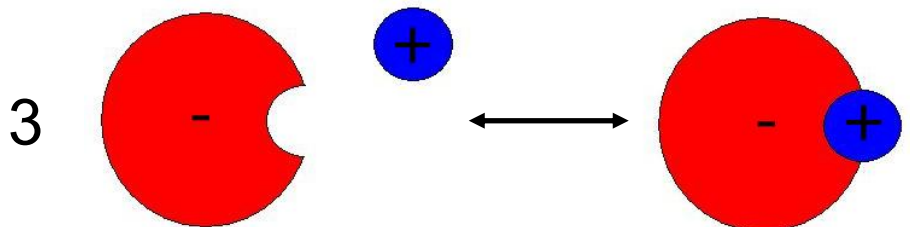
1) According to
Smoluchowski equation,
E-S collision rate is
limited to $\sim 10^9 \text{ M}^{-1}\text{S}^{-1}$



2) **Orientational constraints**
limit the reactive encounter
rate to $\sim 10^6 \text{ M}^{-1}\text{S}^{-1}$

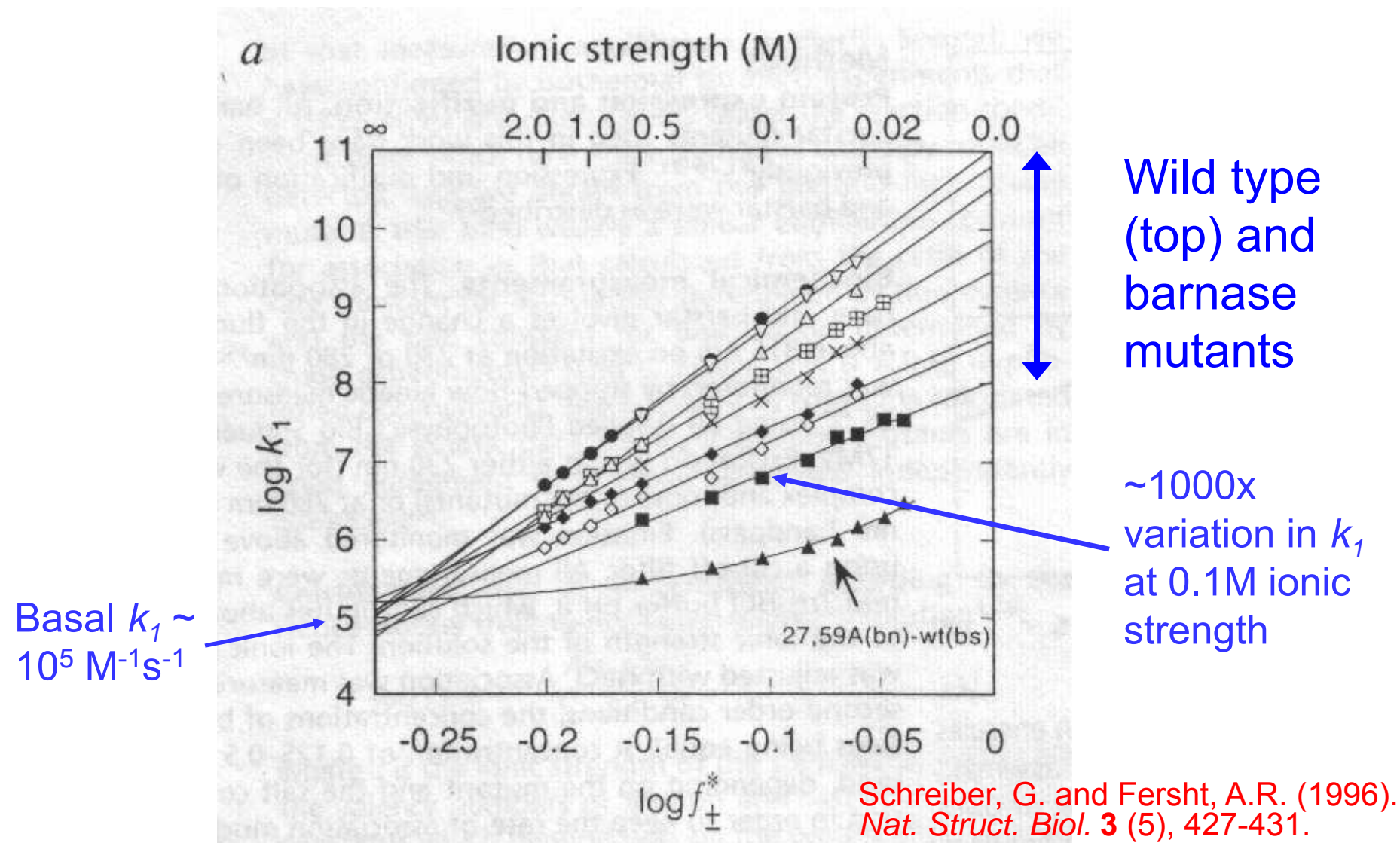


3) **Electrostatic attraction**
or guidance of S to E
can raise the diffusion
limit to $10^8\text{-}10^9 \text{ M}^{-1}\text{S}^{-1}$



Alberty, R.A. and Hammes, G.G.
(1958). *J. Phys Chem* **62**, 154-59

Electrostatics causes large differences in barnase-barstar association rates



Summary: enzymes overcome two physical problems

- Chemical efficiency
 - Geometry (entropic problem)
 - High-energy intermediates (enthalpic problem)
 - Enzyme rate does not appear to be limited by k_{non}
- Molecular encounter
 - Coulomb's law (enthalpic effect)
 - Steering (entropic effect)

Introduction to FEtK

- <http://www.fetk.org/>
- The primary FETK ANSI-C software libraries are:
 - (1) **MALOC** is a Minimal Abstraction Layer for Object-oriented C/C++ programs.
 - (2) **PUNC** is Portable Understructure for Numerical Computing (requires MALOC).
 - (3) **GAMER** is a Geometry-preserving Adaptive MeshER (requires MALOC).
 - (4) **SG** is a Socket Graphics tool for displaying polygons (requires MALOC).
 - (5) **MC** is a 2D/3D AFEM code for nonlinear geometric PDE (requires MALOC; optionally uses PUNC+GAMER+SG).

Smoluchowski Equation

Describes the over-damped diffusion dynamics of non-interacting particles in a potential field.

$$\frac{\partial p(\vec{r}, t \mid \vec{r}_0, t_0)}{\partial t} = \nabla \cdot D [\nabla - \beta \vec{F}(\vec{r})] p(\vec{r}, t \mid \vec{r}_0, t_0)$$

Or for $\vec{F}(\vec{r}) = -\nabla U(\vec{r})$

$$\frac{\partial p(\vec{r}, t \mid \vec{r}_0, t_0)}{\partial t} = \nabla \cdot D e^{-\beta U(\vec{r})} \nabla e^{\beta U(\vec{r})} p(\vec{r}, t \mid \vec{r}_0, t_0)$$

Steady-state Formation

$$\frac{\partial p(\vec{r}, t)}{\partial t} = 0$$

$$\Rightarrow \nabla \cdot D(\vec{r})[\nabla p(\vec{r}) + \beta p(\vec{r}) \nabla U(\vec{r})] = 0$$

Or in flux operator \mathbf{J} :

$$\nabla \cdot \vec{J}p(\vec{r}) = 0$$

where

$$\vec{J}p(\vec{r}) = D(\vec{r})[\nabla p(\vec{r}) + \beta p(\vec{r}) \nabla U(\vec{r})]$$

Poisson-Boltzmann Equation

$$-\nabla \cdot \varepsilon(x) \nabla U(x) + \bar{\kappa}^2(x) \sinh U(x) = \frac{4\pi e_c^2}{kT} \sum_i z_i \delta(x - x_i)$$

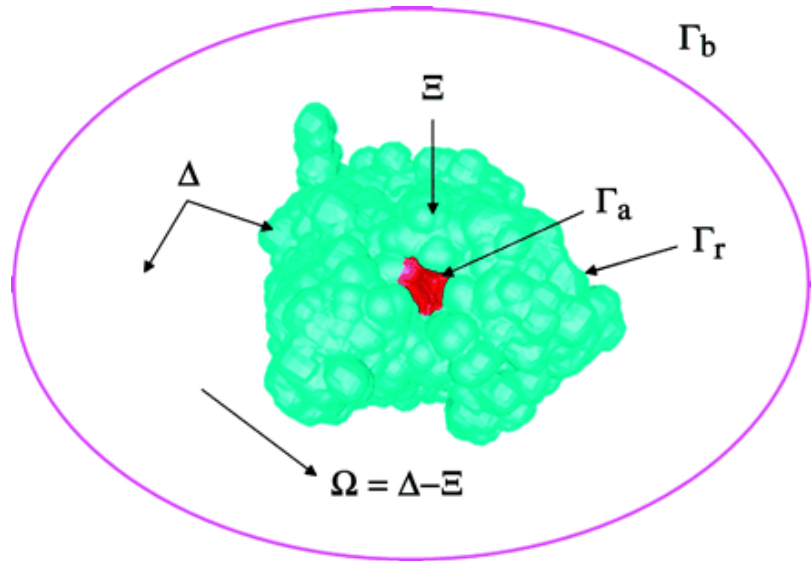
$$-\nabla \cdot \varepsilon(x) \nabla u(x) + \bar{\kappa}^2(x) \sinh[u(x) + G] = \nabla \cdot ((\varepsilon - \varepsilon_m) \nabla G)$$

$$-\nabla \cdot \varepsilon(x) \nabla G_i = q_i \delta_i$$

$$G_i = \frac{q_i}{\varepsilon_m} \frac{1}{|x - x_i|}$$

$$U(x) = u(x) + \sum_{i=1}^{N_m} G_i$$

Boundary conditions for Smoluchowski Equation



- Δ -- whole domain
- Ξ -- biomolecular domain
- Ω -- free space in Δ
- Γ_a – reactive region
- Γ_r – reflective region
- Γ_b – boundary for Δ

- (1) $p(\vec{r}) = p_{bulk}$ for $\vec{r} \in \Gamma_b$
- (2) $p(\vec{r}) = 0$ (Dirichlet BC) for $\vec{r} \in \Gamma_a$
or $\vec{n} \cdot \vec{J}p(\vec{r}) = \alpha(\vec{r})p(\vec{r})$ (Robin BC)
- (3) $\vec{n} \cdot \vec{J}p(\vec{r}) = 0$ for $x \in \Gamma_r$

Diffusion rate:

$$k = \frac{\int_{\Gamma_a} \vec{n} \cdot \vec{J}p(\vec{r}) dS}{p_{bulk}}$$

Finite element discretization of SSSE

1. Define a function space $V_h = \{v_i\}$ (v_i : piece-wise linear FE basis functions defined over each tetrahedral vertex), and assume the solution to SSSE has the form of

$$p_h(\vec{r}) = \sum_i a_i v_i(\vec{r}), \quad p_h \in \bar{p}_h + V_h$$

2. The second derivatives of V_h are not well defined, thus need reformulation of SSSE by integrating it with a test function v :

$$\int_{\Omega} v(\vec{r}) \nabla \cdot \vec{J}p(\vec{r}) d\vec{r}^3 = 0$$

Weak form of SSSE

$$\Rightarrow \int_{\Omega} \nabla v(\vec{r}) \cdot \vec{J}p(\vec{r}) d\vec{r}^3 - \int_{\Gamma_a} v(s) \alpha(s) p(s) ds - \int_{\Gamma_b} v(s) \vec{J}p(s) \cdot \vec{n}(s) ds = 0$$

$$\text{or } \int_{\Omega} \nabla v(\vec{r}) \cdot \vec{J}p(\vec{r}) d\vec{r}^3 - \int_{\Gamma_a \cup \Gamma_b} v(s) \vec{J}p(s) \cdot \vec{n}(s) ds = 0$$

Weak formation of SSSE

$$\nabla \cdot [v \nabla u] = \nabla u \cdot \nabla v + v \nabla \cdot \nabla u$$

Find $p_h \in \bar{p}_h + V_h$ such as $\langle F(p_h), v_i \rangle = 0$ for all $v_i \in V_h$

$$\langle F(p_h), v_i \rangle = \int_{\Omega} \nabla v(x) \cdot Jp(x) dx - \int_{\Gamma_a} v(s) \alpha(s) p(s) ds - \int_{\Gamma_b} v(s) \bar{Jp}(s) \cdot n(s) ds$$

$$\langle F(p_h), v_i \rangle = \int_{\Omega} \nabla v(x) \cdot Jp(x) dx - \int_{\Gamma_a \cup \Gamma_b} v(s) \bar{Jp}(s) \cdot n(s) ds$$

Note that the boundary integral on Γ_b vanishes due to the test function vanishes on the non-reactive boundaries.

Bilinear linearization form of SSSE

To apply a Newton iteration, we need to linearize $\langle F(u), v \rangle$

$$\langle DF(u)w, v \rangle = \frac{d}{dt} \langle F(u + tw), v \rangle = \int_{\Omega} D\nabla w \cdot \nabla v dx$$

Algorithm 3.2. (*Damped-inexact-Newton*)

- Given an initial u
- While $|\langle F(u), v \rangle| > TOL$ for some v) do:
 - (1) Find δ such that $\langle DF(u)\delta, v \rangle = -\langle F(u), v \rangle + r, \forall v$
 - (2) Set $u = u + \lambda\delta$
- end while

Posteriori ERROR ESTIMATOR

$$\eta_s^2 = h_s^2 \|\nabla \cdot J_h\|_{L^2(s)}^2 + \frac{1}{2} \sum_{f \in I(s)} h_f^2 \| [n_f \cdot (D\nabla p(r))] \|_{L^2(f)}^2$$

h_s represent the size of the element.

$J_h(p;x)$ is the current estimate of the flux.

$f \in S$ denotes a face of simplex

h_s is the size of the face f

$[n \cdot J_h]$ denotes to the ``jump'' term across faces interior to the simplex.

$$err = \sqrt{\sum_s \eta_s^2}$$

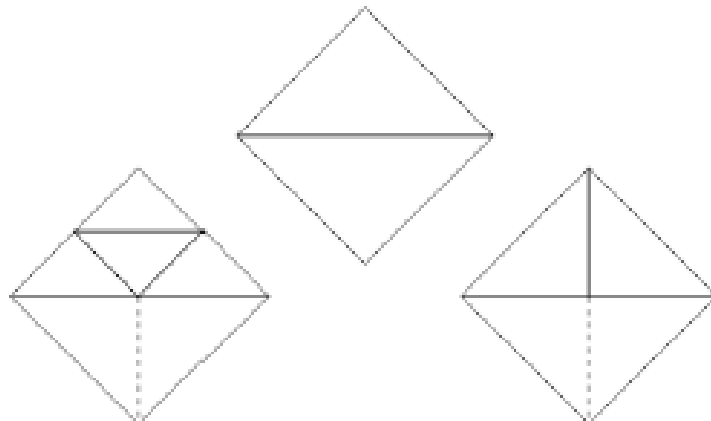


Mesh Marking and Refinement

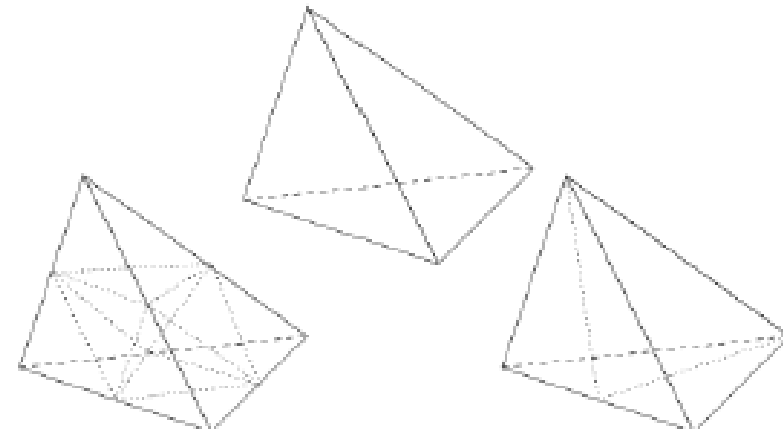
Algorithm 3.1. (*Adaptive multilevel finite element approximation*)

- While $(\|u - u_h\|_X > \epsilon)$ do:
 - (1) Find $u_h \in \bar{u}_h + V_h \subset H_0^1(\Omega)$ such that $\langle F(u_h), v_h \rangle = 0, \forall v_h \in V_h \subset H_0^1(\Omega)$.
 - (2) Estimate $\|u - u_h\|_X$ over each element.
 - (3) Initialize two temporary simplex lists as empty: $Q1 = Q2 = \emptyset$.
 - (4) Place simplices with large error on the “refinement” list $Q1$.
 - (5) Bisect all simplices in $Q1$ (removing them from $Q1$),
and place any nonconforming simplices created on the list $Q2$.
 - (6) $Q1$ is now empty; set $Q1 = Q2, Q2 = \emptyset$.
 - (7) If $Q1$ is not empty, goto (5).
- End While.

Subdividing 2-simplices (triangles)



Subdividing 3-simplices (tetrahedra)



Potential gradient mapping

Currently, we have three ways to obtain potential gradient $\nabla U(r)$:

- Boundary element method:

Pro: it can easily calculate the $\nabla U(r)$ at any spatial position.

Con: $\nabla U(r)$ near the protein surface is hard to calculate accurately.

- Finite difference method:

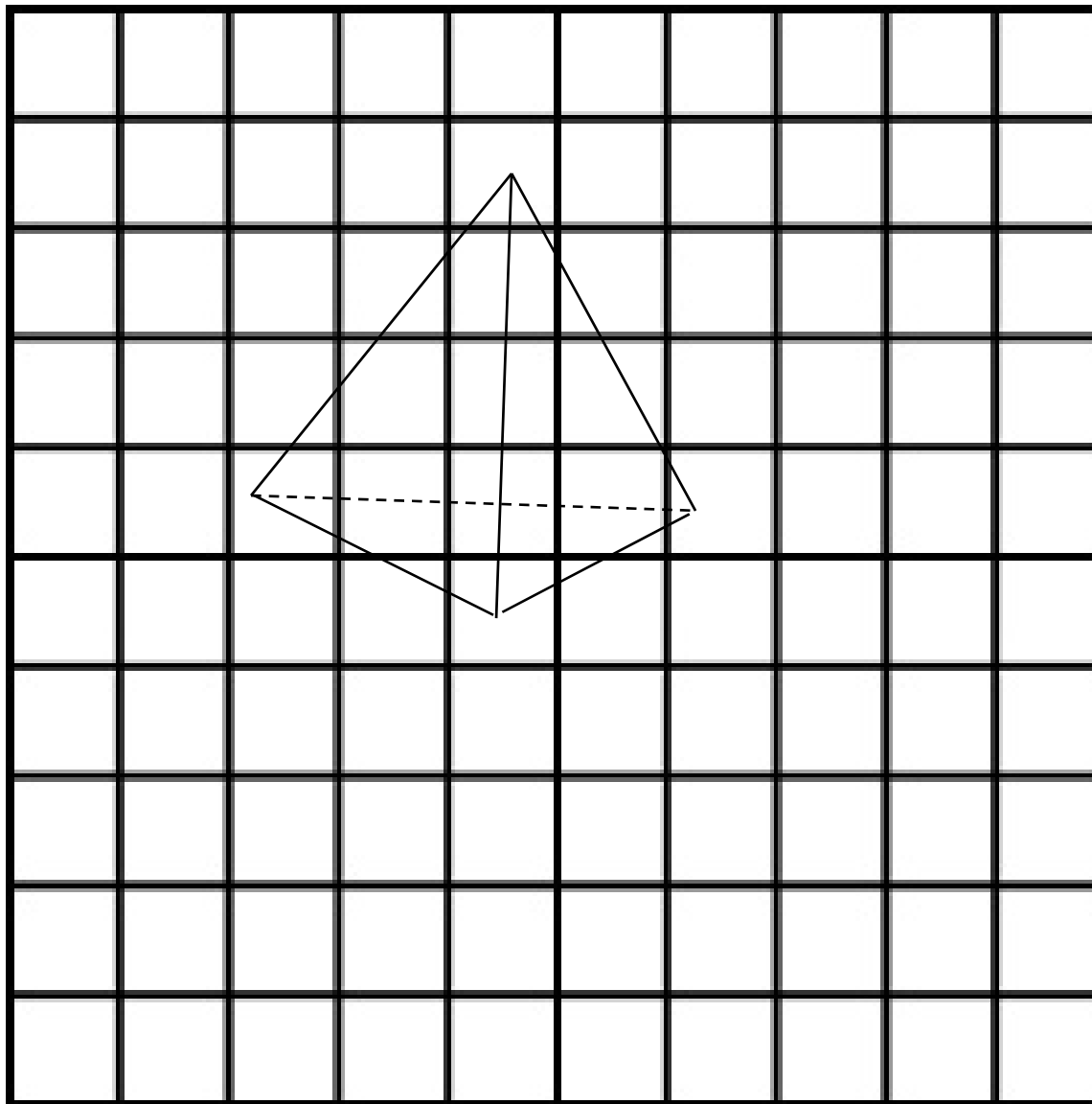
$$\text{APBS: } \nabla U(r_j) = \frac{U(r_{j+1}) - U(r_{j-1})}{2h}$$

- Finite element method:

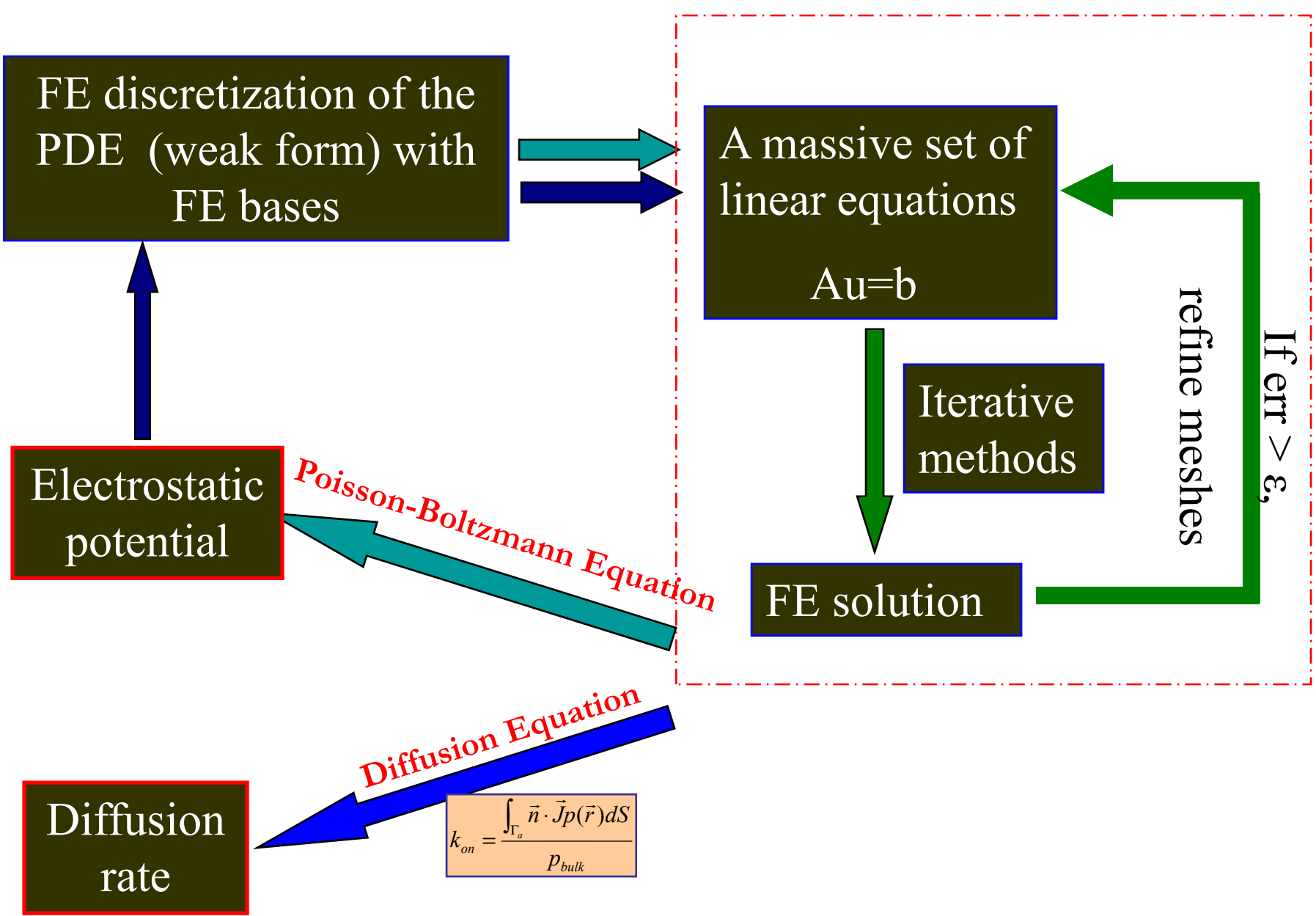
Treat the cubic grid as the FE cubic mesh

Use basis functions to calculate the force on the tetrahedral FE node position.

Potential gradient mapping



Solving Electrostatics and Diffusion by FEtK



Sample input files

- **NOTE:**

```
# model parameters
charge 0.0      /* ligand charge */
conc 1.0        /* initial ligand concentration at the outer boundary */
diff 78000.0    /* diffusion coefficient, unit: Å²/μs */
temp 300.0      /* temperature, unit: Kelvin */
# potential gradient methods
METHtype BEM          /* you can choose BEM or FEM */
# mapping method
map NONE           /* you can choose NONE/DIRECT/FEM */
# steady-state or time-dependent
tmkey TDSE         /* you can choose SSSE or TDSE */
# input paths
mol ../../pqr/ion_yuhui.pqr
mesh ../../mesh/sphere_4.m
mgrid ../../potential/pot-0.dx      /* for APBS input */
dPMF ../../force/evosphere_4.dat   /* for BEM input */
end 0
```

Manage your input parameters

- **NOTE:**

`${solver}`

- the default input file: `smol.in`

`${solver} -ifnam filename`

- the default iteration method: `CG(lkey=2)`.

`BCG (lkey=4 or 5), BCGSTAB(lkey=6)`

`${solver} -lkey 2`

- default maximal number of iterative steps: 5000

`${solver} –lmax 8000`

Manage your input parameters (cont.)

- **NOTE:**

- the default timestep: $5.0 \times 10^{-6} \mu\text{s}$

`${solver} -dt 5.0*10-5`

- the default number of time steps: 500

`${solver} –nstep 1000`

- the default concentration output frequency: 50

`${solver} –cfreq 100`

- the default reactive integral output frequency: 1

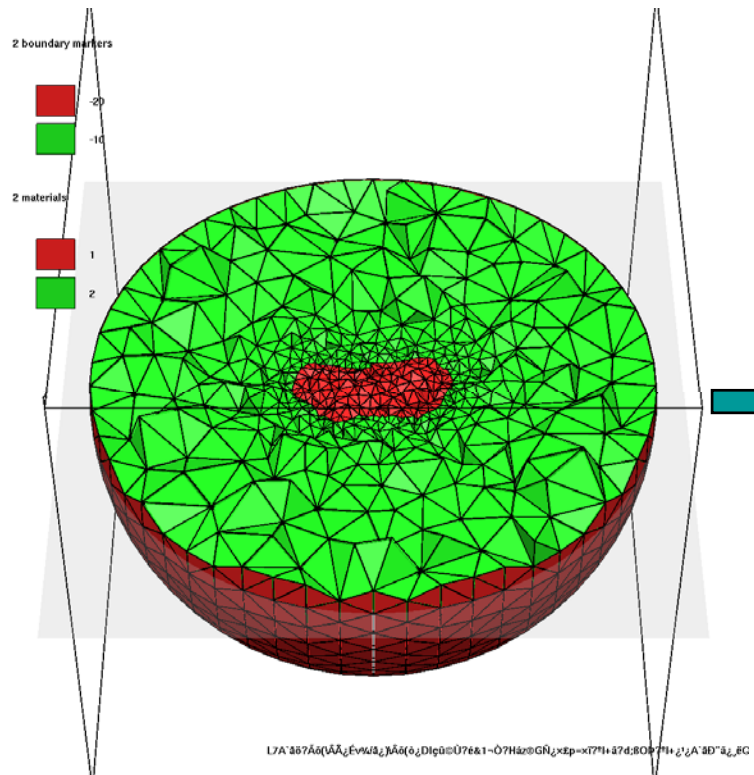
`${solver} –efreq 5`

- the default restart file writing frequency: 1000

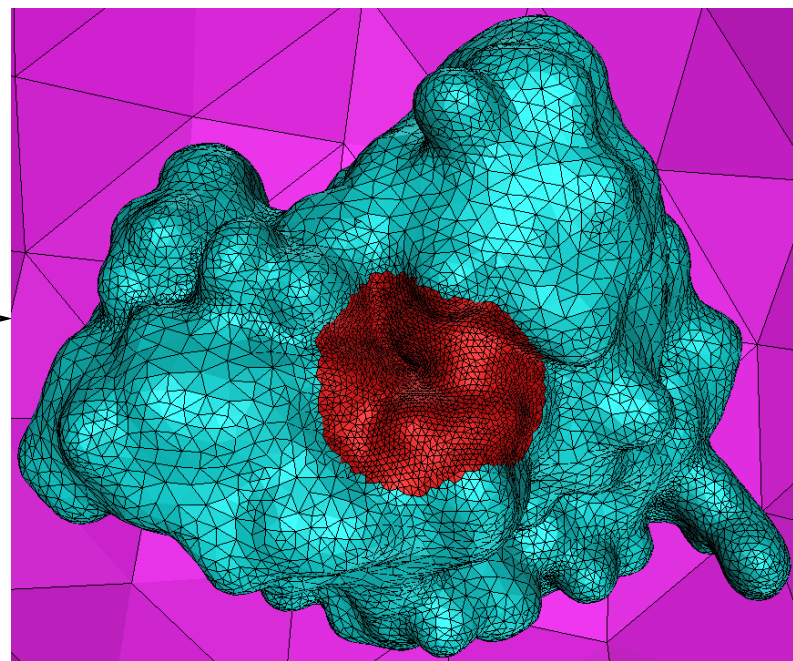
`${solver} –pfreq 5000`

Tetrahedral mesh generation: GAMer

PBE solver



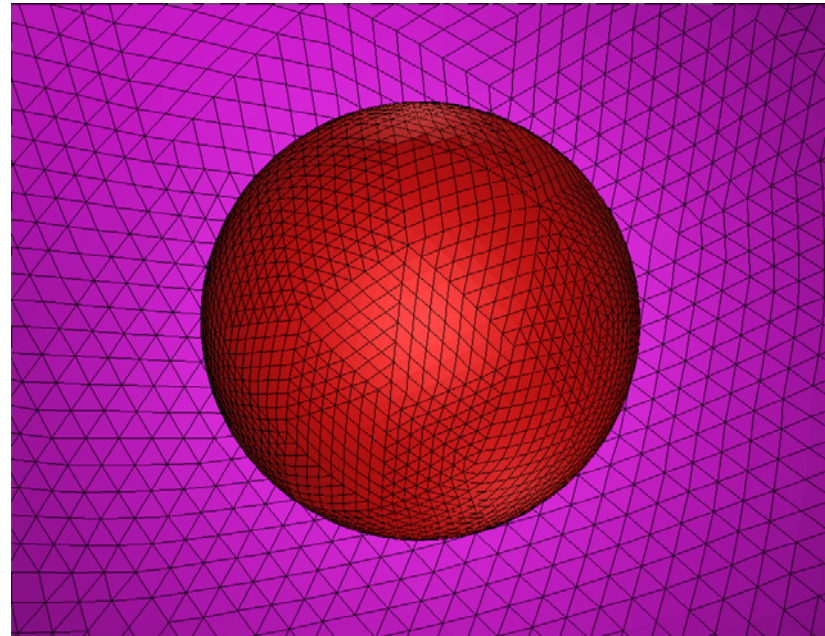
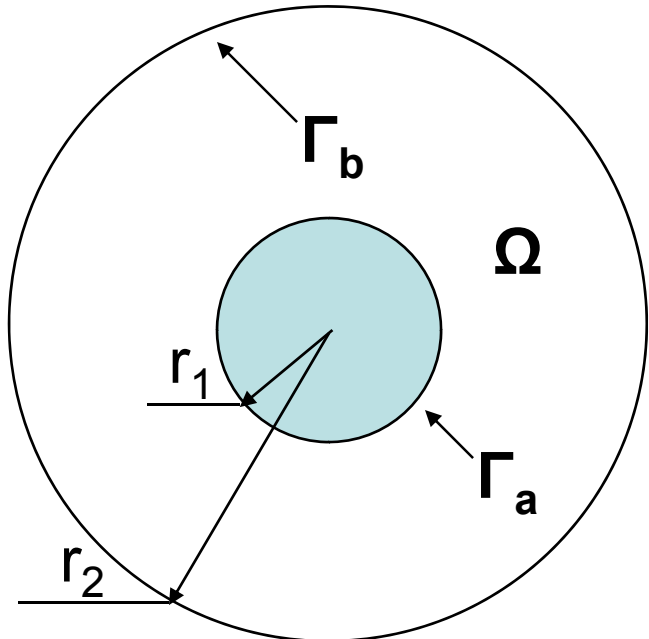
SMOL solver



<http://www.fetk.org/codes/gamer/>

Example 1: Analytical test

The finite element problem domain is the space between two concentric spheres. The boundary Γ_b is Dirichlet, and Γ_a is reactive Robin.



Example 1: Analytical test

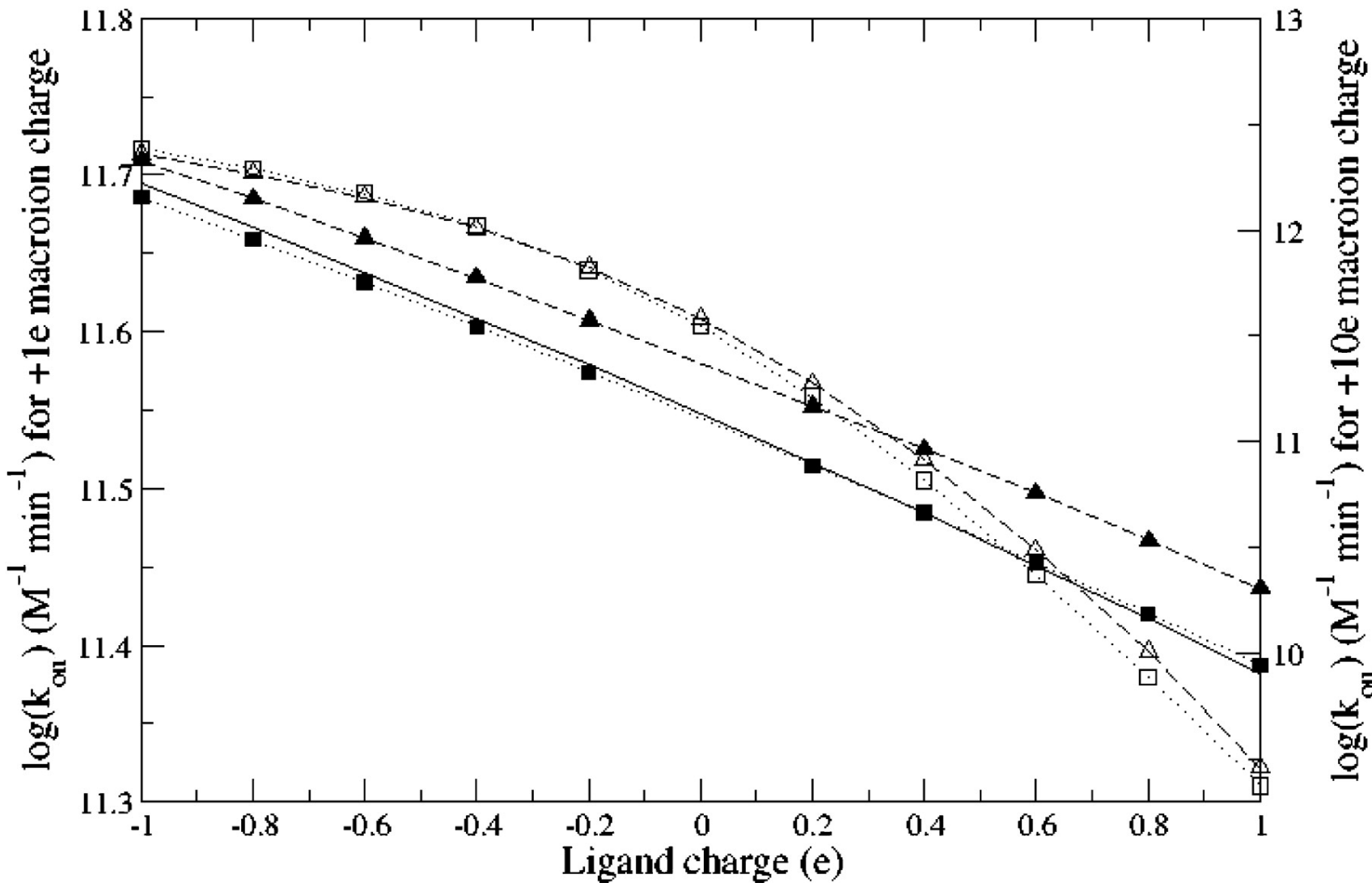
For a spherically symmetric system with a Coulombic form of the PMF, $W(r) = q/(4\pi \epsilon r)$, the SSSE can be written as

$$\frac{1}{r^2} \frac{\partial}{\partial r} (r^2 J_p) = \frac{1}{r^2} \frac{\partial}{\partial r} \left(r^2 D \left(\frac{\partial p}{\partial r} - \beta p \frac{qq_l}{4\pi\epsilon r^2} \right) \right) = 0$$

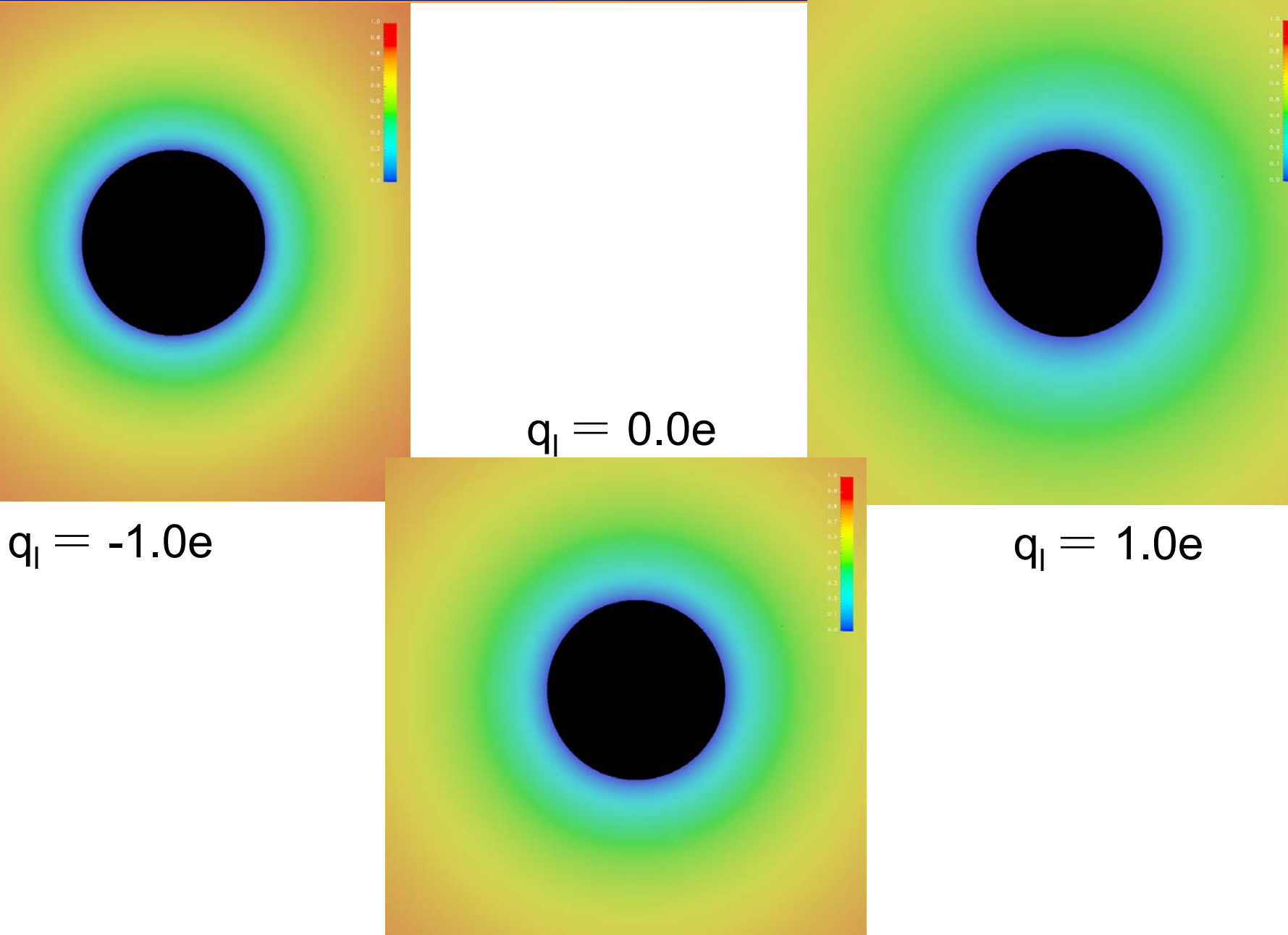
Suppose $Q = \frac{\beta qq_l}{4\pi\epsilon}$, $p(r_1) = 0; p(r_2) = p_{bulk}$

Then, $k_{on} = \frac{4\pi Q D r_1^2}{e^{-\frac{Q}{r_2}} - e^{-\frac{Q}{r_1}}}$ If $Q = 0$, $k_{on} = \frac{4\pi D r_1^2}{\frac{1}{r_1} - \frac{1}{r_2}}$

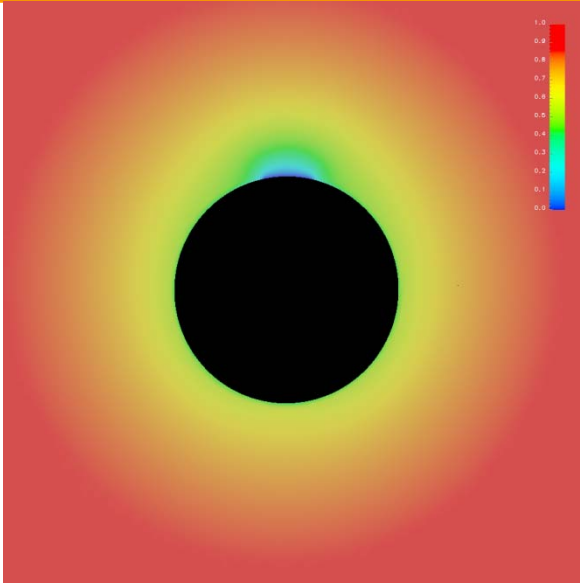
Example 1: Analytical test



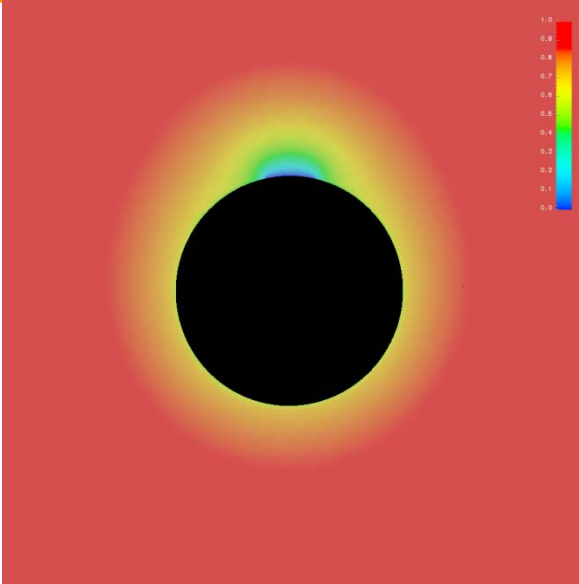
Example 1: Analytical test ($q = 1.0$)



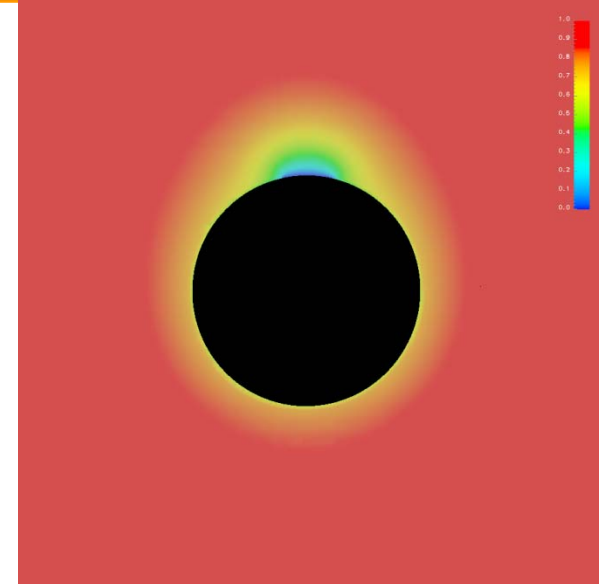
Example 1: Analytical test ($qq_l = 1.0$)



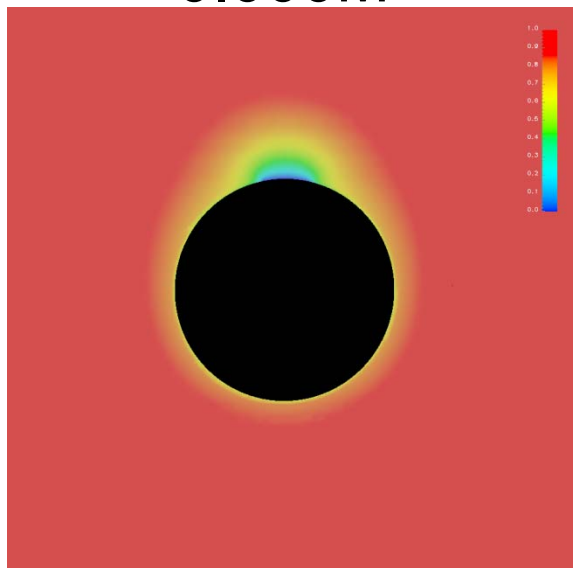
0.000M



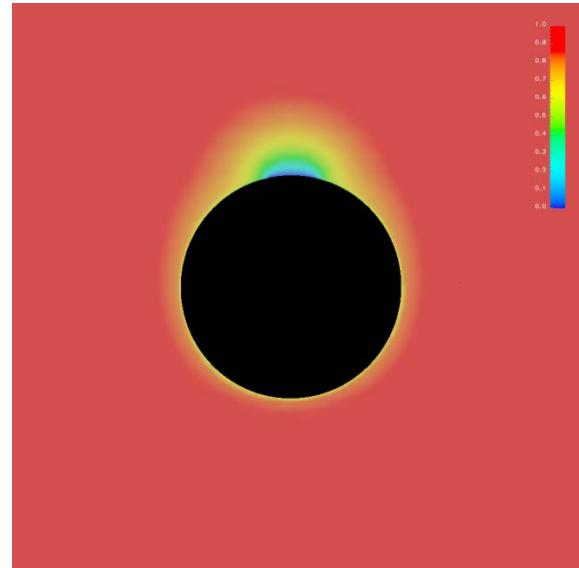
0.075M



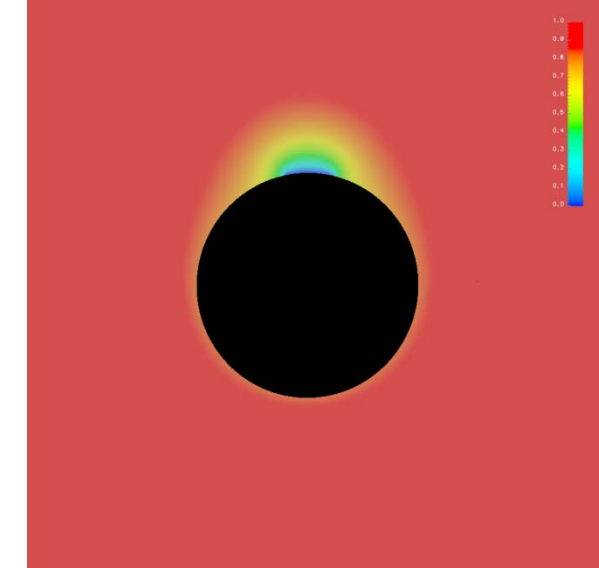
0.150M



0.300M

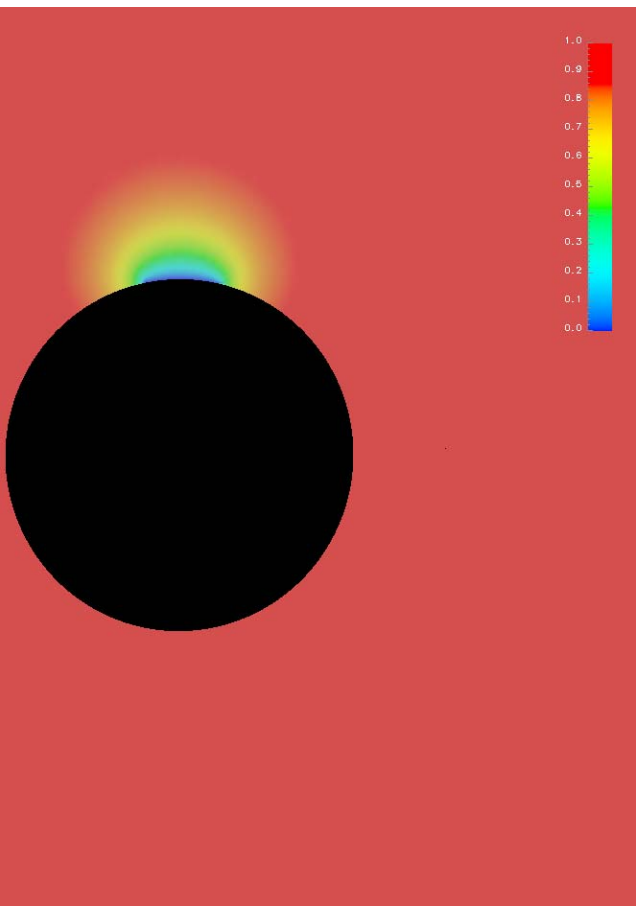


0.450M

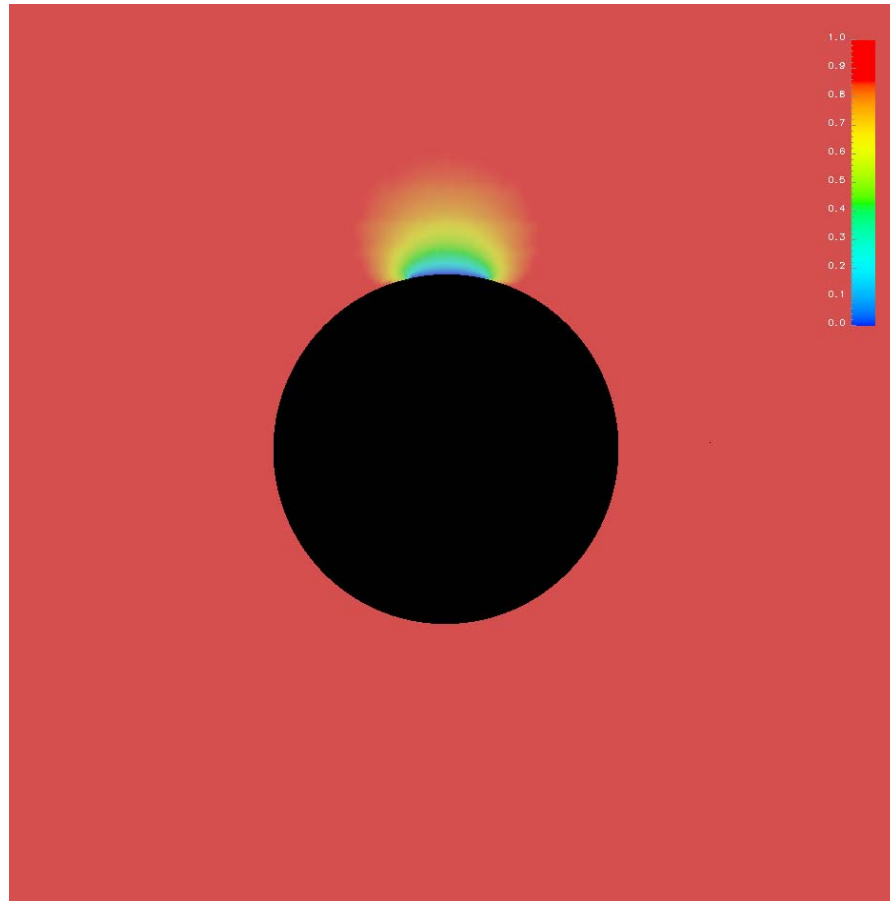


0.670M

Example 1: Analytical test ($qq_l = 0.0$)



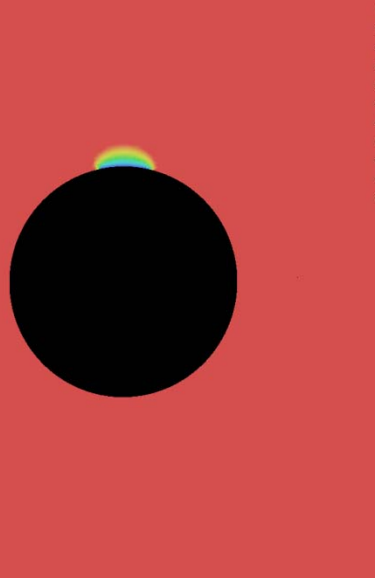
0.000M



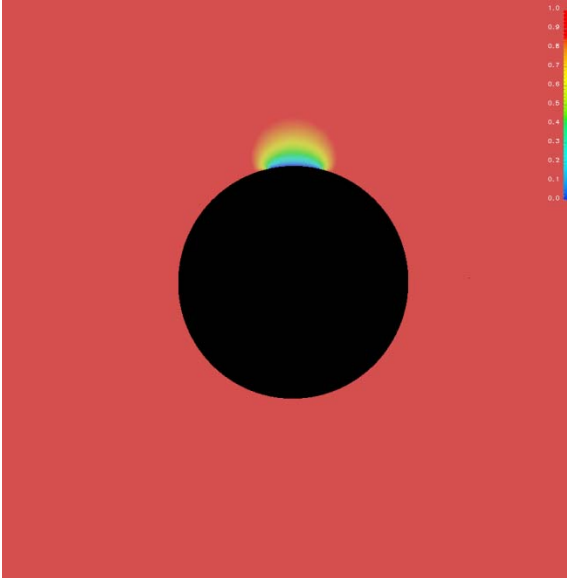
0.600M

Certainly, there is no difference at any ionic strength.

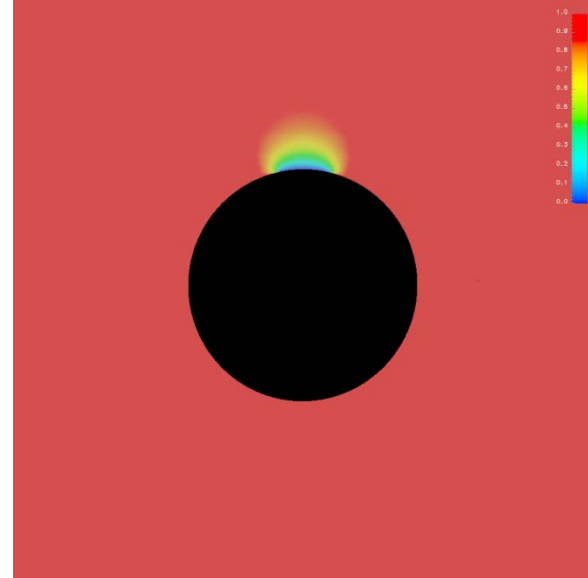
Example 1: Analytical test ($qq_l = -1.0$)



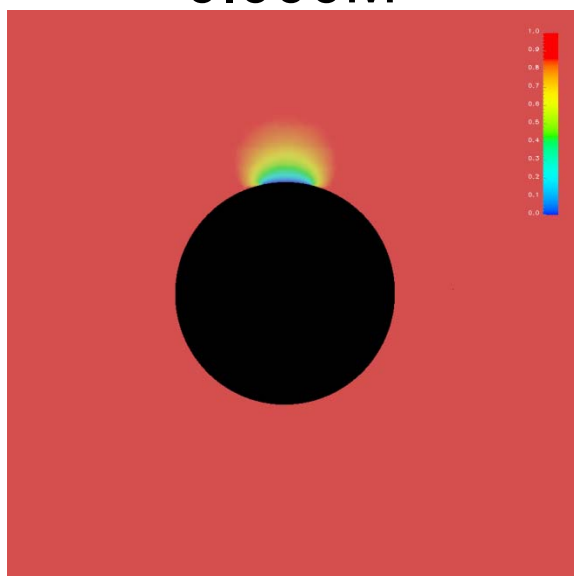
0.000M



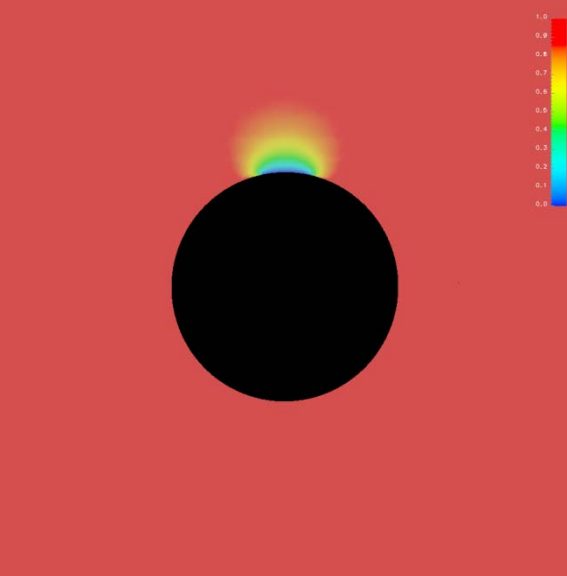
0.075M



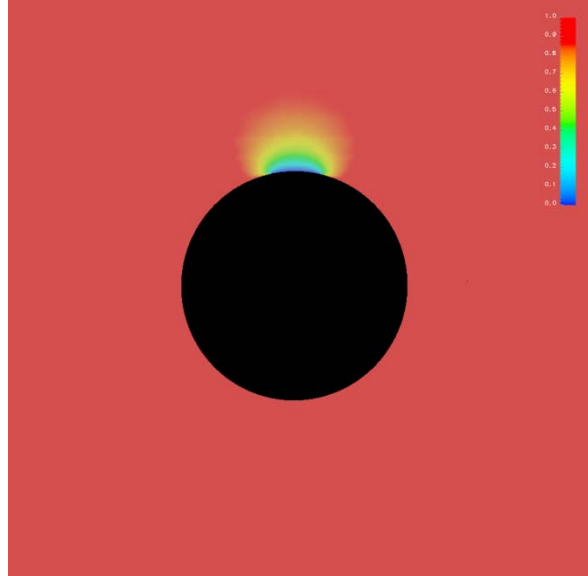
0.150M



0.300M



0.450M



0.600M

Example 2: mAChE monomer

Why Study AChE?

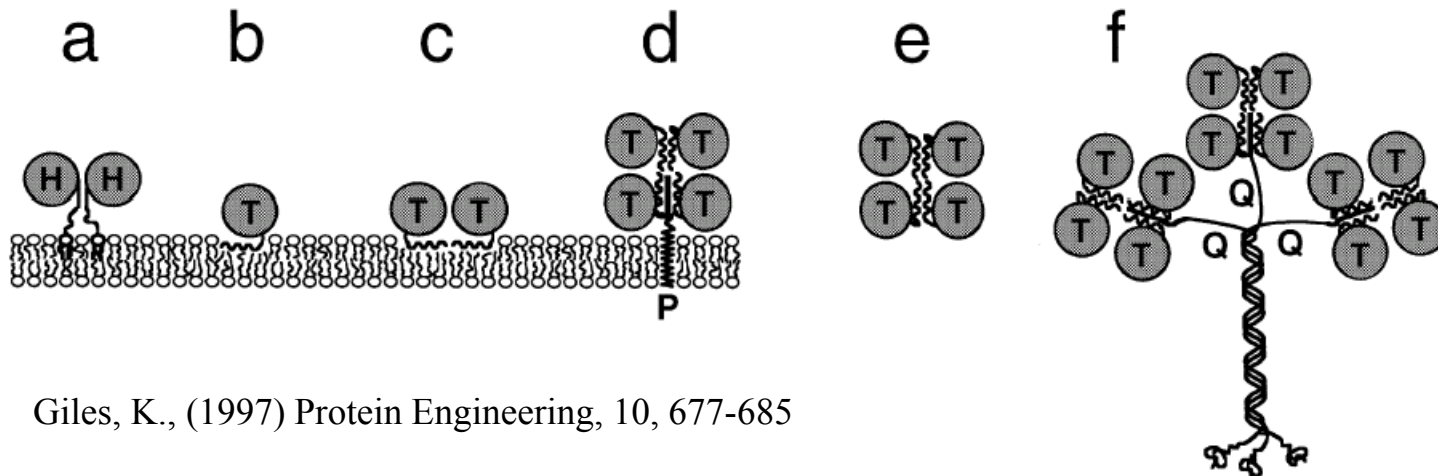
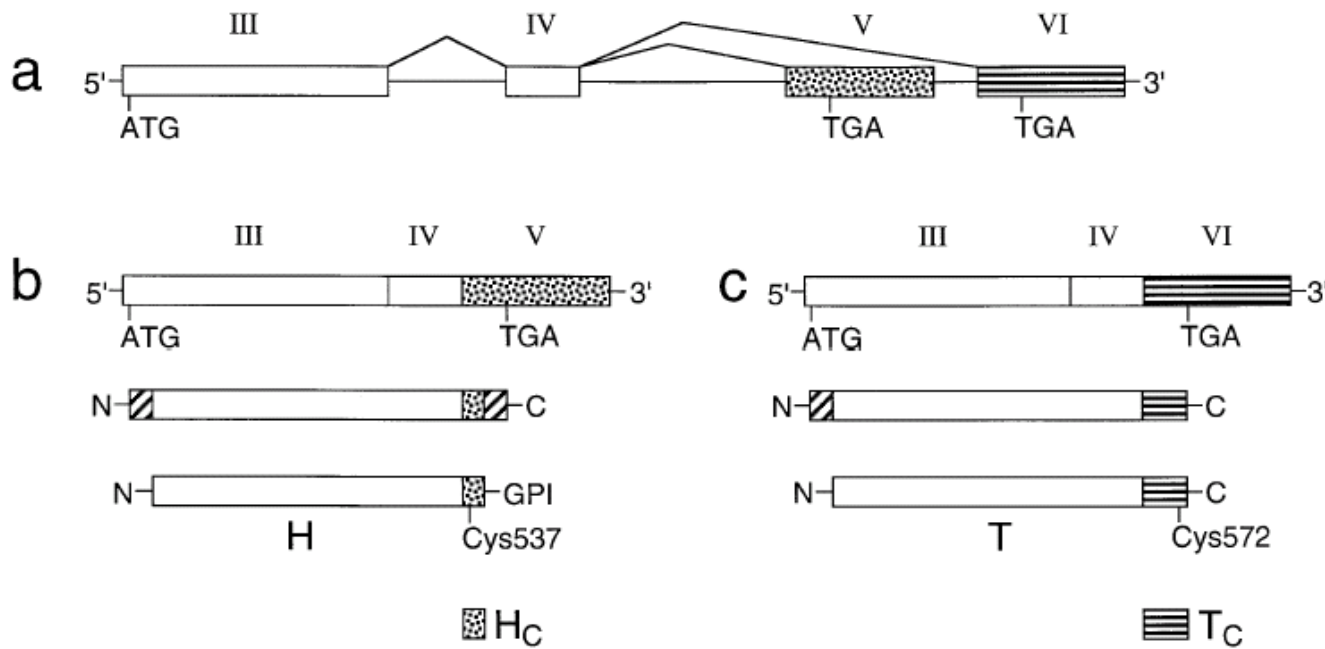
- AChE breaks down ACh at the post-synapse in the neuromuscular junction, terminating the neural signal
- Because of its critical function, AChE is a target for medical agents, insecticides, chemical warfare agents
- The reaction is extremely fast, approaching diffusion limit. Thus a good target to study diffusion both experimentally and computationally
- Part of efforts toward synapse simulation at cellular level

Sub-types of AChE

Three different types of AChE subunits from the same gene, but with alternative splicing of the C-terminal:

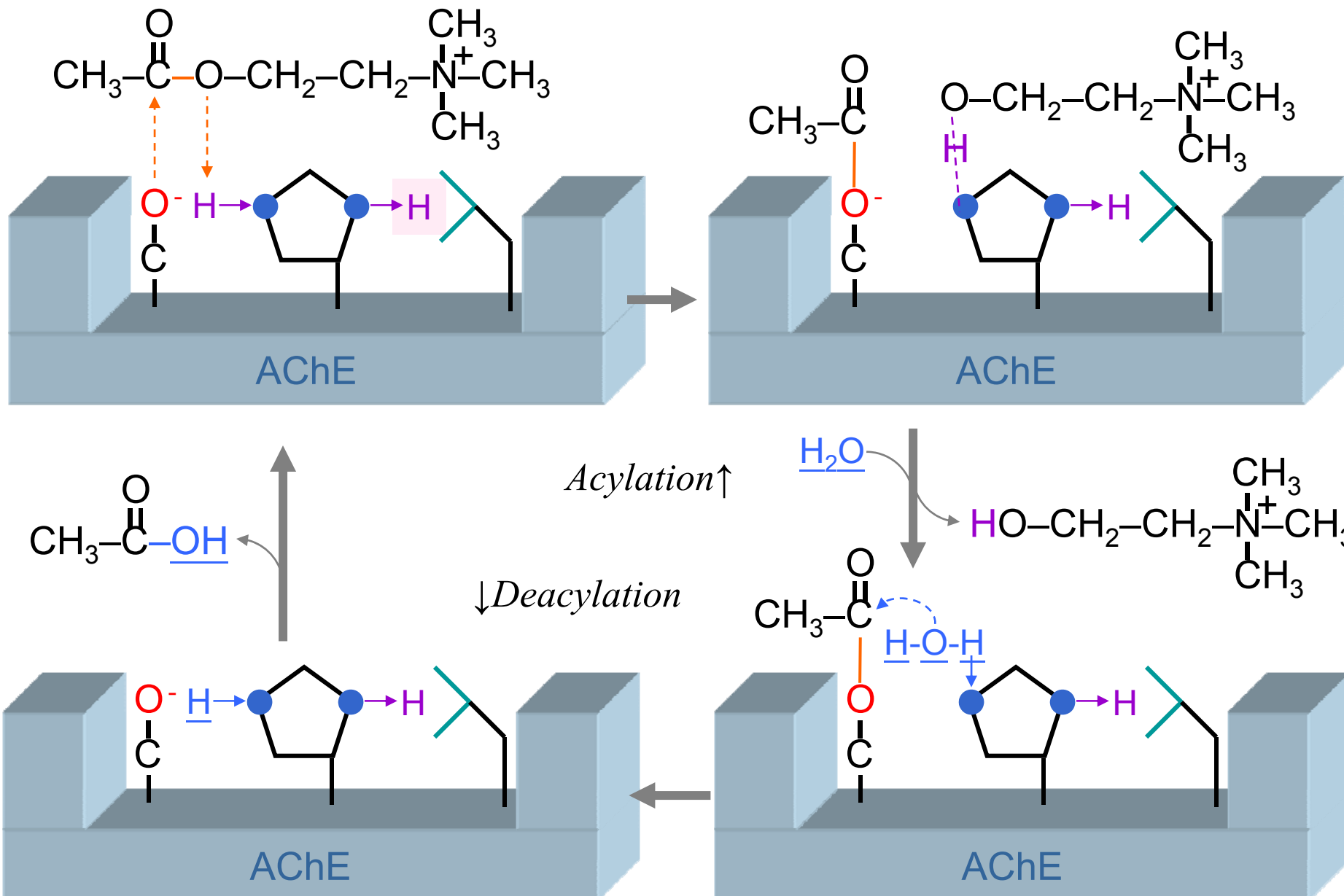
- Type R ('readthrough') produce soluble monomers; they are expressed during development and induced by stress in the mouse brain.
- Type H ('hydrophobic') produce GPI-anchored dimers, but also secreted molecules; they are mostly expressed in red blood cells, where their function is unknown.
- Type T ('tailed') represent the forms expressed in brain and muscle. This is the dominate form of AChE, and also exists for butyrylcholinesterase (BChE).

From Gene to protein



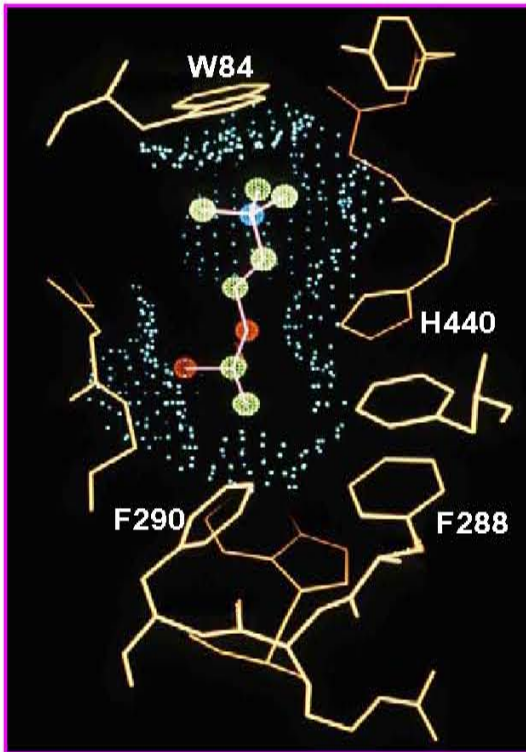
Giles, K., (1997) Protein Engineering, 10, 677-685

Catalytic Mechanism in AChE

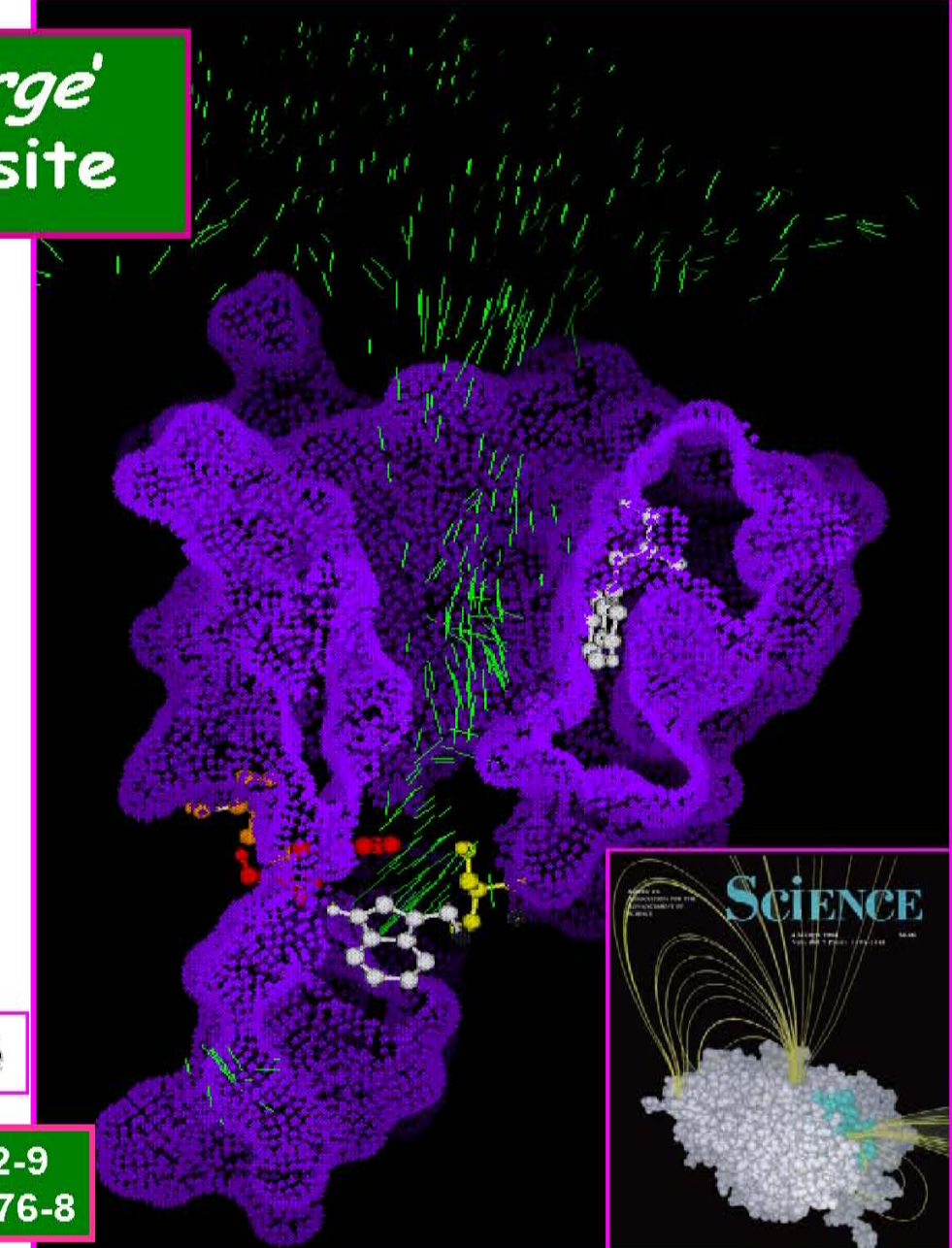


AChE Catalytic Center

AChE has a '*deep gorge*' leading to its active site



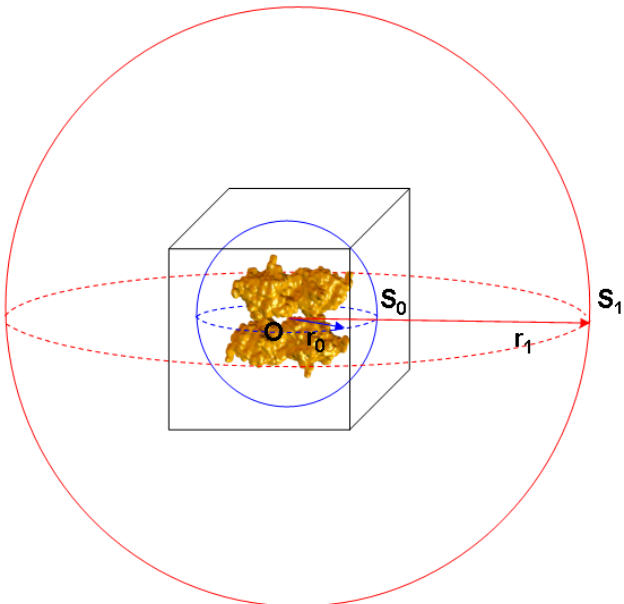
ACh bound in AChE active site



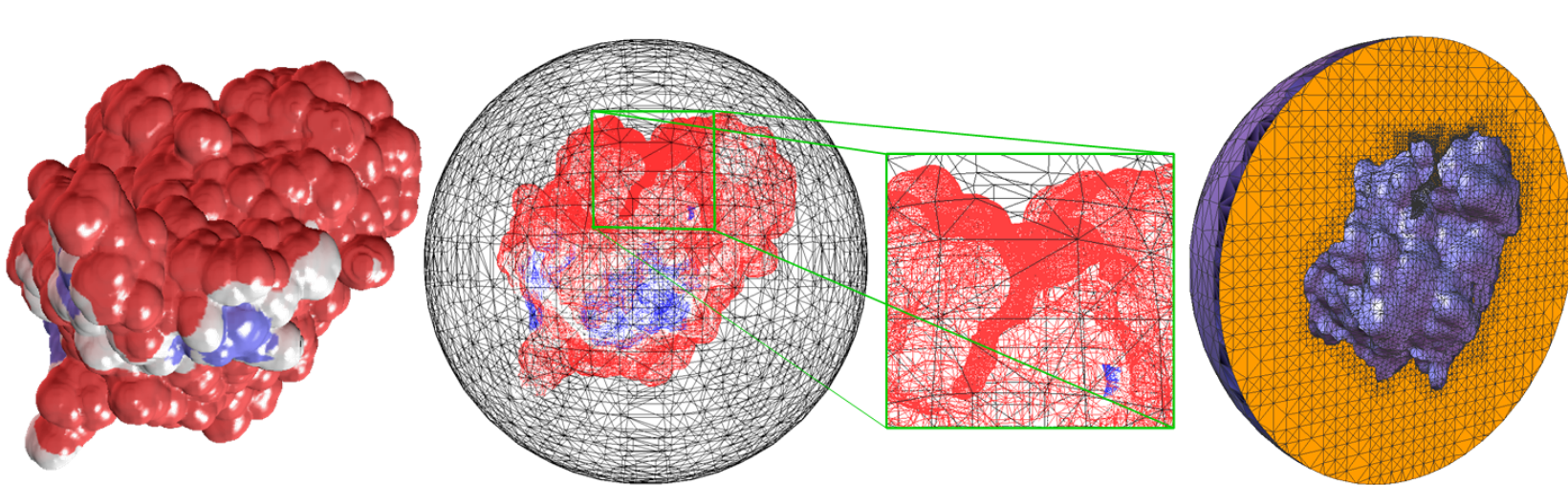
Sussman et al Sllman (1991) *Science* 253, 872-9

Gillson et al Sussman (1994) *Science* 263, 1276-8

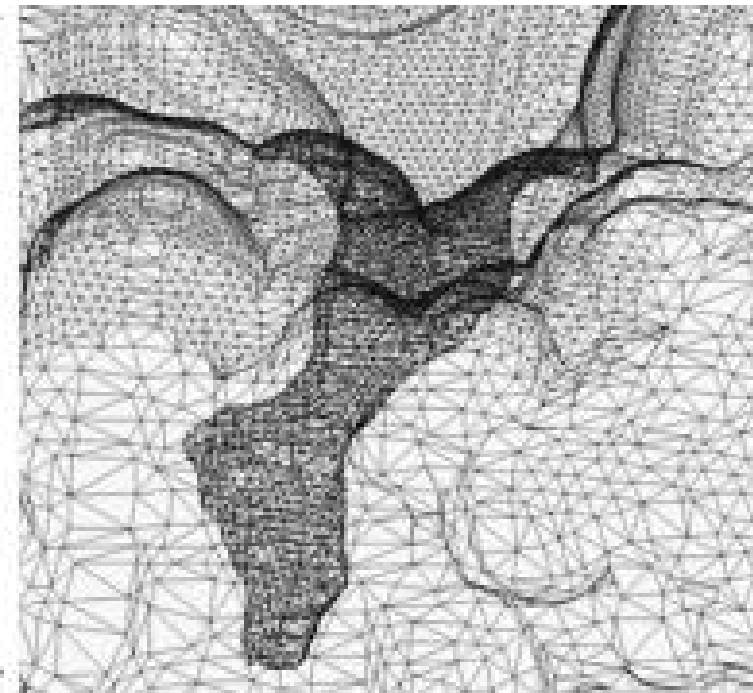
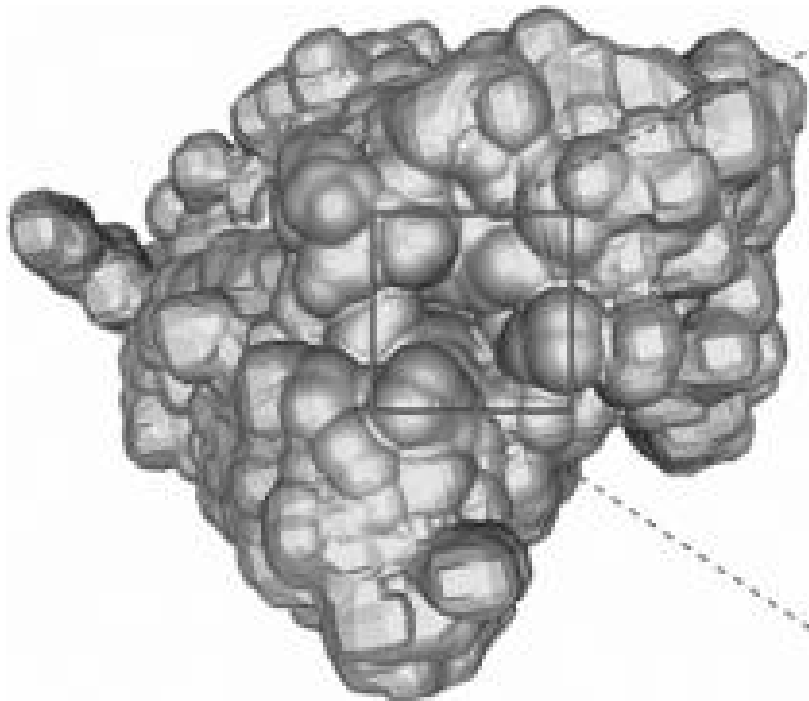
Finite element mesh generation



- GAMer (Holst Group @ UCSD):
[\(<http://www.fetk.org/codes/gamer/>\)](http://www.fetk.org/codes/gamer/)
- $r_1 \sim 40r_0$ (r : biomolecule size)
- Adaptive tetrahedral mesh generation by contouring a grid-based inflated vdW accessibility map for region S_0
- Extend mesh to region S_1 spatial adaptively



Reactive boundary assignment



The origin: carbonyl carbon of Ser203

Sphere 1: $(0.0, 16.6, 0.0)$ $r = 12\text{\AA}$

Sphere 2: $(0.0, 13.6, 0.0)$ $r = 6\text{\AA}$

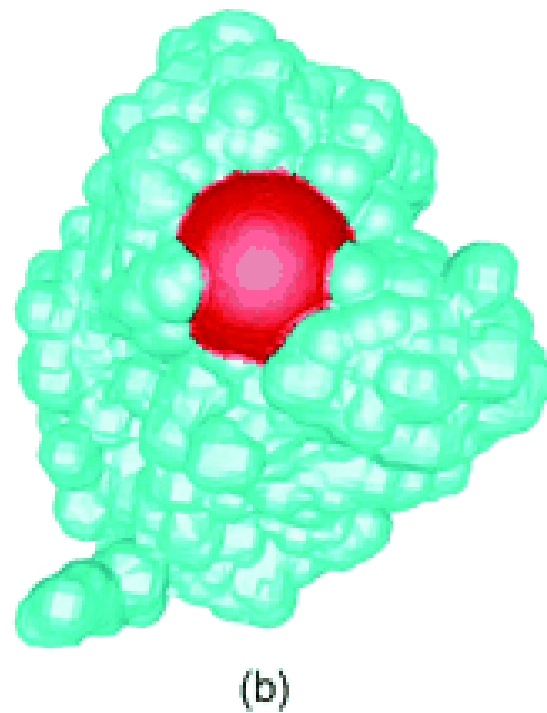
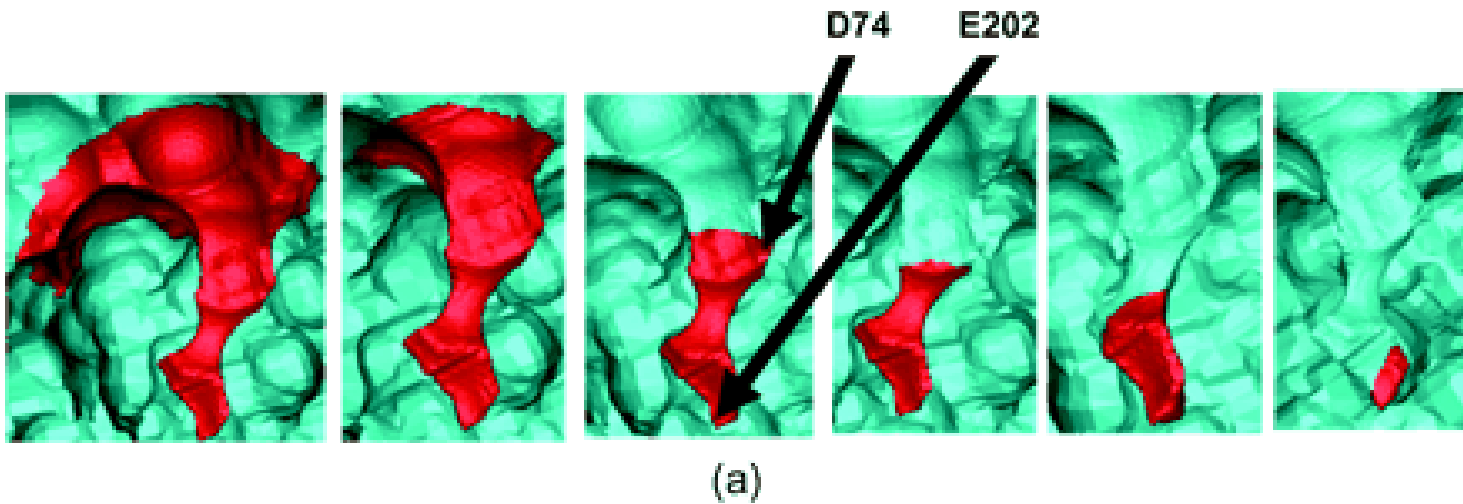
Sphere 3: $(0.0, 10.6, 0.0)$ $r = 6\text{\AA}$

Sphere 4: $(0.0, 7.6, 0.0)$ $r = 6\text{\AA}$

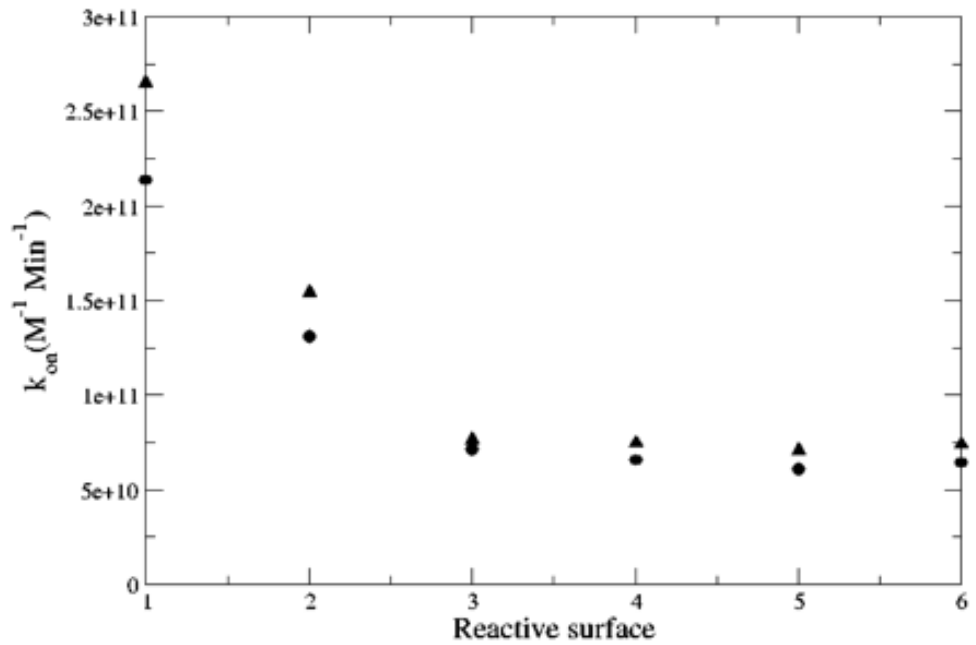
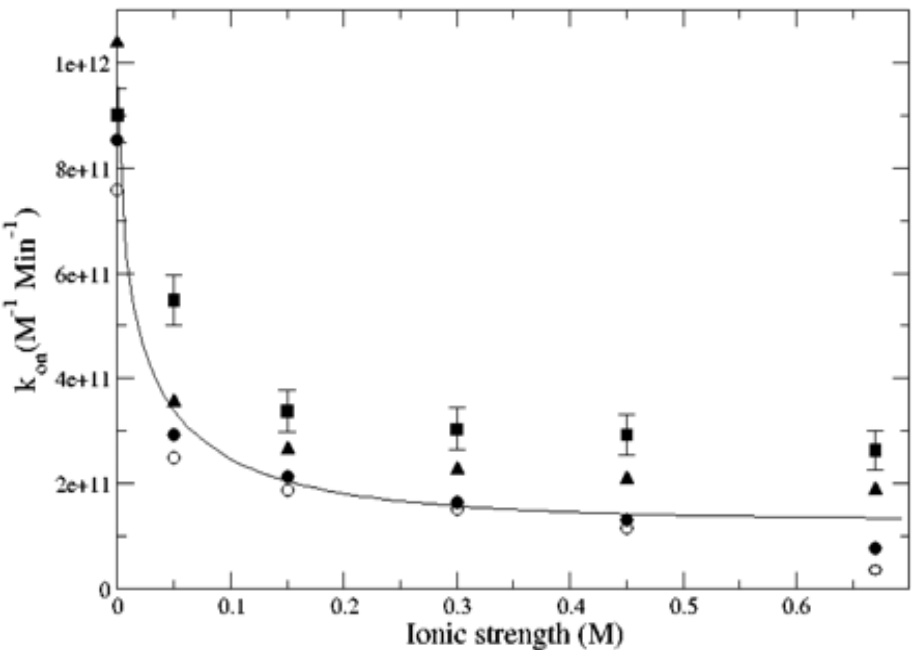
Sphere 5: $(0.0, 4.6, 0.0)$ $r = 6\text{\AA}$

Sphere 6: $(0.0, 1.6, 0.0)$ $r = 6\text{\AA}$

Reactive boundary assignment



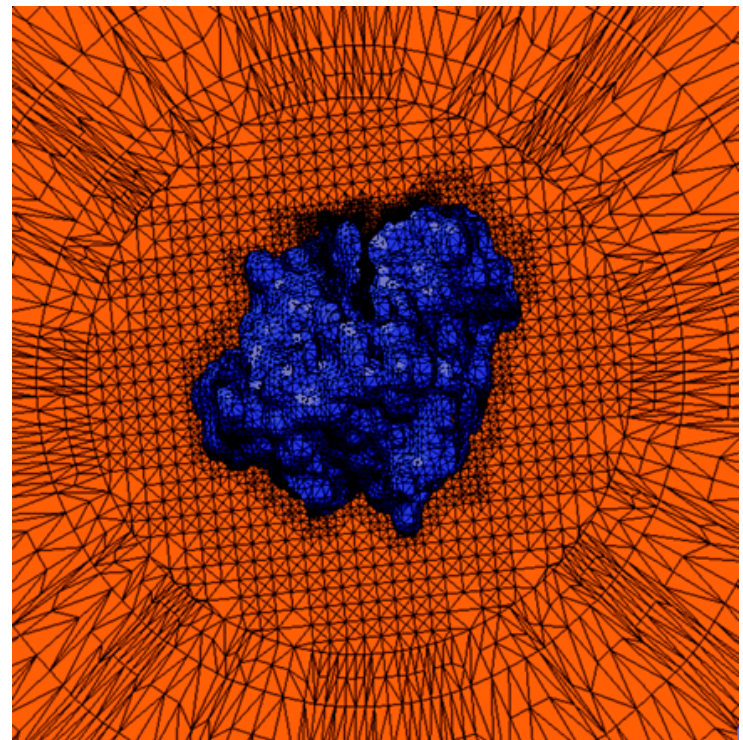
mAChE wild-type ligand binding rate



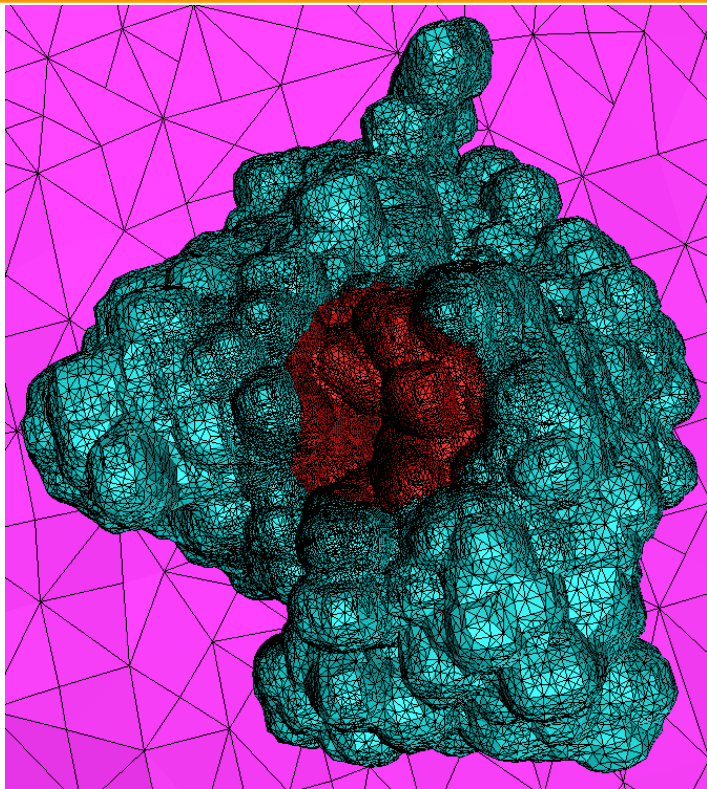
Debye-Hückel limiting law:

$$k_{on} = (k_{on}^0 - k_{on}^H) 10^{-1.18|z_E z_I| \sqrt{I}} + k_{on}^H$$

Mesh quality and refinement



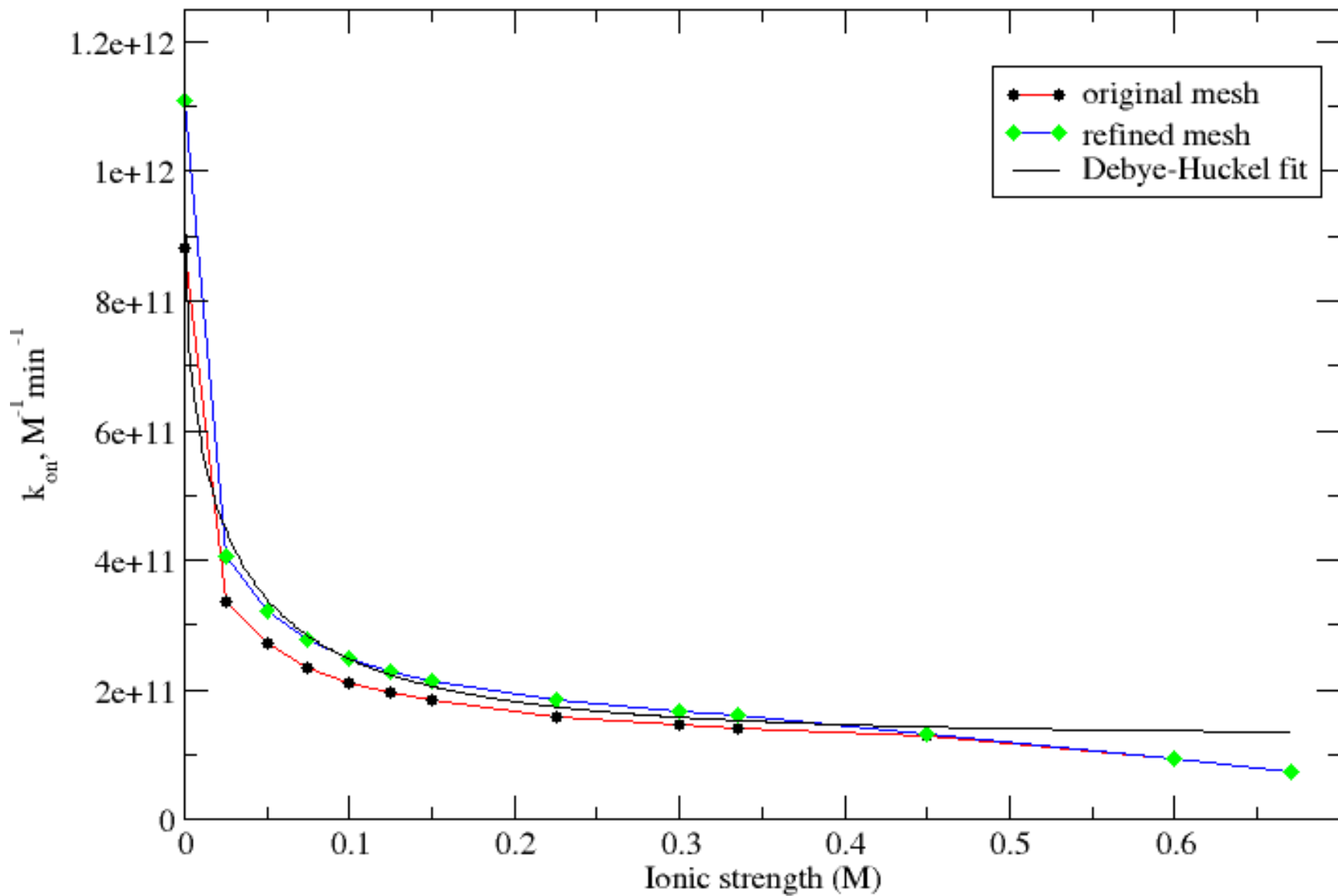
$\varepsilon < 5.0 \times 10^5$



original: 121,670 node,
656,823 simplexes.

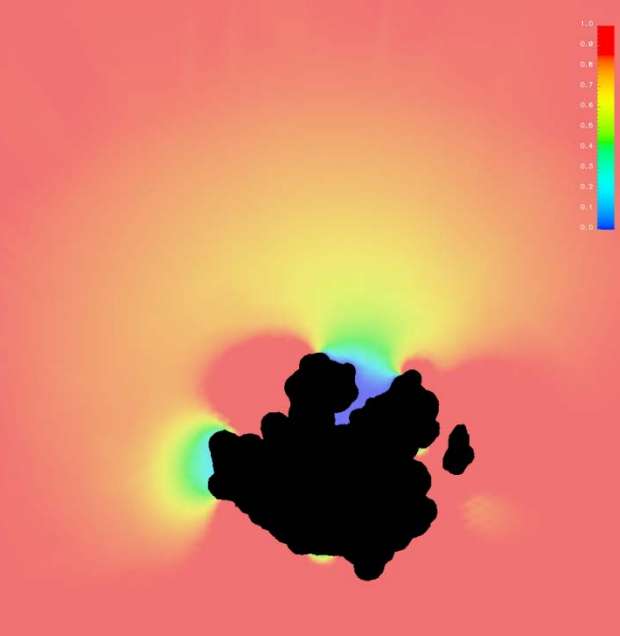
final: 1,144,585 node,
6,094,440 simplexes.

Why do we need to refine the mesh?

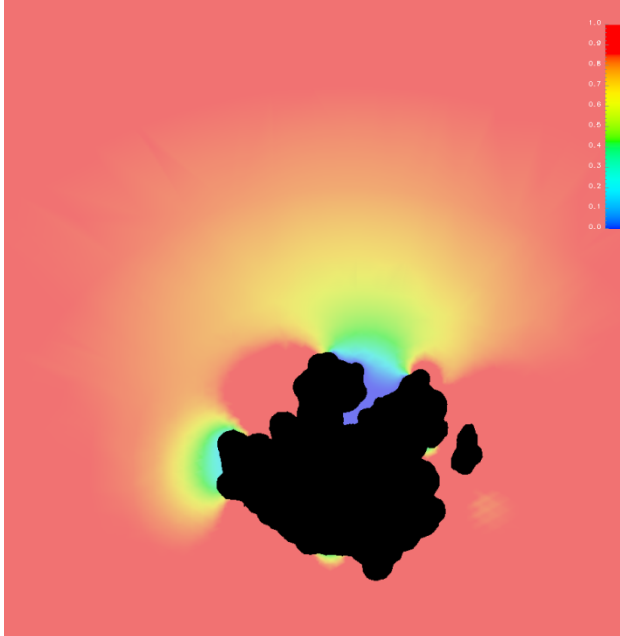




0.025 M



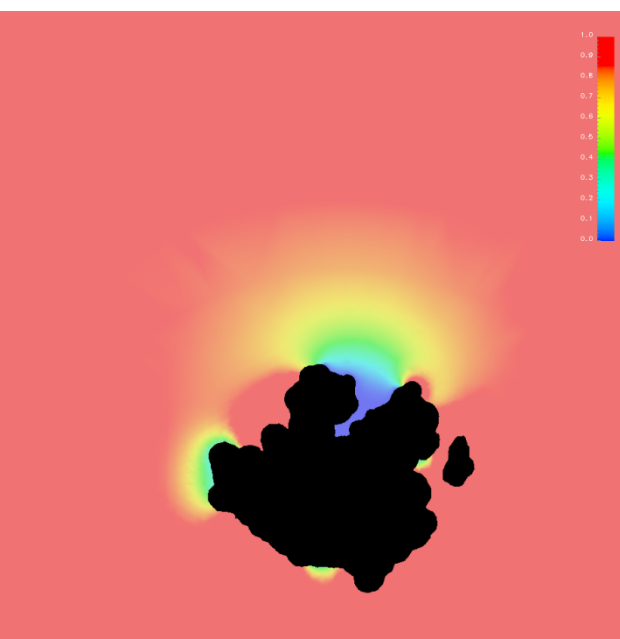
0.050 M



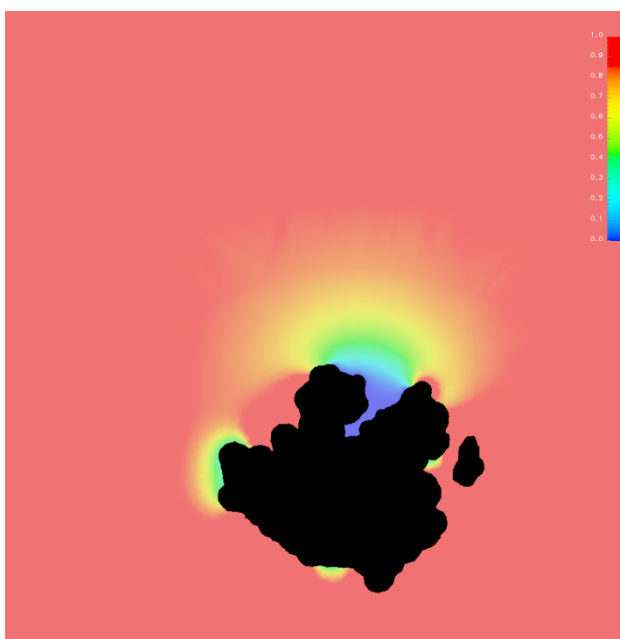
0.100 M



0.225 M



0.450 M



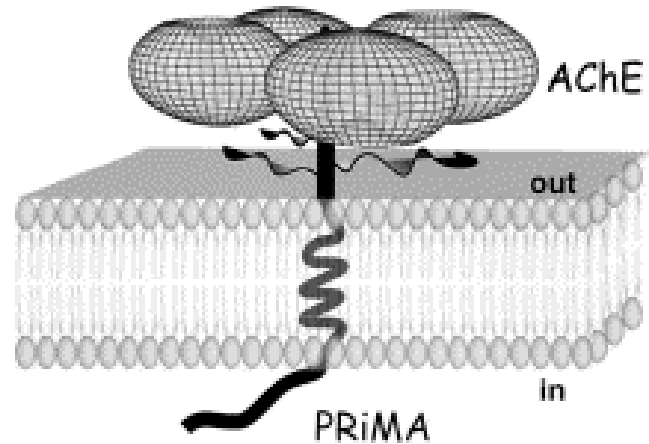
0.670 M

What can we learn from last several cases?

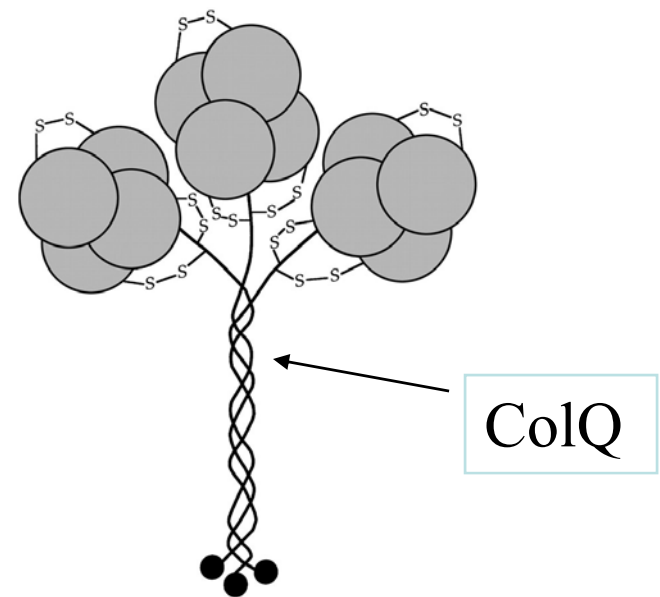
- ⊕ The concentration distribution is affected by the ionic strength substantially.
- ⊕ k_{on} exhibits an ionic strength dependence strongly indicative of electrostatic acceleration. The high ionic strength environment lessens the electrostatic interactions between the active site and the ligand, (cf. J. Mol. Biol. 1999, 291, 149-162)

The Quaternary Association of AChE

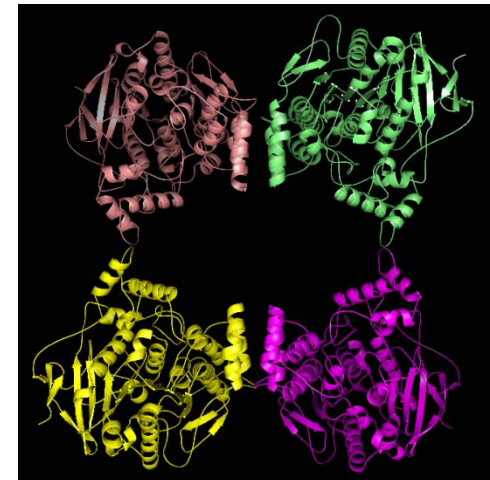
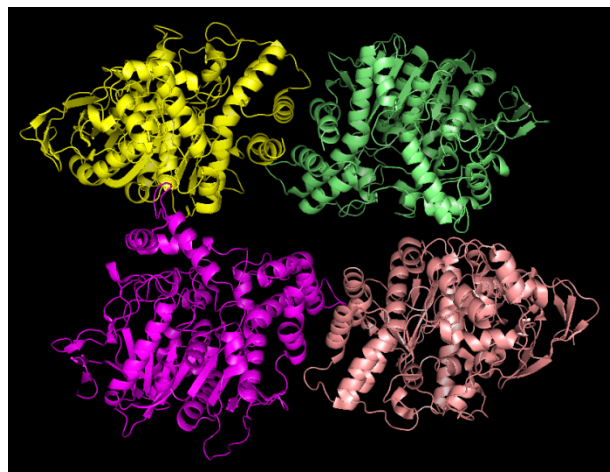
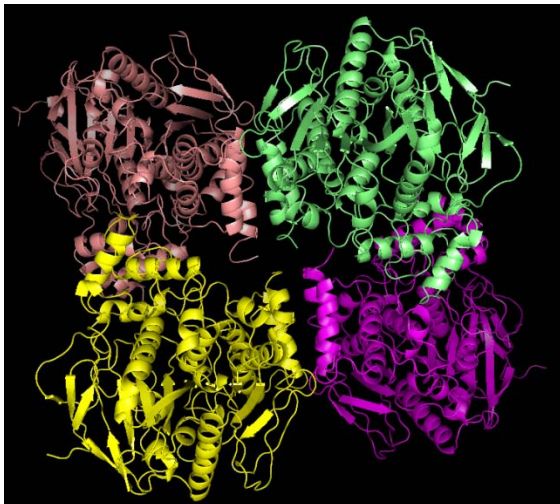
- In mammalian CNS, AChE exists as an amphiphilic tetramer anchored to the membrane by a hydrophobic non-catalytic subunit (PRiMA)



- In NMJ, AChE is an asymmetric form containing 1-3 tetramers associated with the basal lamina by a collagen-like structural subunit ColQ



Tetramer: Dimer of Dimers



- PDB: 1MAA
- Residues 549-583 deleted
- Only forms monomer or dimer in solution
- Dimer-dimer interaction similar to Fas2-AChE (omega loop = loop II), resulting in two occluded gorges

- PDB: 1C2O
 - Trypsin released form of AChE from *E. electrocetus*
 - Crystal grown at pH8 4°C
 - Compact, square nonplanar
 - four-helix boundle parallel
 - two gorges partially blocked
 - additional density for C-terminal t peptide observed, but not resolved.
- 1C2B(1EAA)
 - pH6 20°C
 - Loose, pseudo-square planar;
 - anti-parallel
 - all gorges open

Heteromeric Association with PRAD



Giles, K. (1997) Protein Engineering, 6, 677-685

- t peptide sequence (40 or 41 res) highly conserved
- PRAD = Proline Rich Attachment Domain
- PRAD is required to form tetramer in solution

Bon,S. Coussen, F., Massoulie, J. (1997) JBC, 272, 3016-3021

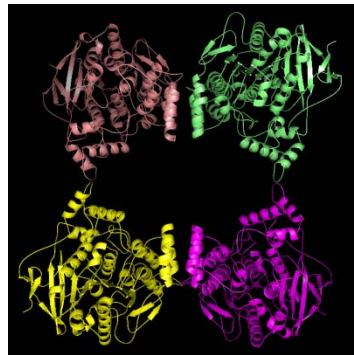
Bon, S. et al. (2003) Eur. J. Biochem, 271, 33-47

ColQ_Mouse
L**P**GLDQKKRG SHKACCLL**M**P **PPPPLF**PPPF FRGSRS**P**LLS PDMKNLLELE AS**PSPCIQGS**
LGSP**PG**PPGQG **PPGLP**GKTGP KGEKGDLGR**P** GRKGR**PG**PPG VPGMPGPVGW **PG**PEG**PR**GEK
GDLGMMGL**P**G SRG**PM**GSKGF **P**GSRGEKGSR GERGDLG**P**KG EKGFPGFPGM LGQKGEM**GPK**
GESGLAGHRG **PTGR**PGKRGK QGQKGDSGIM GPHGK**PG**PSG Q**P**GRQG**PP**GA **PG**PPSA

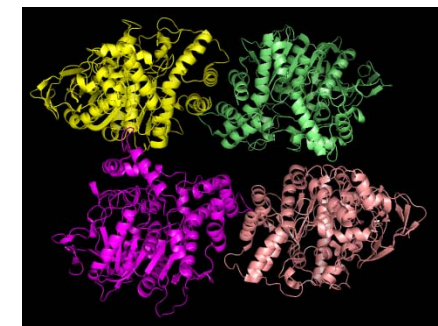
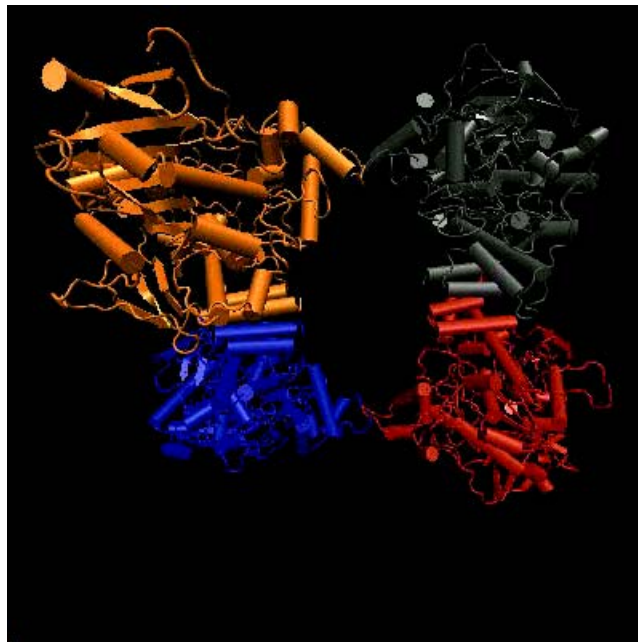
PRMA_Mouse

MLLRDLV**PR**H GCCW**P**SLLLH CALH**P**LWGLV QVT~~HAE~~**P**QKS CSKVTDSCQH ICQC**RP**PPPL
PPPPPPPPPP RLLSAP**A**PNS TSCP**AED**SWW SGLVIIIVAVV CASLVFLT**V**L VIICYKAIKR
KPLRKDENGT SVAEY**P**MSSS QSHKGVDVNA AVV

A flexible Tetramer?

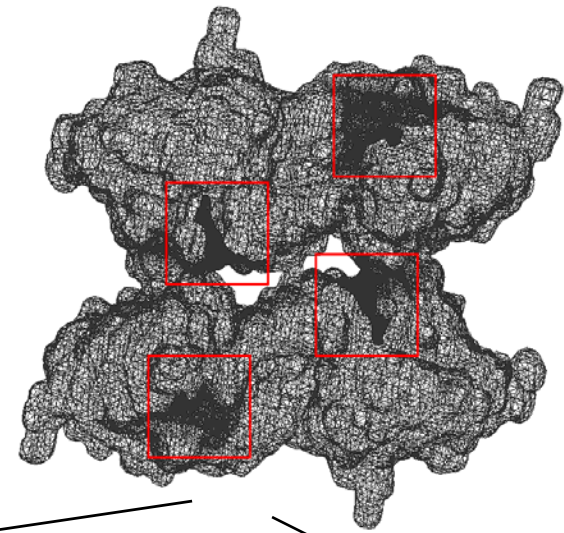
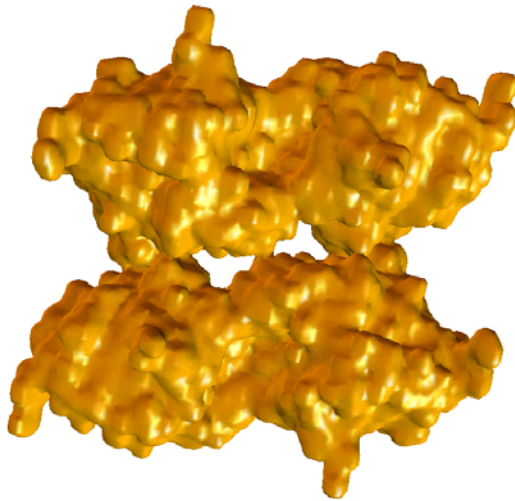
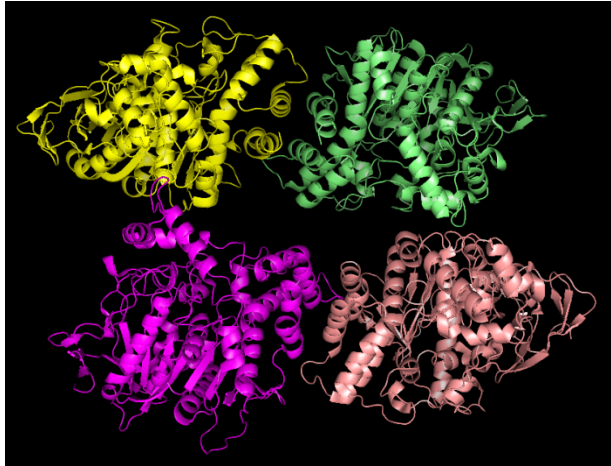


1C2B
Flat square
Quasi-planar

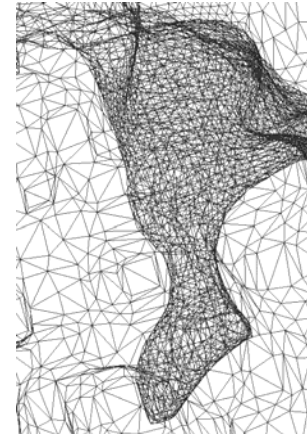
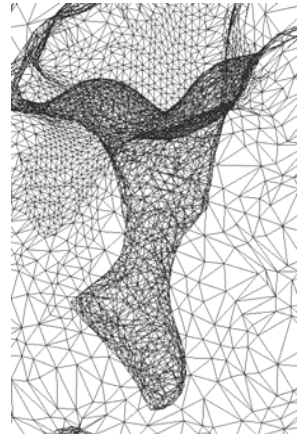
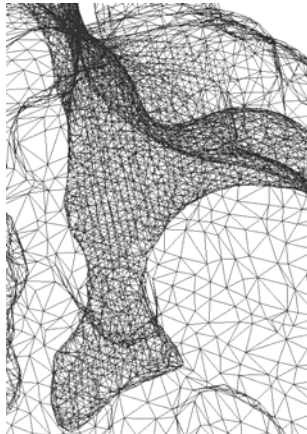
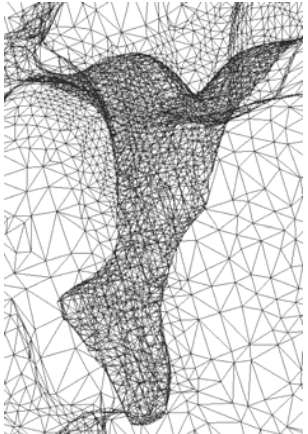


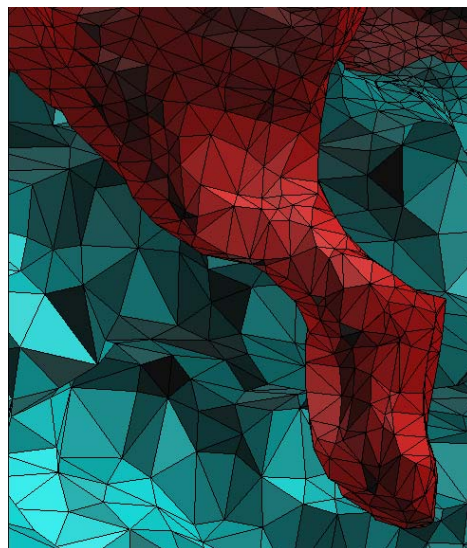
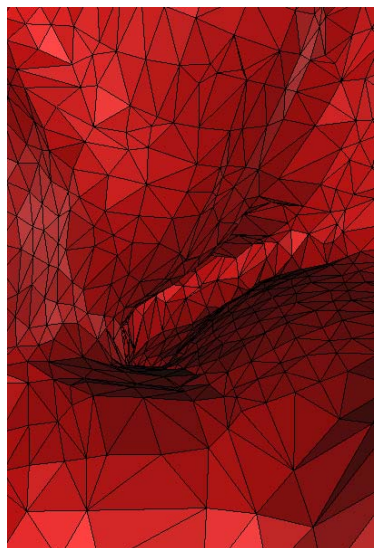
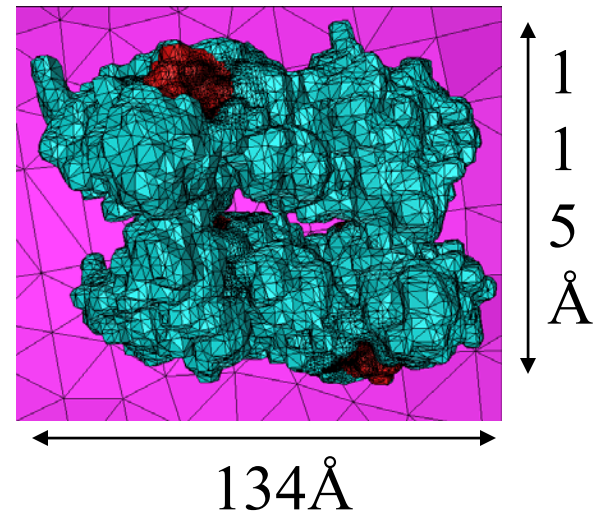
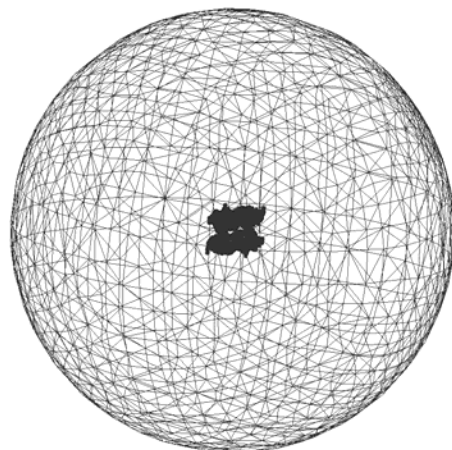
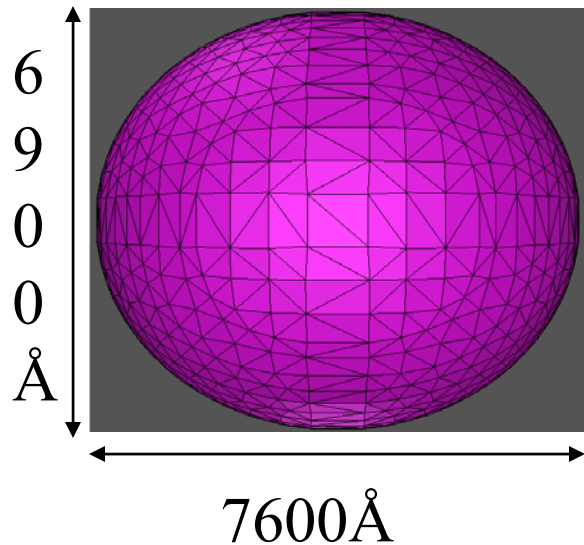
1C2O
Compact

Tetrahedral Mesh for mAChE Tetramer



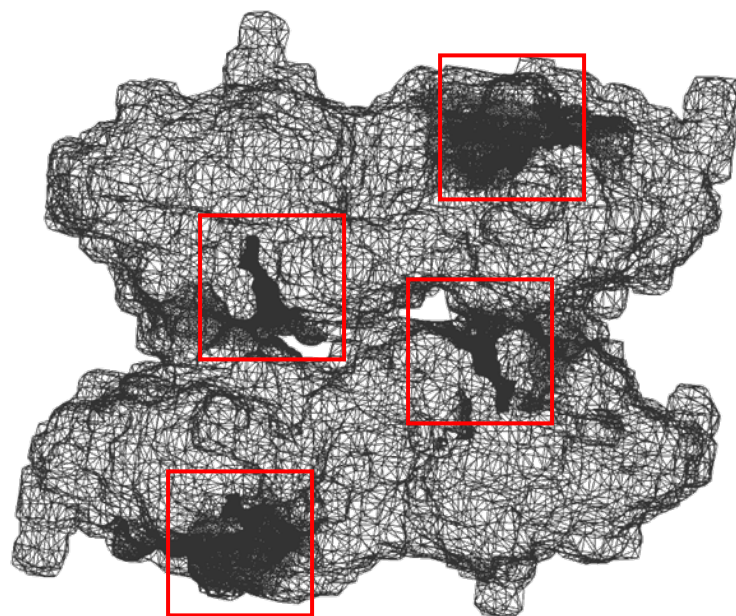
Reactive
surface is
assigned
according
to previous
studies on
monomeric
mAChE



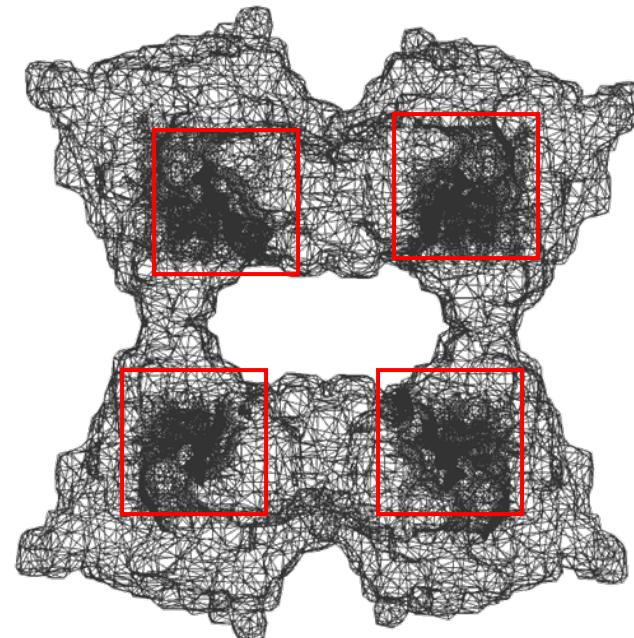


Typical Mesh quality:

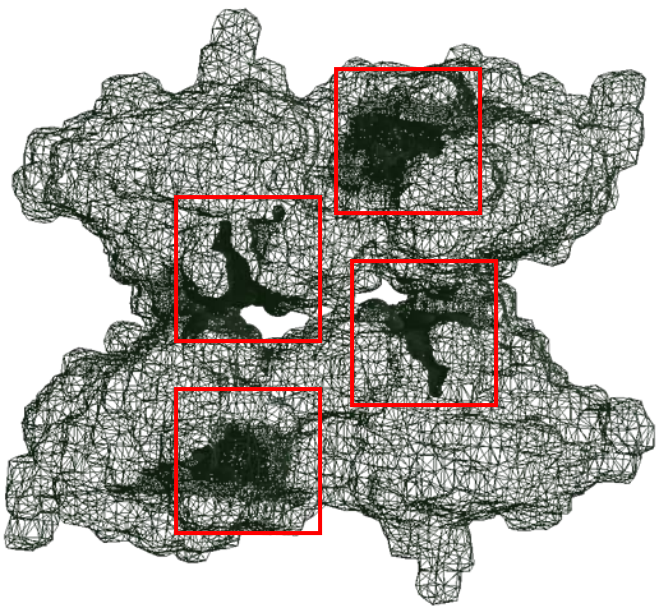
726186 simplices, 142643 vertices
 Joe-Liu: 0.999(best), 0.0154(worst)
 Edge-Ratio: 1.03(best), 8.48(worst)
 Volume: 1.73e-4(S), 9.35e8(L)
 Short Edge: 0.039(S), 363 (L)
 Long Edge: 0.148 (S), 861 (L)



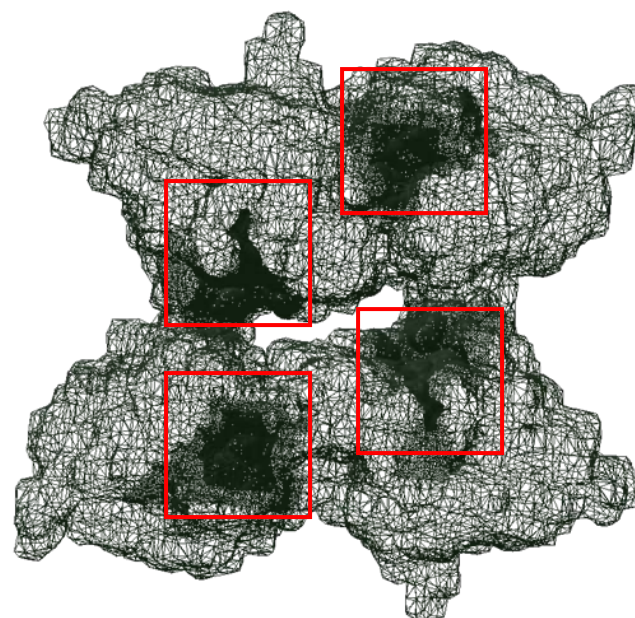
1C2O



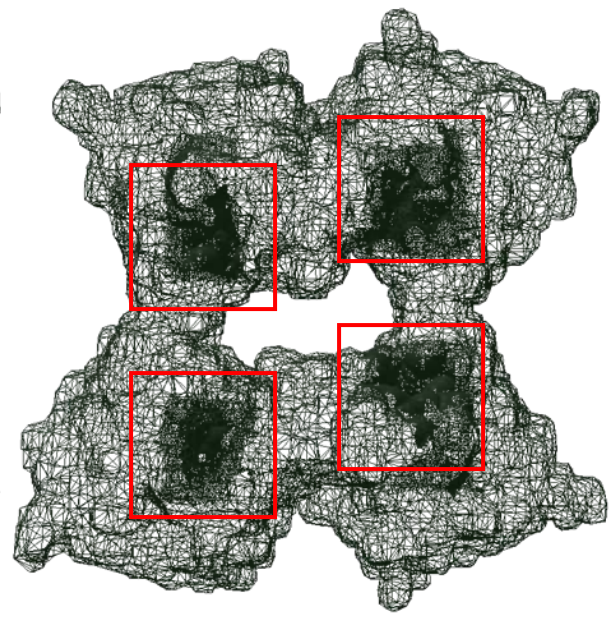
1C2B



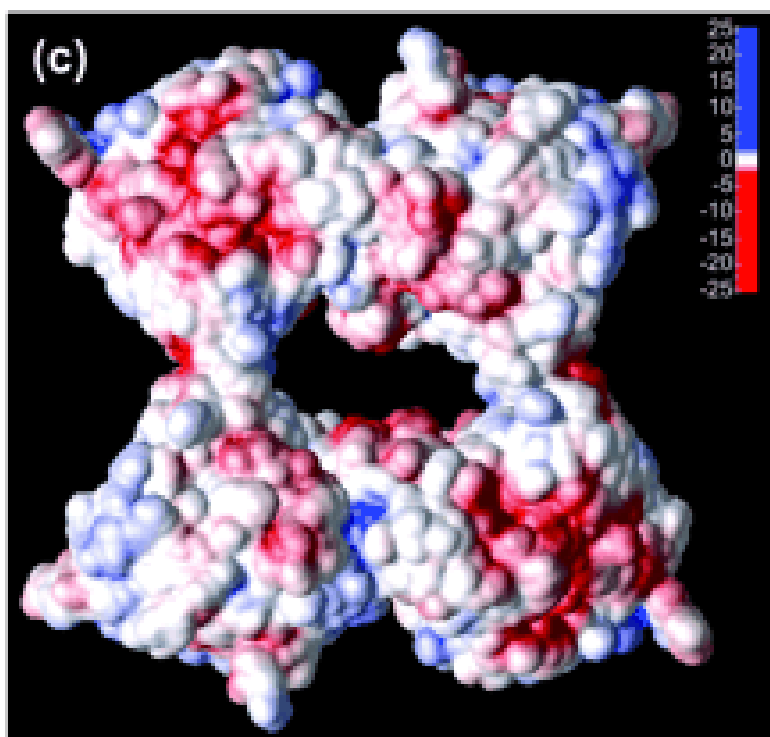
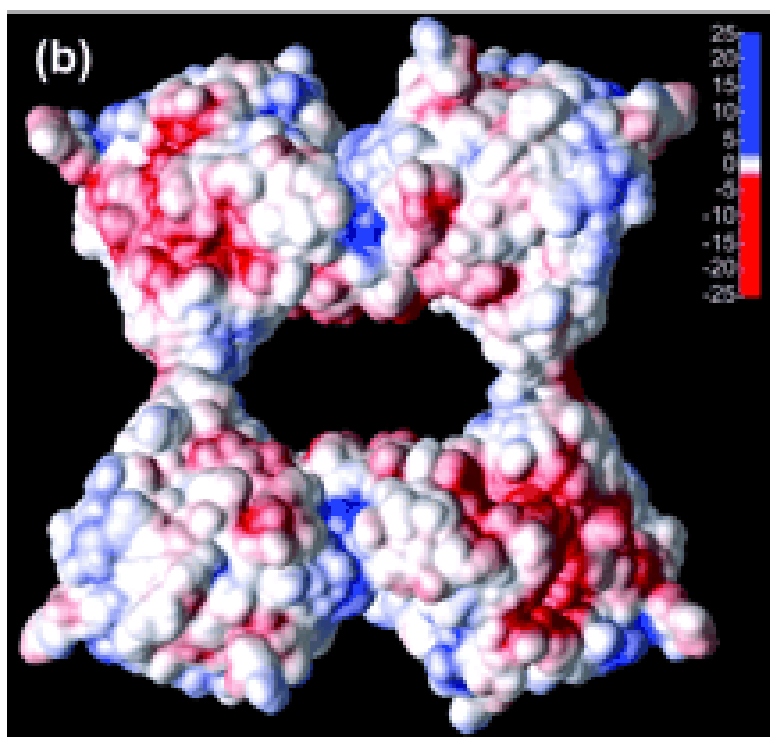
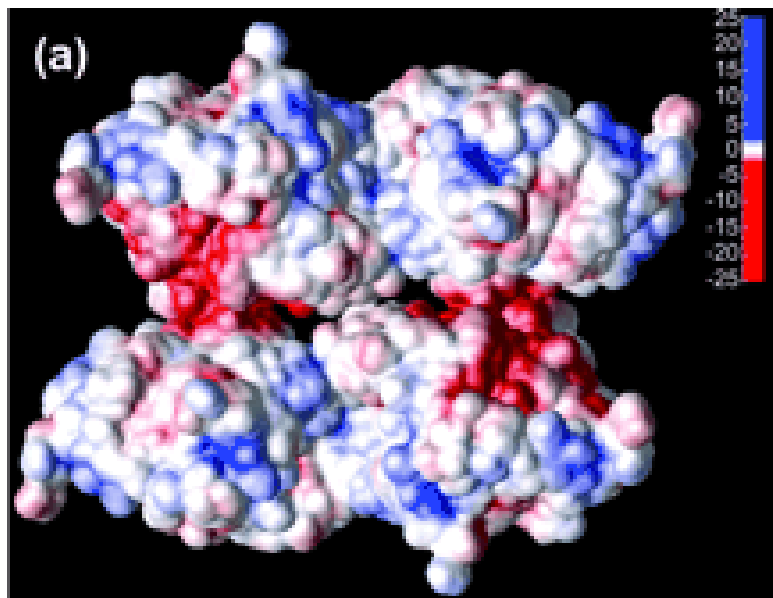
Int4



Int3



Int2



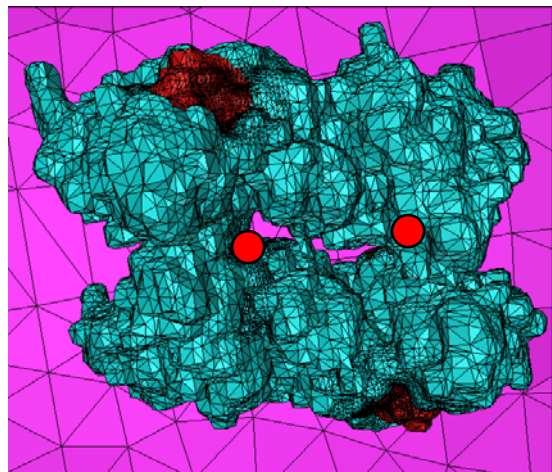
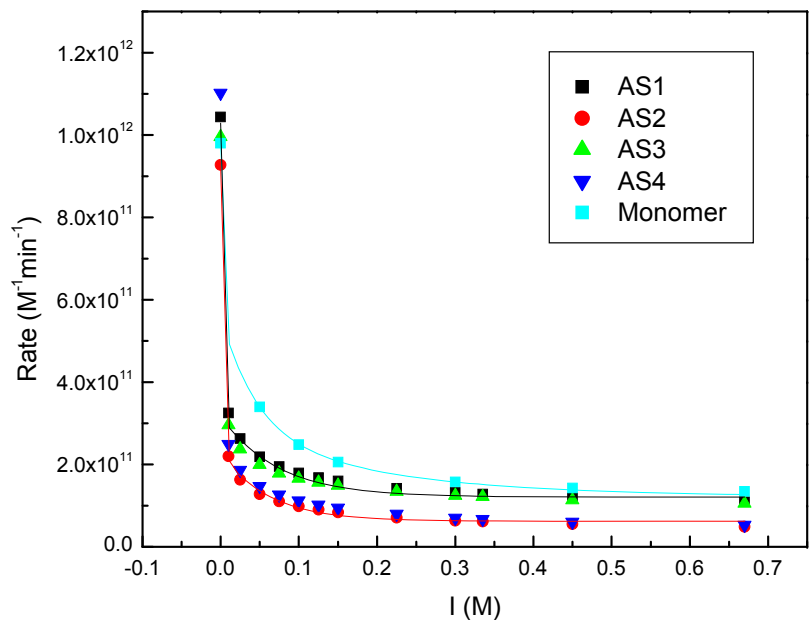
PMF Calculation

- APBS 0.5.1
(<http://agave.wustl.edu/>)
- Grid hierarchy (0-10)
- Apolar forces and dielectric boundary omitted
- No coupling b/w PMF and diffusing particle
(Poisson-Nerst-Plank Eqn)
- No correlation b/w diffusing species

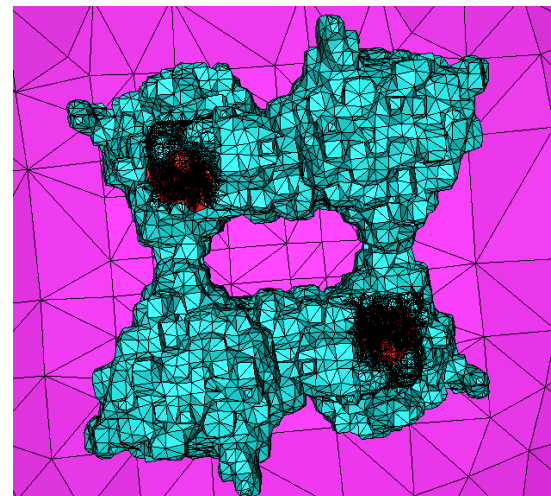
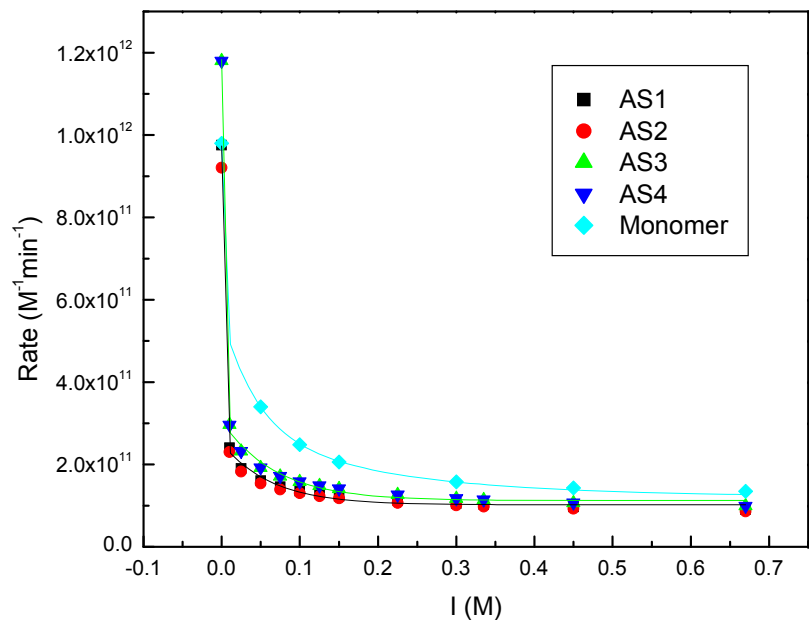
Grid#	dx(Å)	dy(Å)	dz(Å)	*x	*y	*z
0	0.44	0.38	0.38	-	-	-
1	0.89	0.78	0.80	2.0	2.0	2.0
2	1.33	1.16	1.20	1.5	1.5	1.5
3	2.00	1.73	1.80	1.5	1.5	1.5
4	3.00	2.60	2.71	1.5	1.5	1.5
5	4.49	3.91	4.07	1.5	1.5	1.5
6	6.73	5.87	6.11	1.5	1.5	1.5
7	10.11	8.80	9.16	1.5	1.5	1.5
8	15.16	13.20	13.73	1.5	1.5	1.5
9	22.73	19.80	20.60	1.5	1.5	1.5
10	34.09	29.71	30.89	1.5	1.5	1.5

SSSE Solver Details

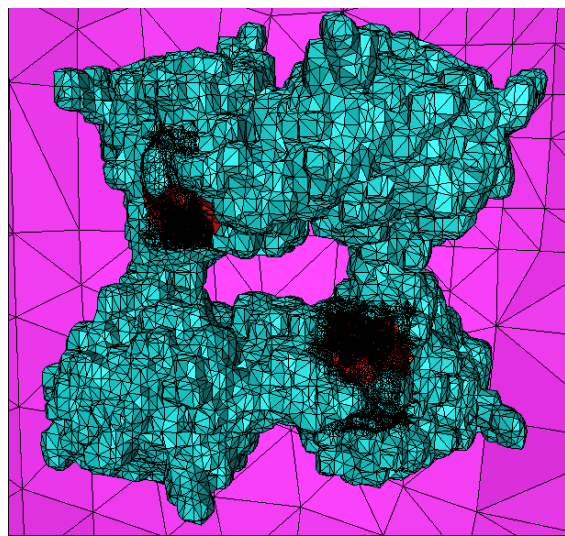
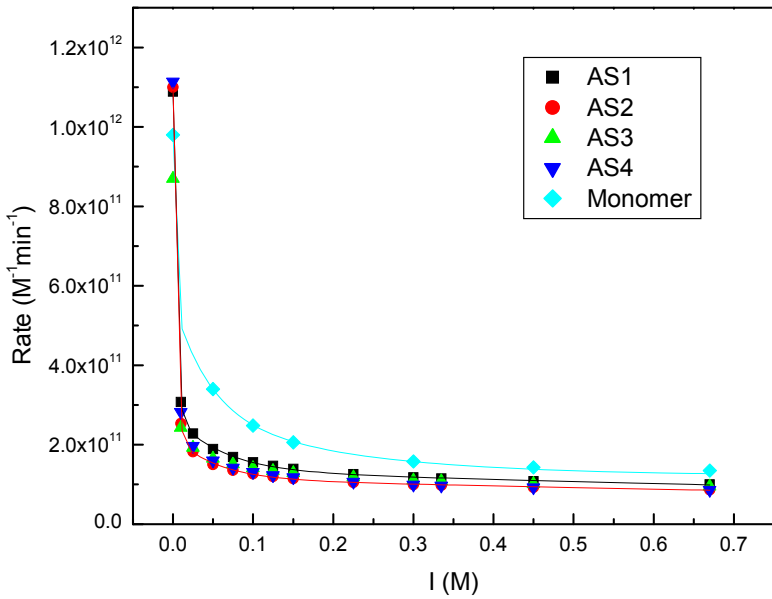
- Smol is developed by Baker's group at WUSTL (<http://agave.wustl.edu/>)
- Based on Mike Holst's Fetk (<http://www.fetk.org>)
- Diffusing particle (based on TFK+): $q = +1e$, $R=2.0 \text{ \AA}$, $D = 78000 \text{ \AA}^2/\mu\text{s}$
- Ionic strengths: 0.00, 0.01, 0.05, 0.10, 0.20, 0.300, 0.450, and 0.670 M.
- Reactive surface is assigned with zero Dirichlet boundary condition (perfectly absorbing)
- $p_{bulk} = 1.0 \text{ M}$



1C2O (compact)



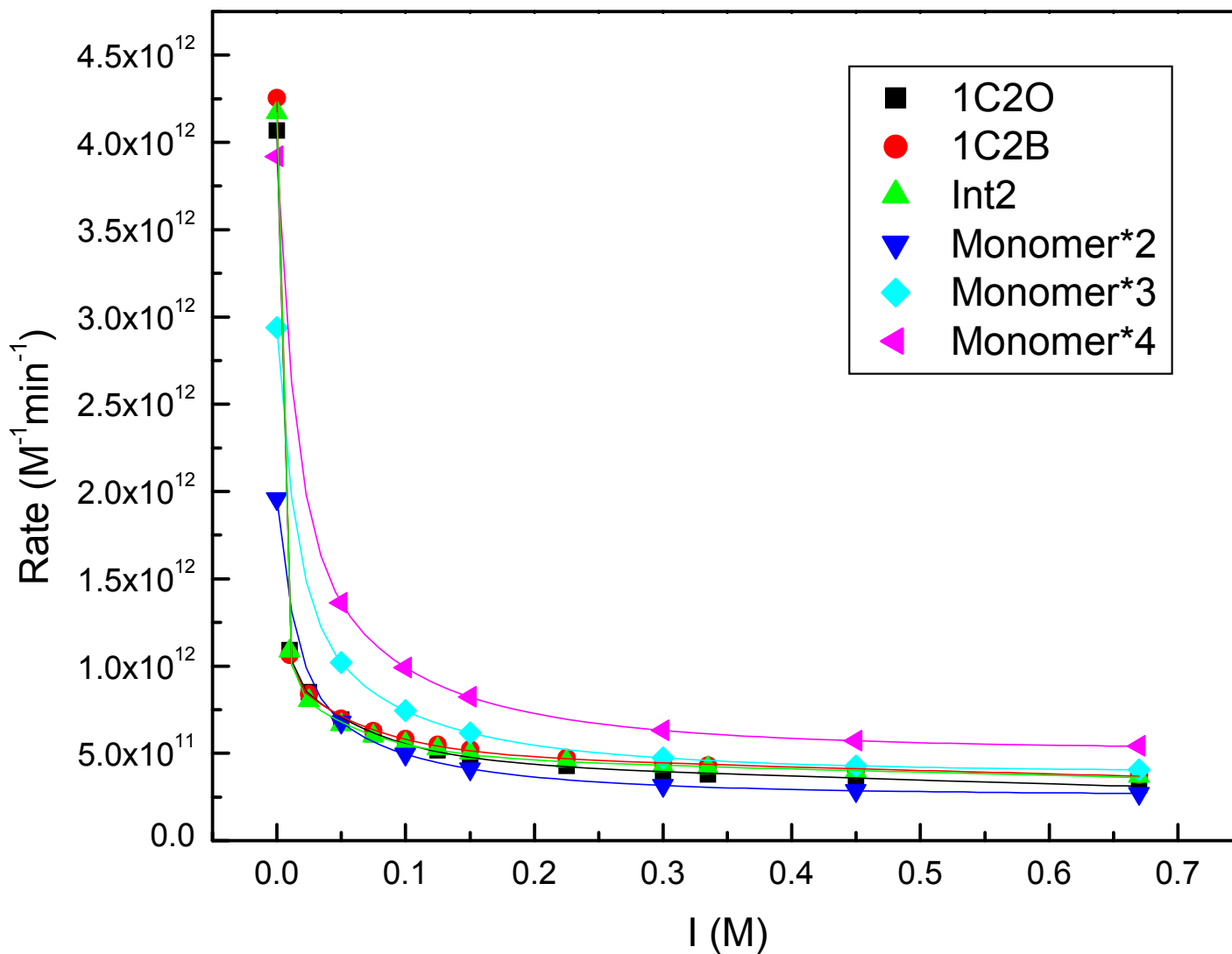
1C2B (loose)



Intermediate b/w

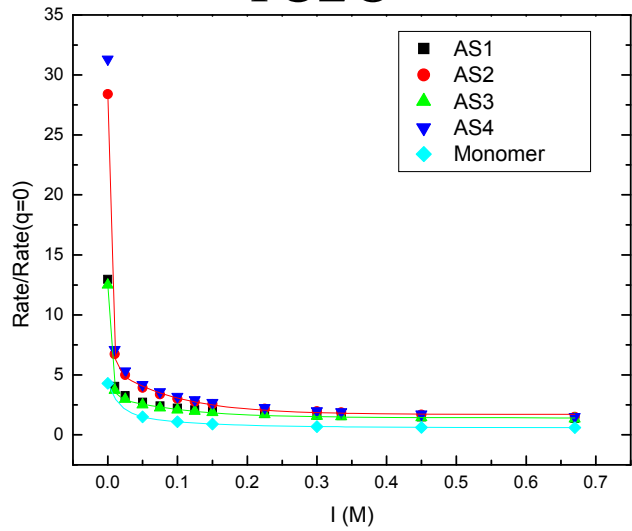
1C2O and 1C2B

All Active Sites

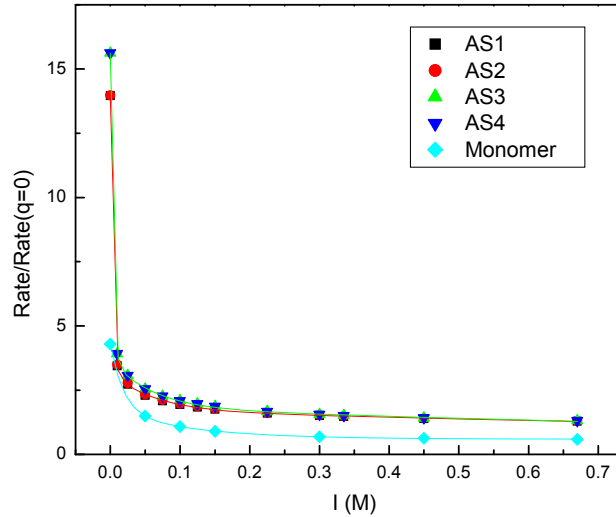


Electrostatic Guidance

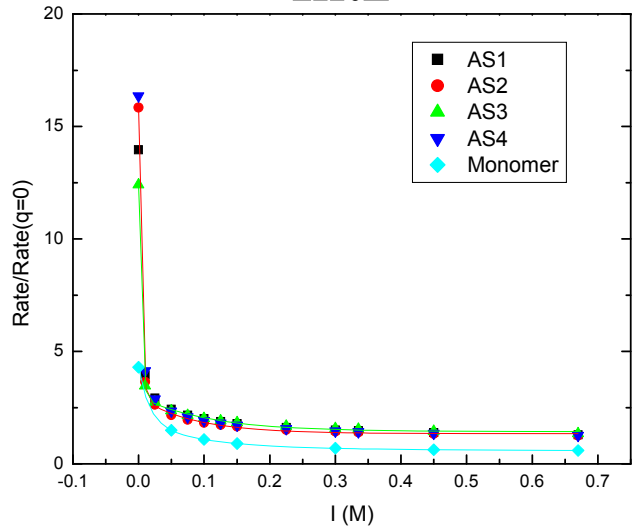
1C2O



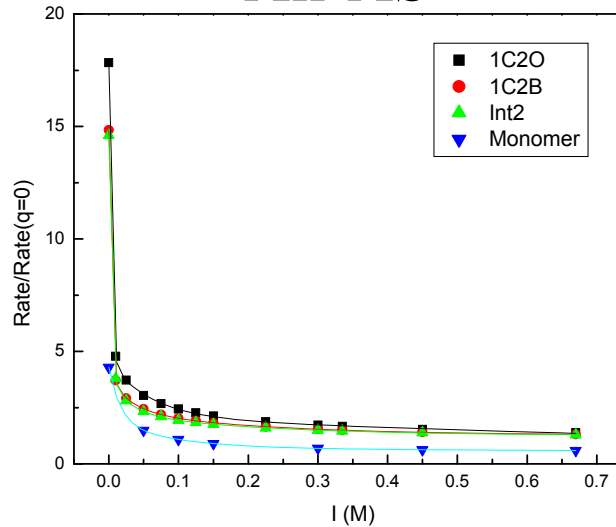
1C2B



Int2



All-AS



Time-dependent Formation

$$\frac{\partial p(\vec{r}, t \mid \vec{r}_0, t_0)}{\partial t} = \nabla \cdot D e^{-\beta U(\vec{r})} \nabla e^{\beta U(\vec{r})} p(\vec{r}, t \mid \vec{r}_0, t_0)$$

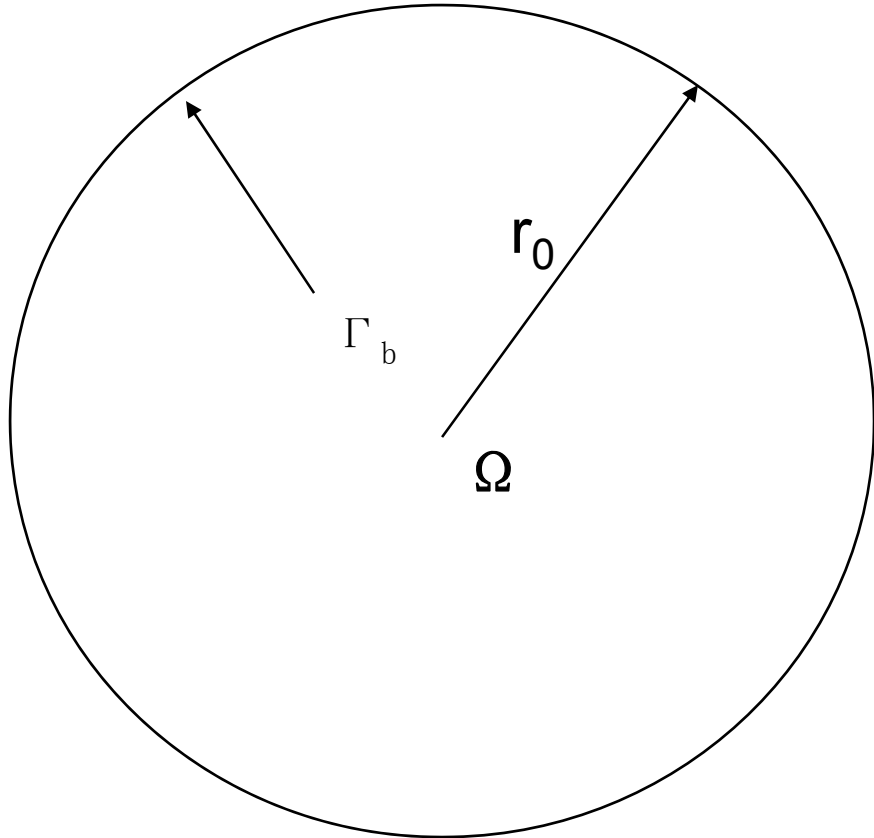
$$D'(\vec{r}) = D e^{-\beta U(\vec{r})} \quad p'(\vec{r}, t) = e^{\beta U(\vec{r})} p(\vec{r}, t \mid \vec{r}_0, t_0)$$

$$\frac{\partial p(\vec{r}, t \mid \vec{r}_0, t_0)}{\partial t} = \nabla \cdot D'(\vec{r}) \nabla p'(\vec{r}, t)$$

$$-\nabla \cdot D'(\vec{r}) \nabla p'(\vec{r}, t) + e^{-\beta U(\vec{r})} \frac{\partial p'(\vec{r}, t)}{\partial t} = 0 \quad \xrightarrow{\text{symmetric}}$$

$$\xrightarrow{\text{symmetric}} p(\vec{r}, t \mid \vec{r}_0, t_0) = e^{-\beta U(\vec{r})} p'(\vec{r}, t)$$

Analytical test



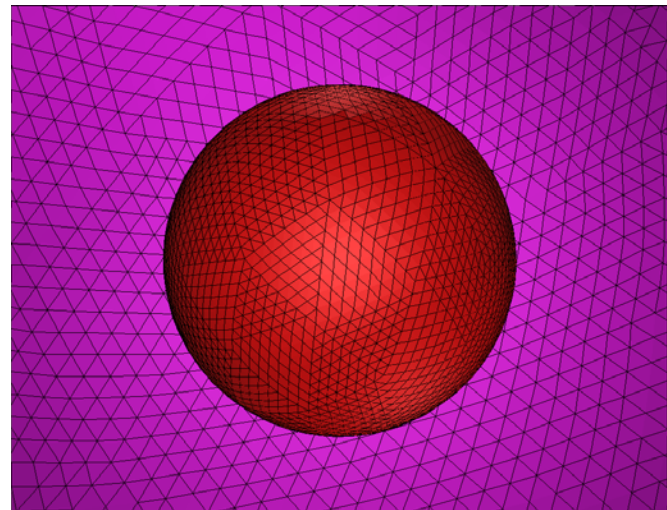
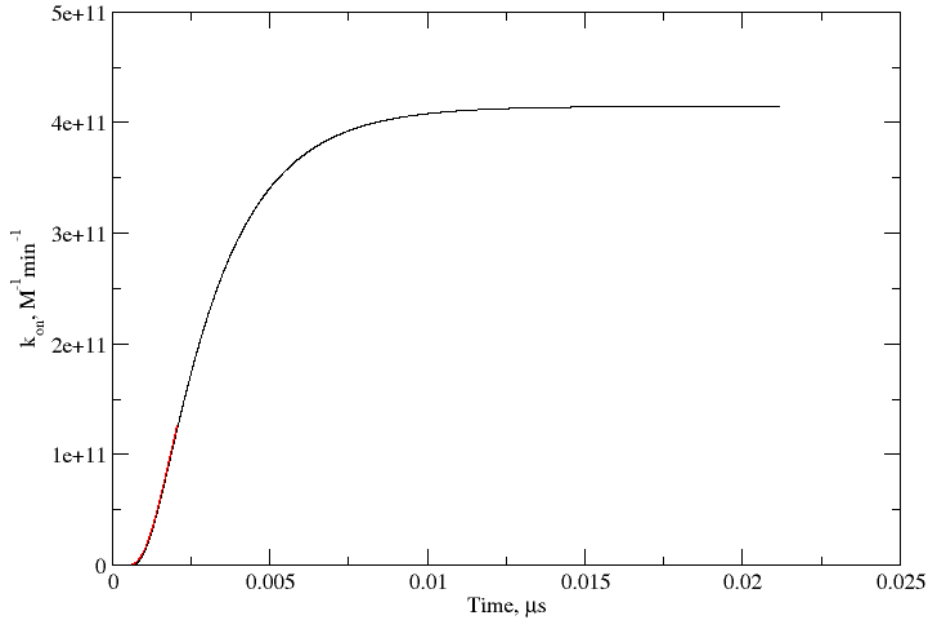
When the potential inside the sphere and the radius of the inner sphere are zero, the analytical solution can be easily written as below:

$$\left\{ \begin{array}{l} \frac{\partial p(r;t)}{\partial t} - D\Delta_3 p(r;t) = 0 \\ p(r;0) = 0 \\ p(r_0;t) = p_{bulk} \end{array} \right.$$

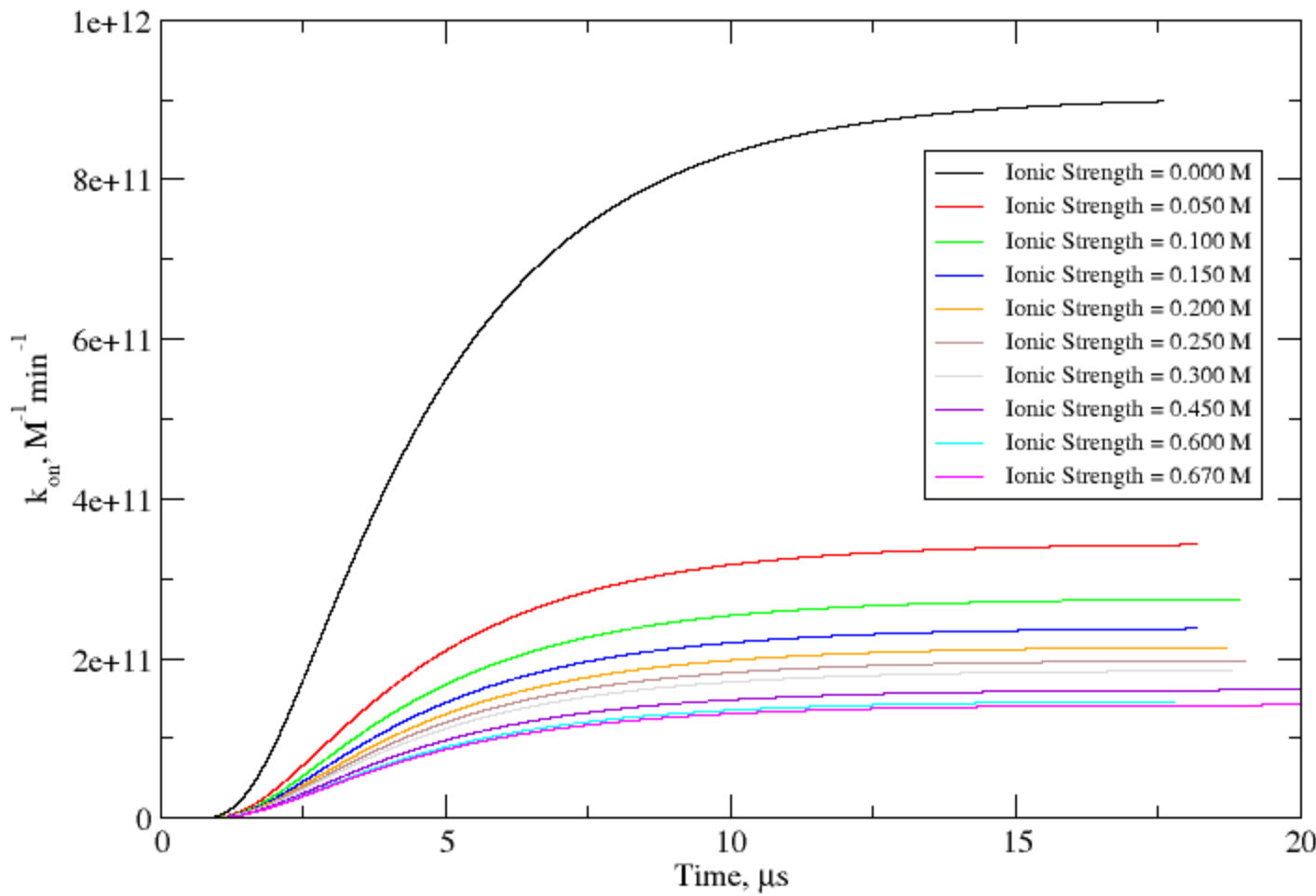
$$p(r;t) = p_{bulk} + \frac{2p_{bulk}r_0}{\pi r} \sum_{n=1}^{\infty} \frac{(-1)^n}{n} \sin \frac{n\pi r}{r_0} \exp \left\{ -D \left(\frac{n\pi}{r_0} \right)^2 t \right\}$$

Analytical test

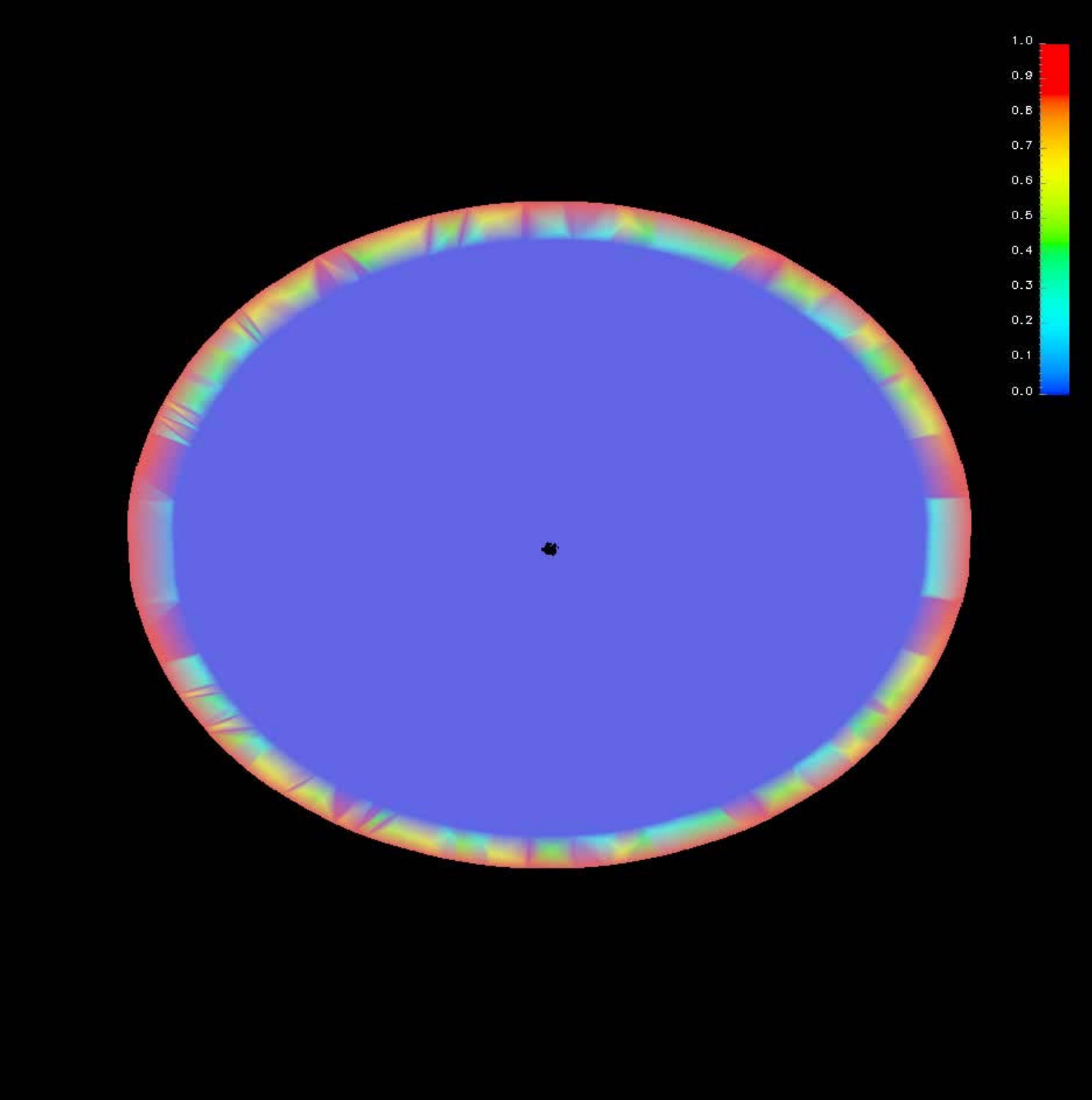
- Vertex number: 109,478
- Simplex number: 629,760
- Vertex number: 857,610
- Simplex number: 5,038,080
- Inner radius: 10 Å
- Outer radius: 50 Å
- Time step: 5 ps

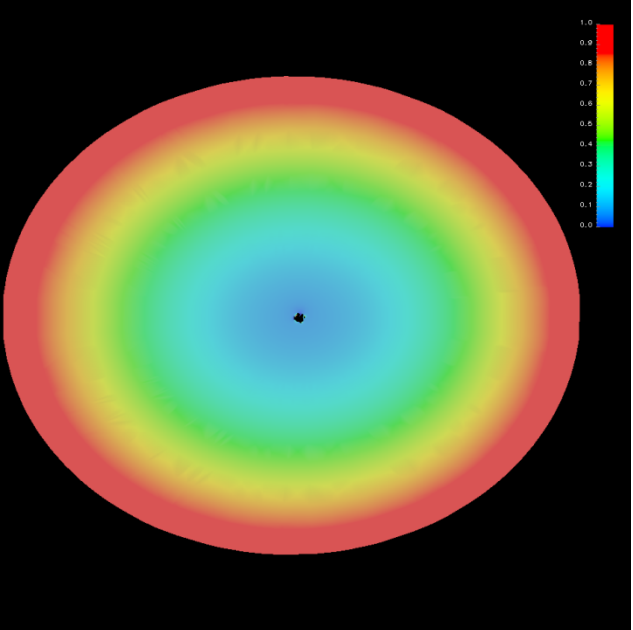


TDSE Results vs. SSSE Results

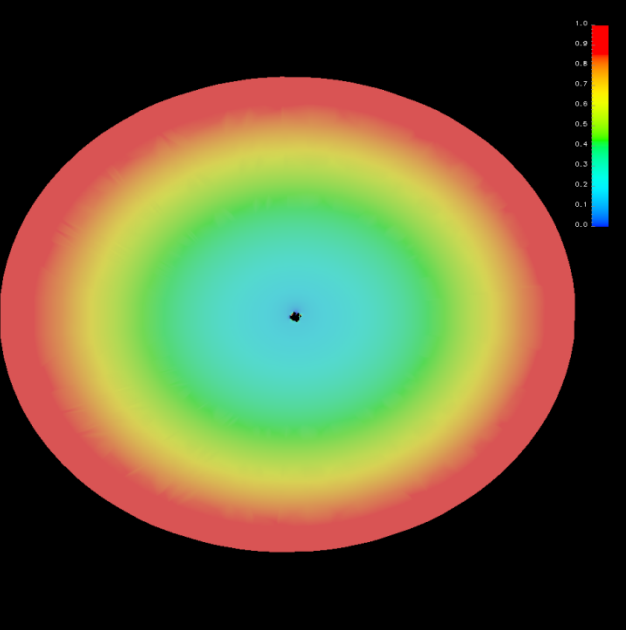


ionic strength (M)	0.000	0.025	0.100	0.300	0.600
SSSE results $k_{on}(10^{11} M^{-1} \text{min}^{-1})$	9.562	3.681	2.304	1.572	1.302
TDSE final results $k_{on}(10^{11} M^{-1} \text{min}^{-1})$	9.535	3.673	2.298	1.569	1.298

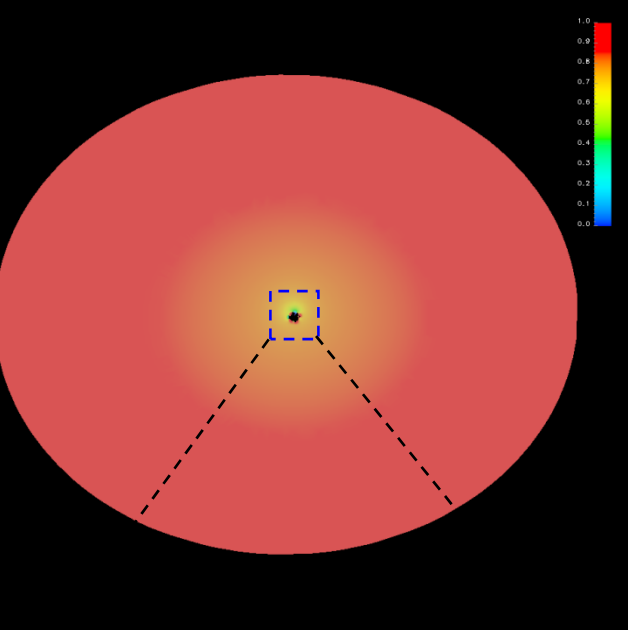




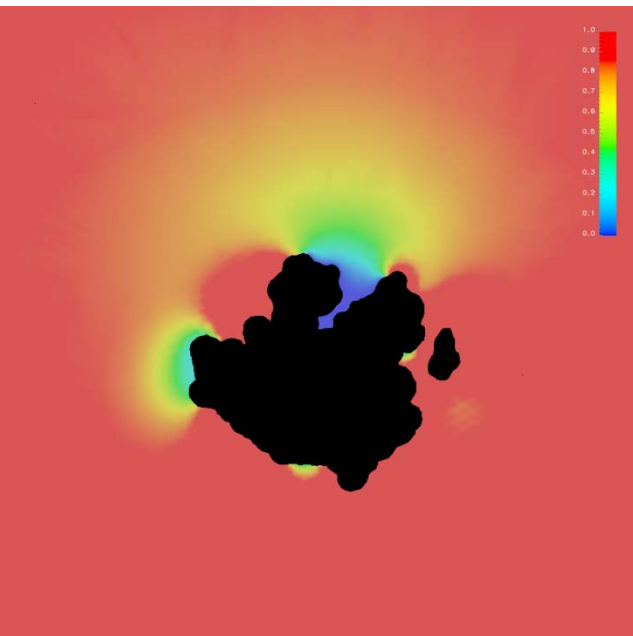
$t = 0.05 \mu\text{s}$



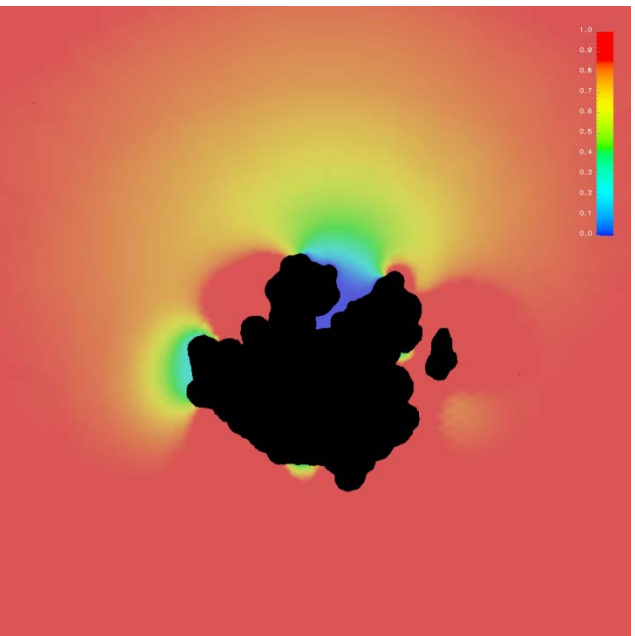
$t = 0.50 \mu\text{s}$



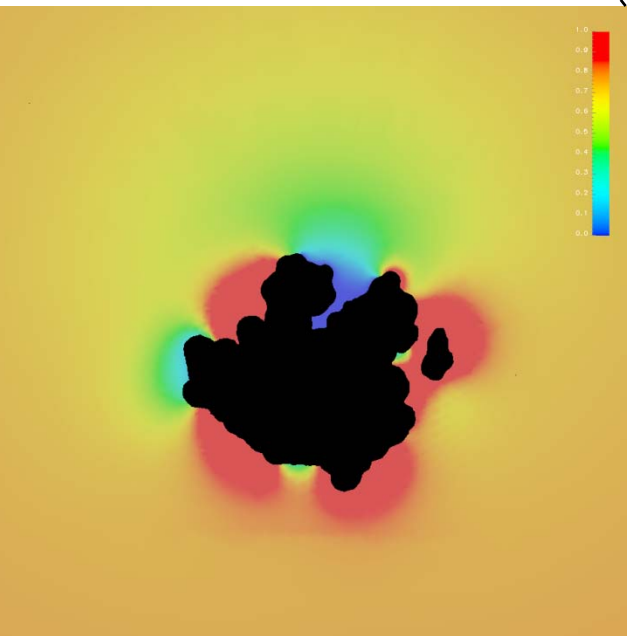
$t = 5.00 \mu\text{s} (\text{global})$



$t = 15.00 \mu\text{s}$

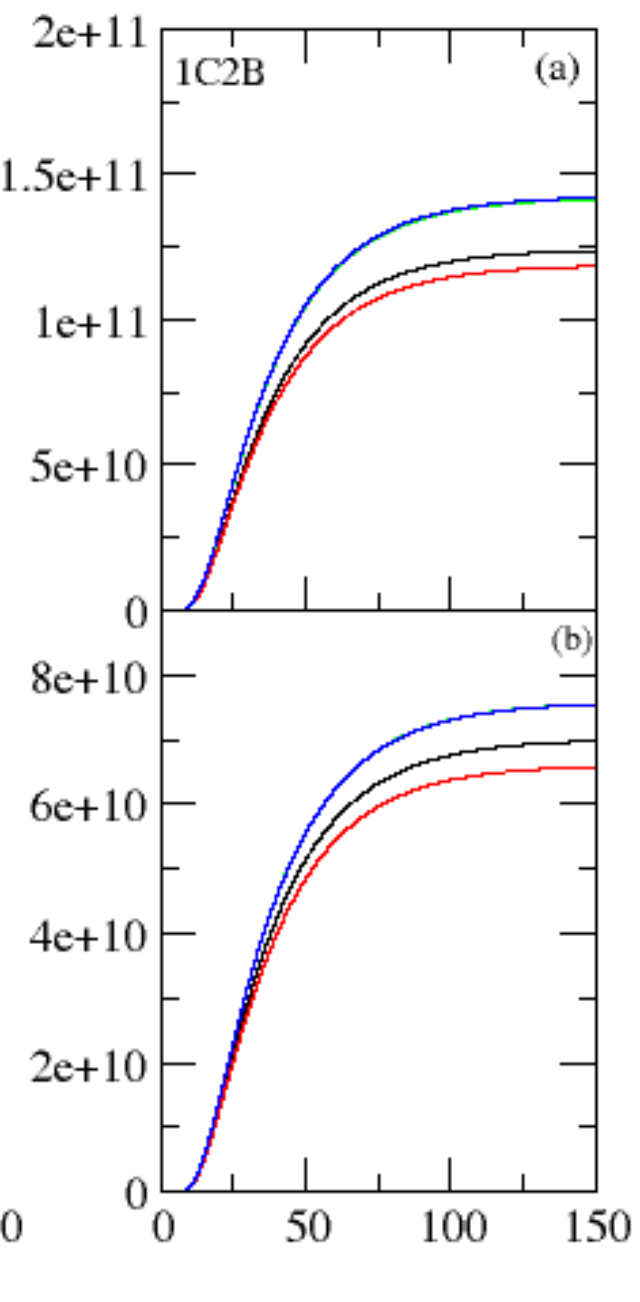
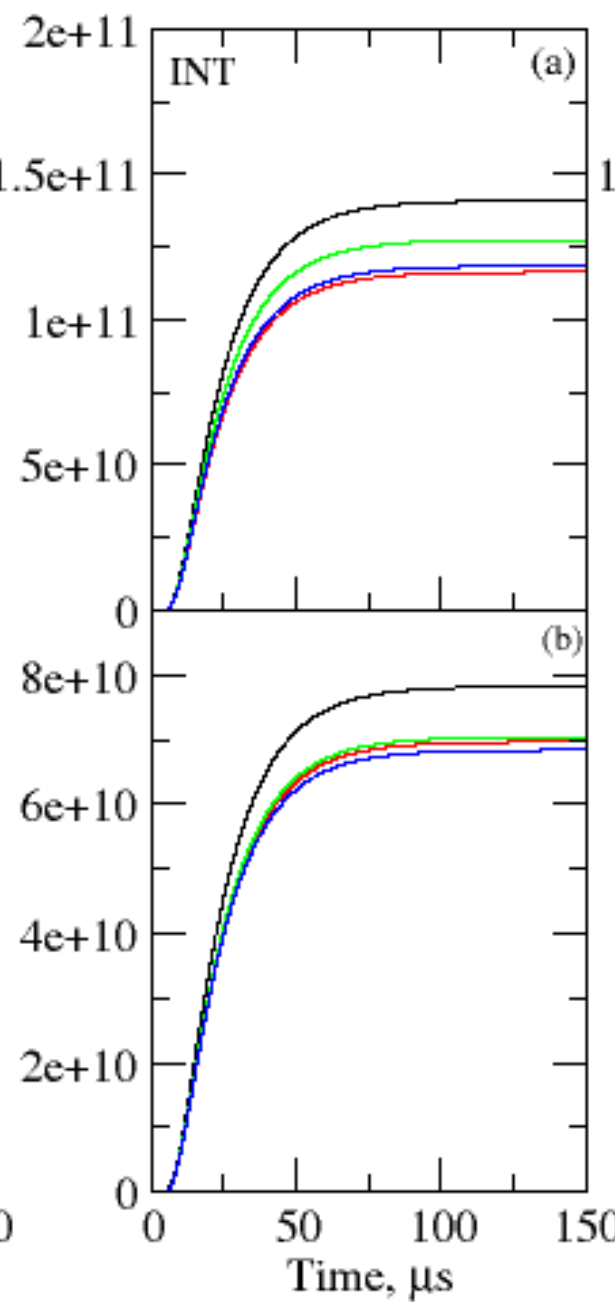
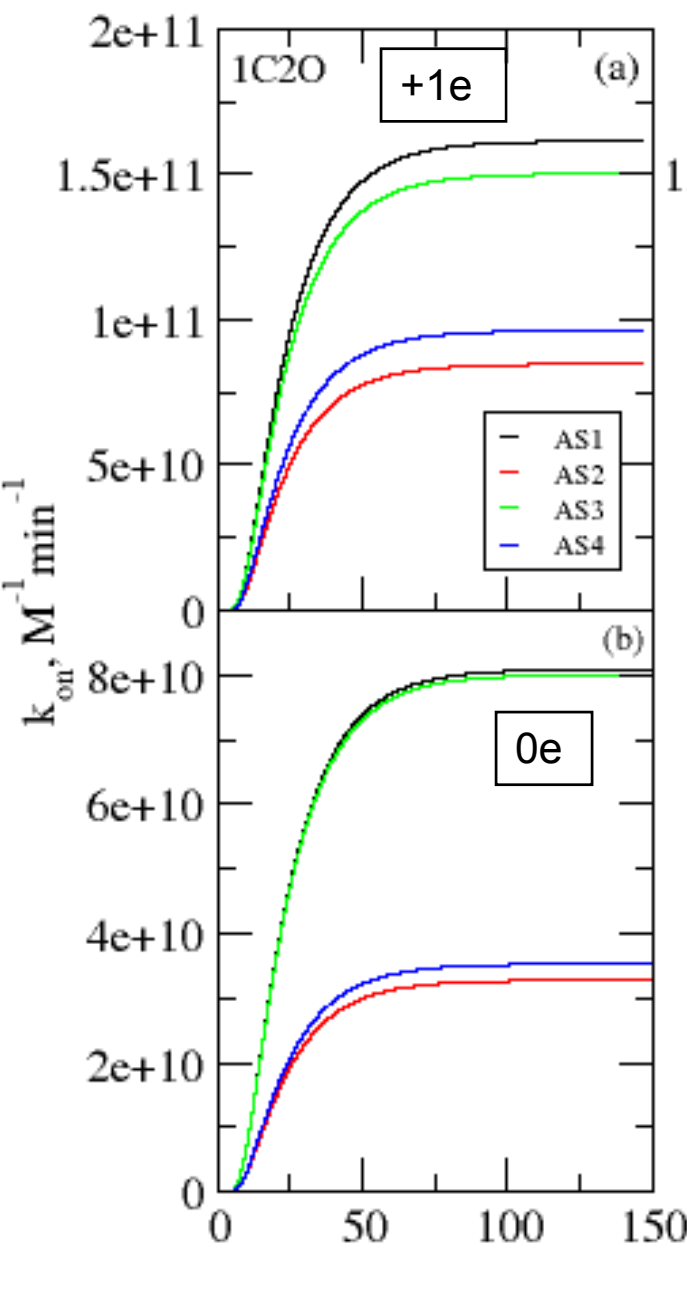


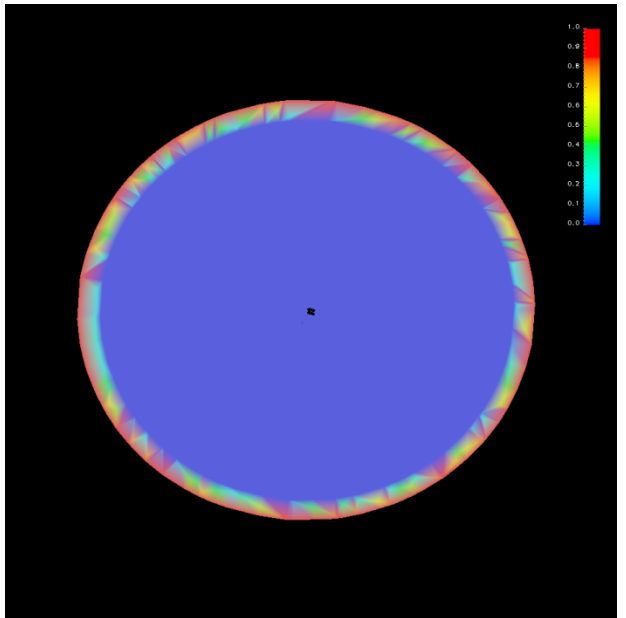
$t = 10.00 \mu\text{s}$



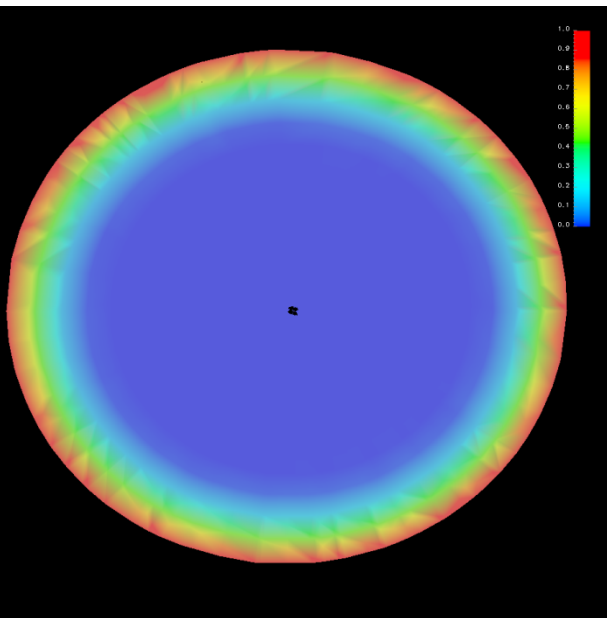
$t = 5.00 \mu\text{s} (\text{close})$

TDSE Results

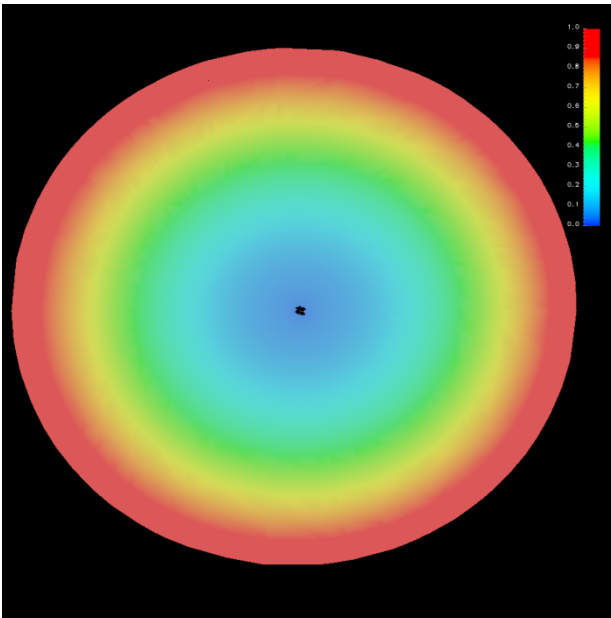




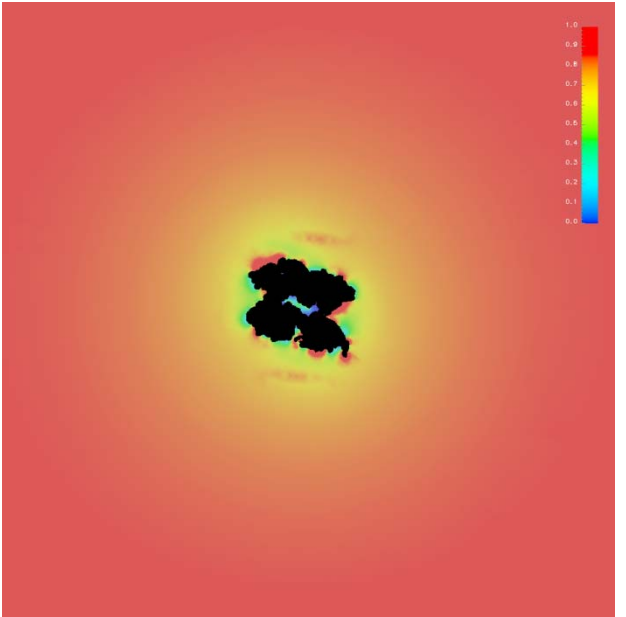
$t = 0.000 \mu\text{s}$



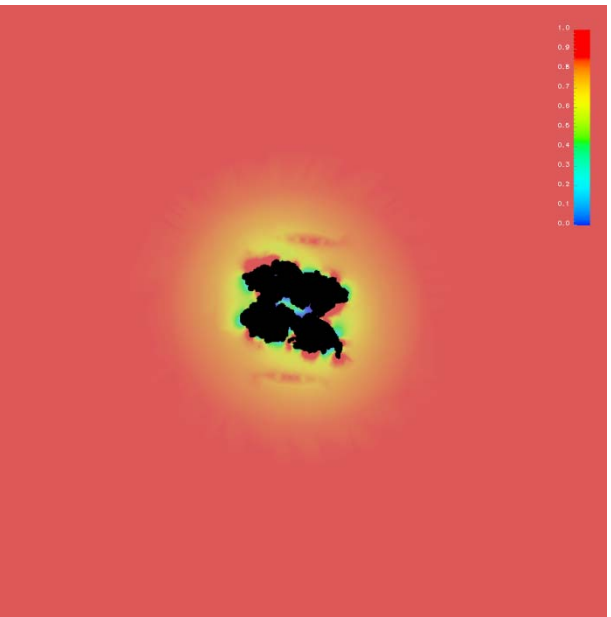
$t = 1.000 \mu\text{s}$



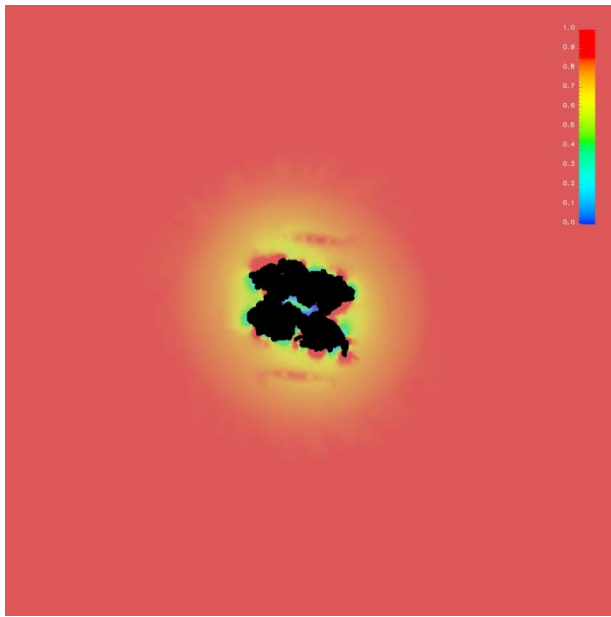
$t = 10.00 \mu\text{s}$



$t = 50.00 \mu\text{s}$



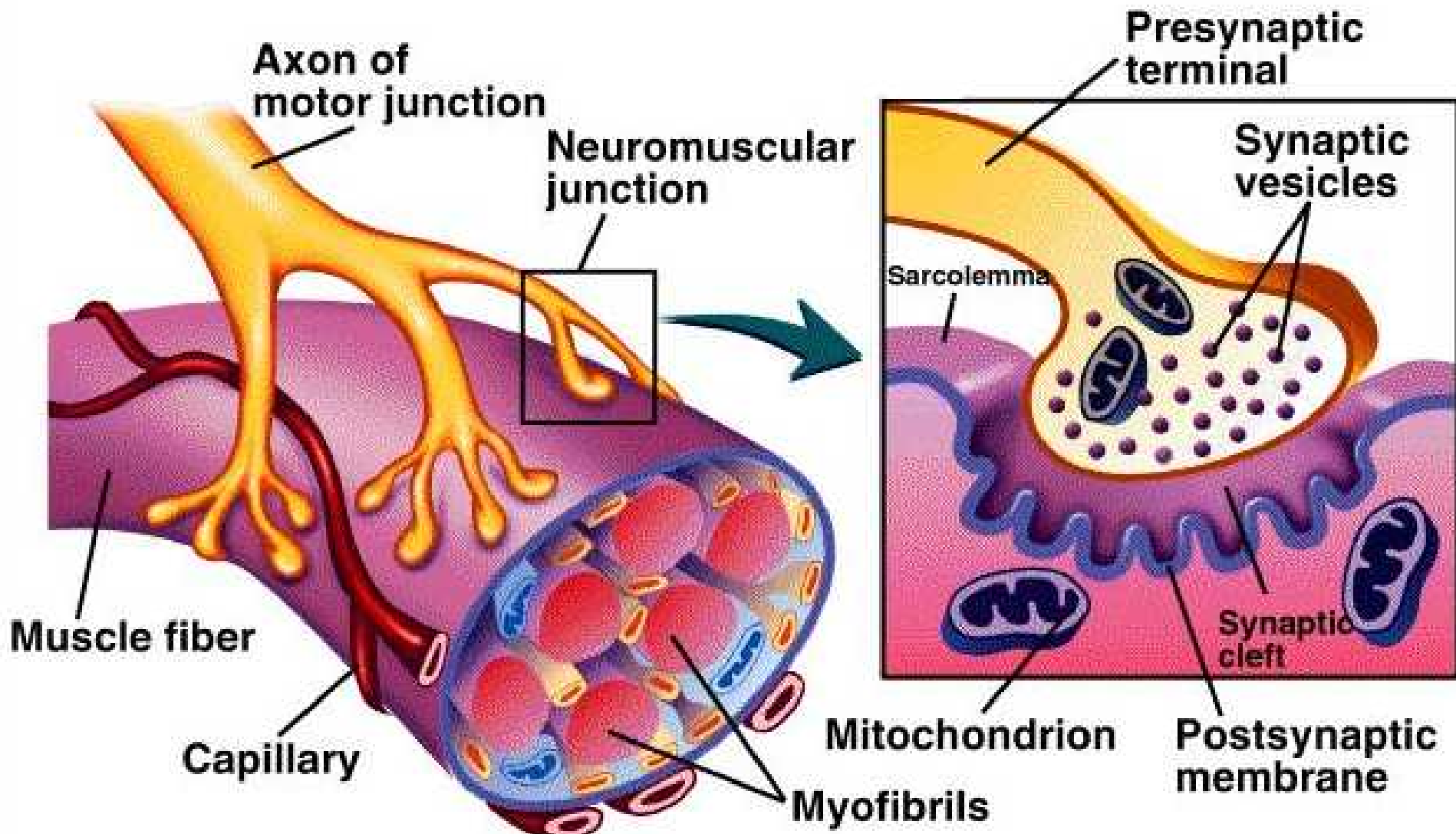
$t = 100.0 \mu\text{s}$



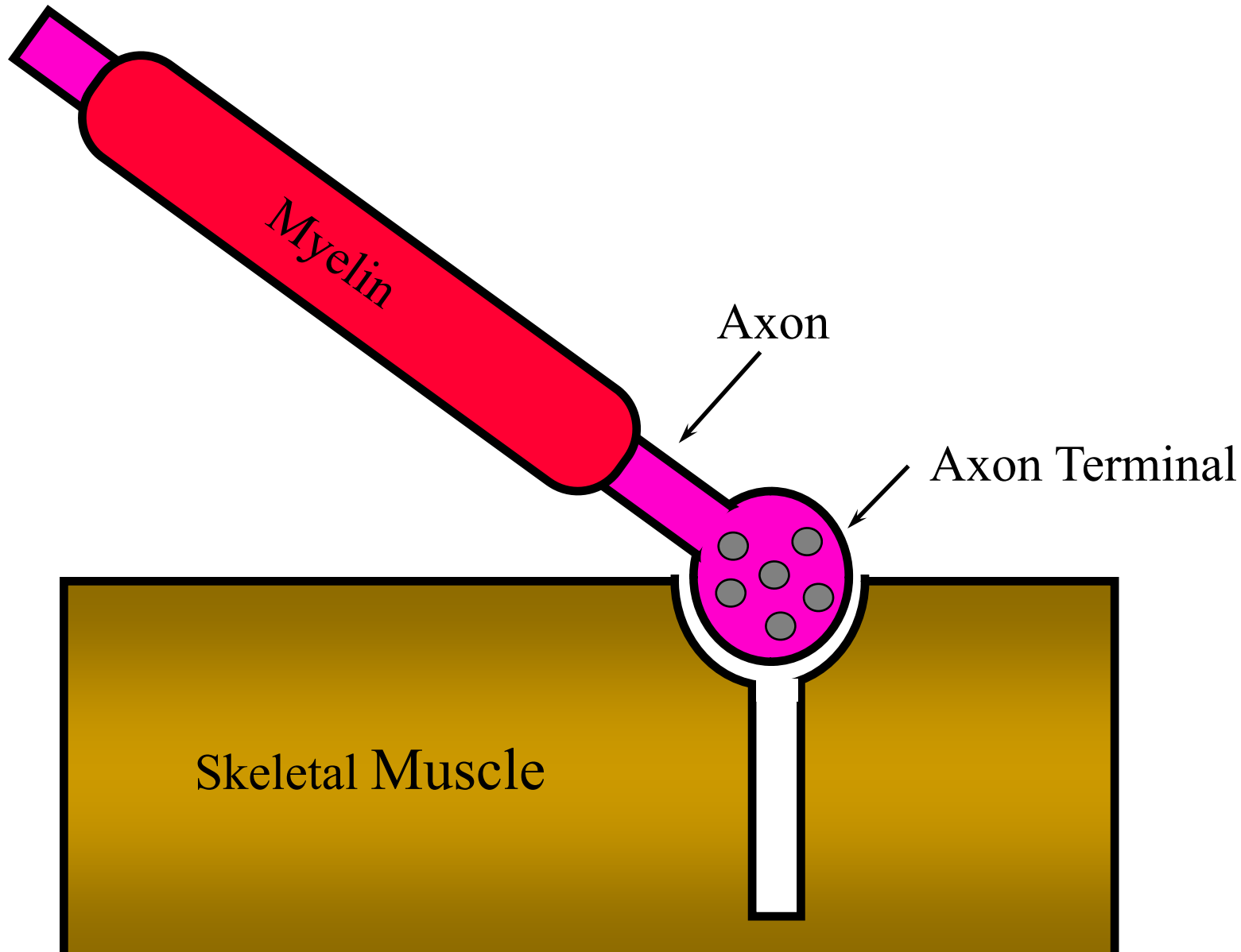
$t = 150.0 \mu\text{s}$

Cellular level diffusion modeling

Neuromuscular Junction

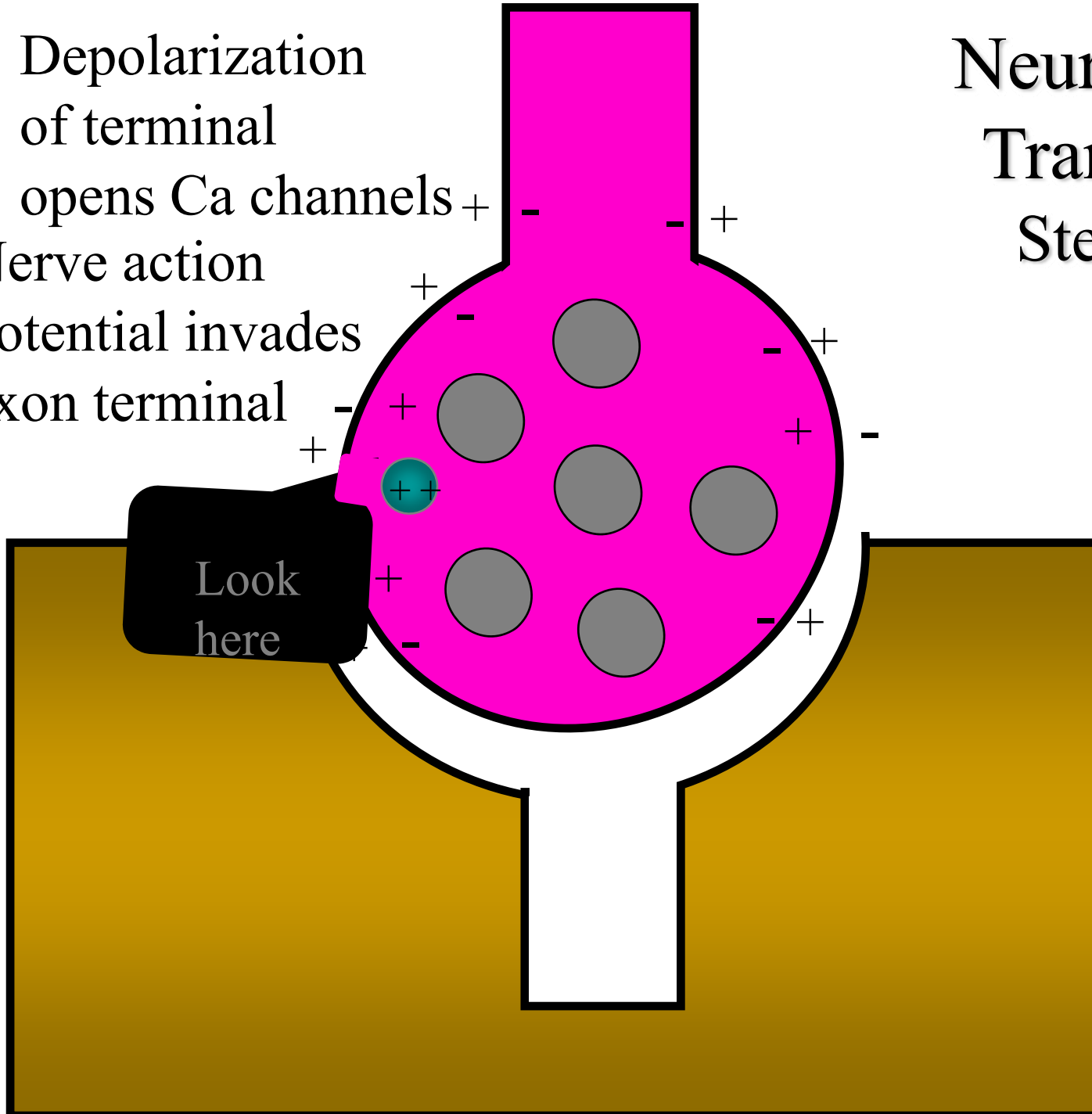


Neuromuscular Transmission

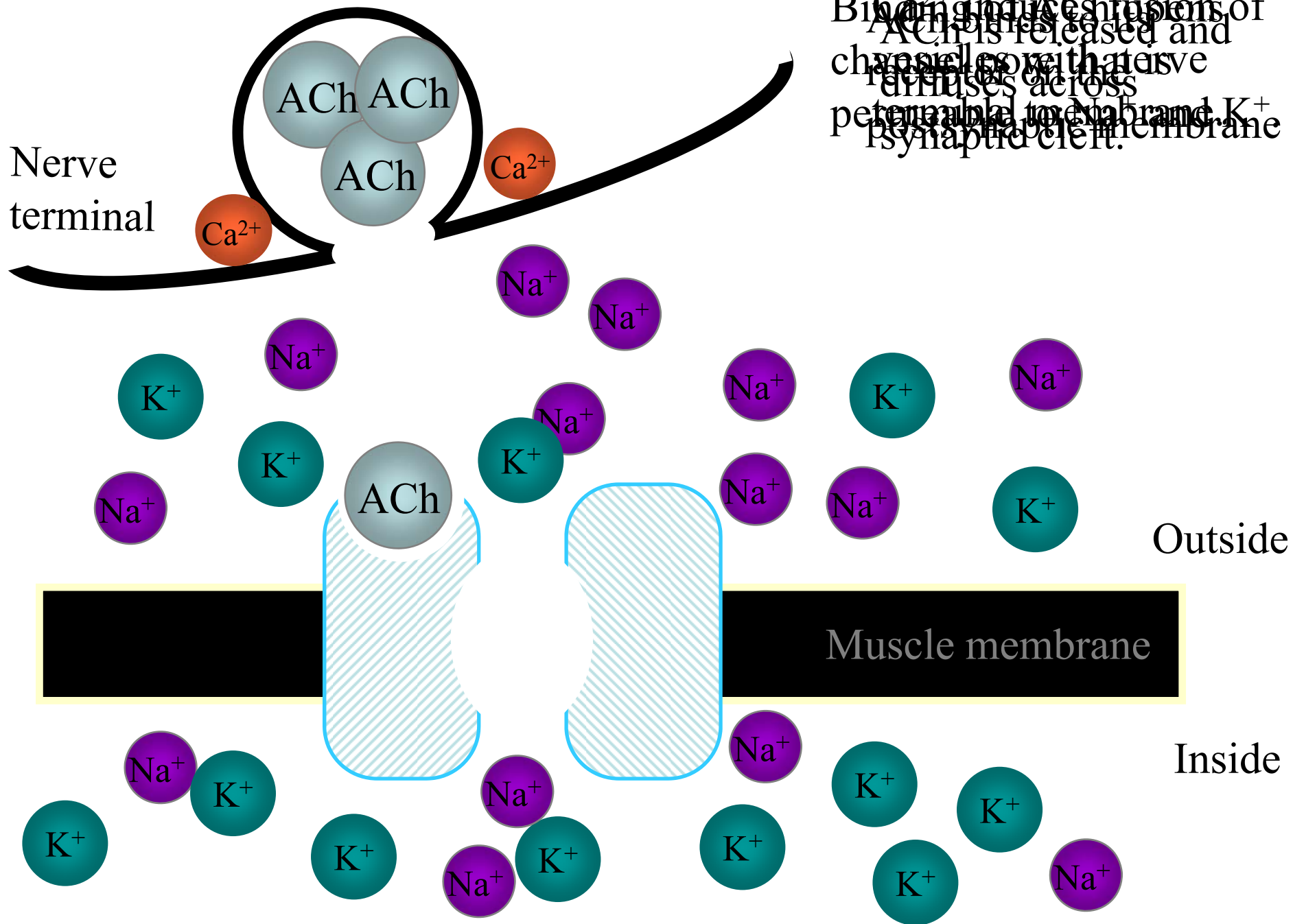


Neuromuscular Transmission: Step by Step

Depolarization
of terminal
opens Ca channels
Nerve action
potential invades
axon terminal



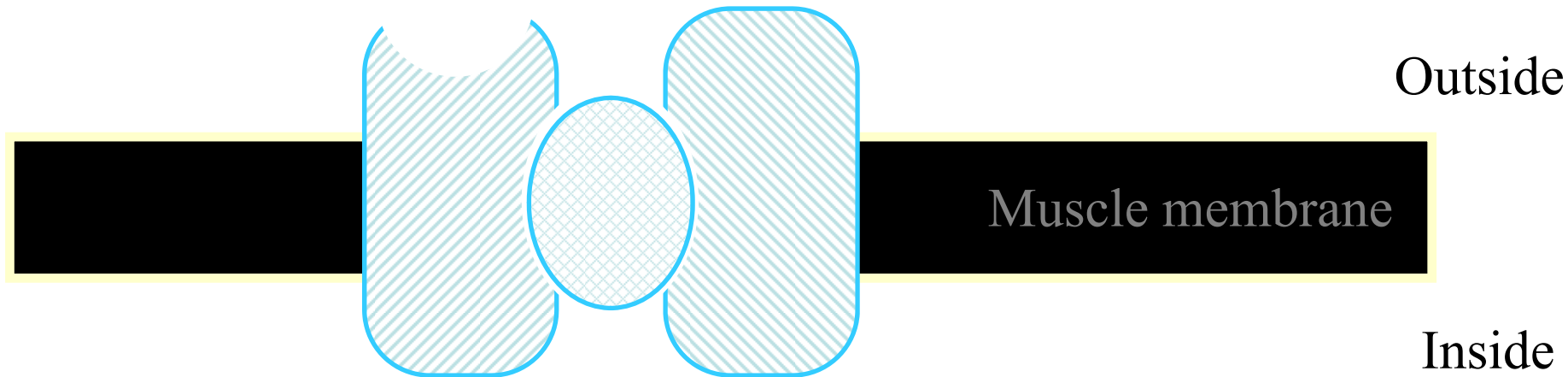
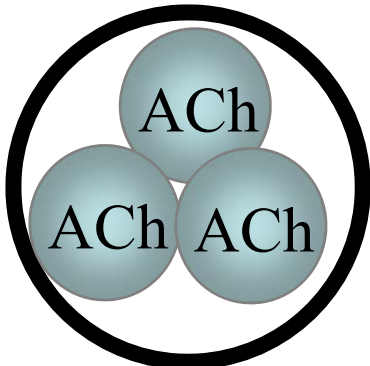
BiCa^{2+} induces fusion of ACh vesicles released and channels open with active diffusion across permeable to Na^+ and K^+ synaptid cleft.



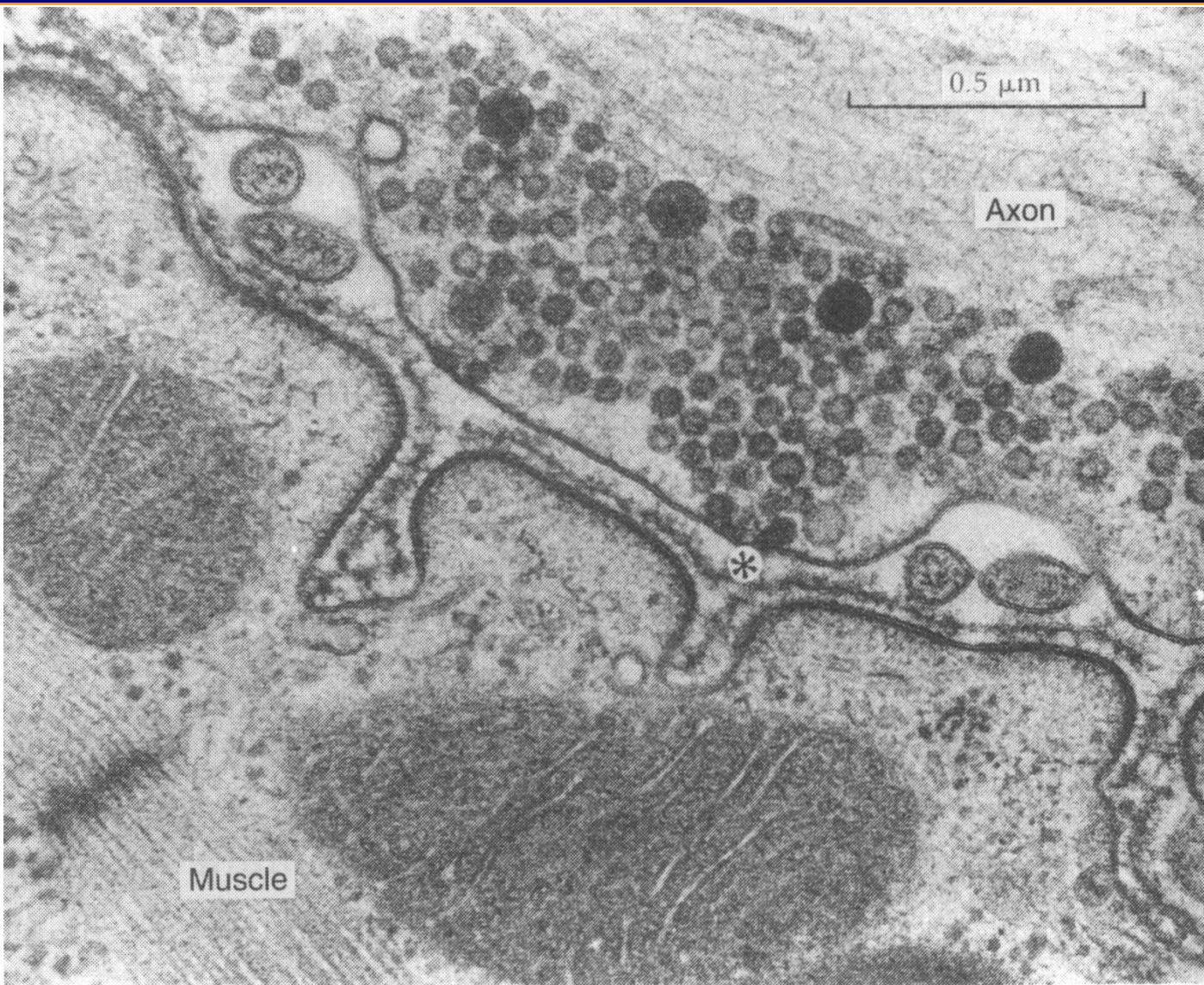
Meanwhile ...

ACh is quickly fixed by
Choline synthetase
ACh is taken up
into AChE and rehacked
into nerve terminal
into vesicle

Nerve terminal

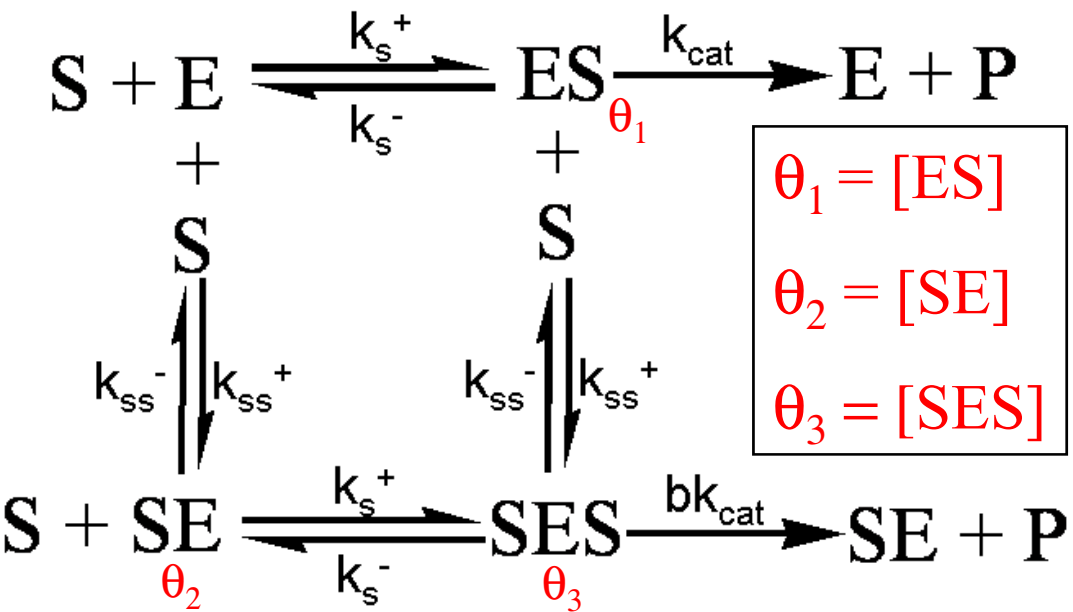
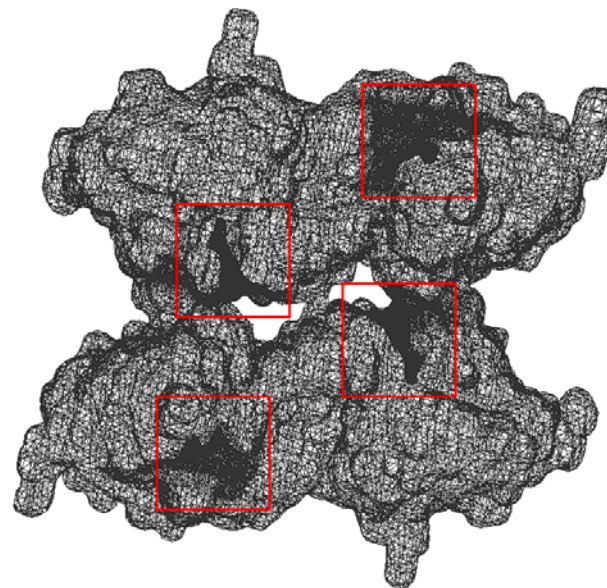
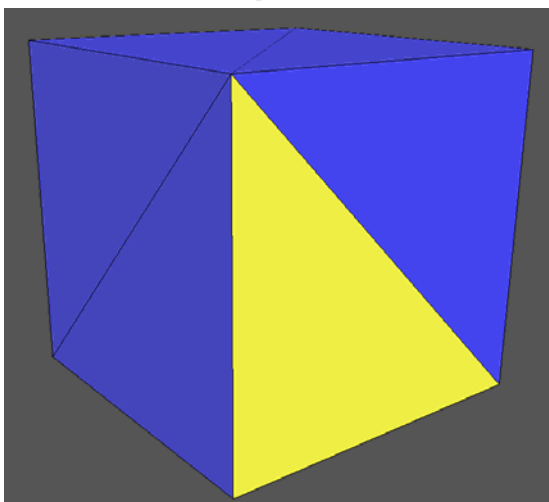
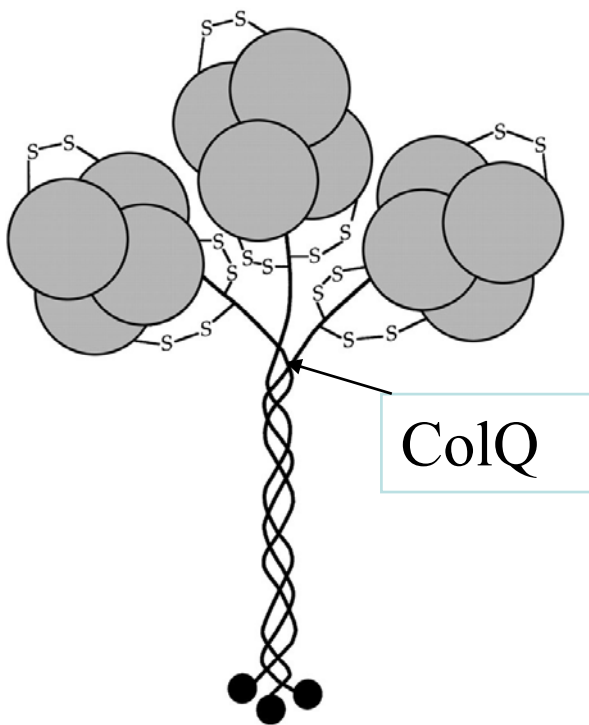


Structural Reality

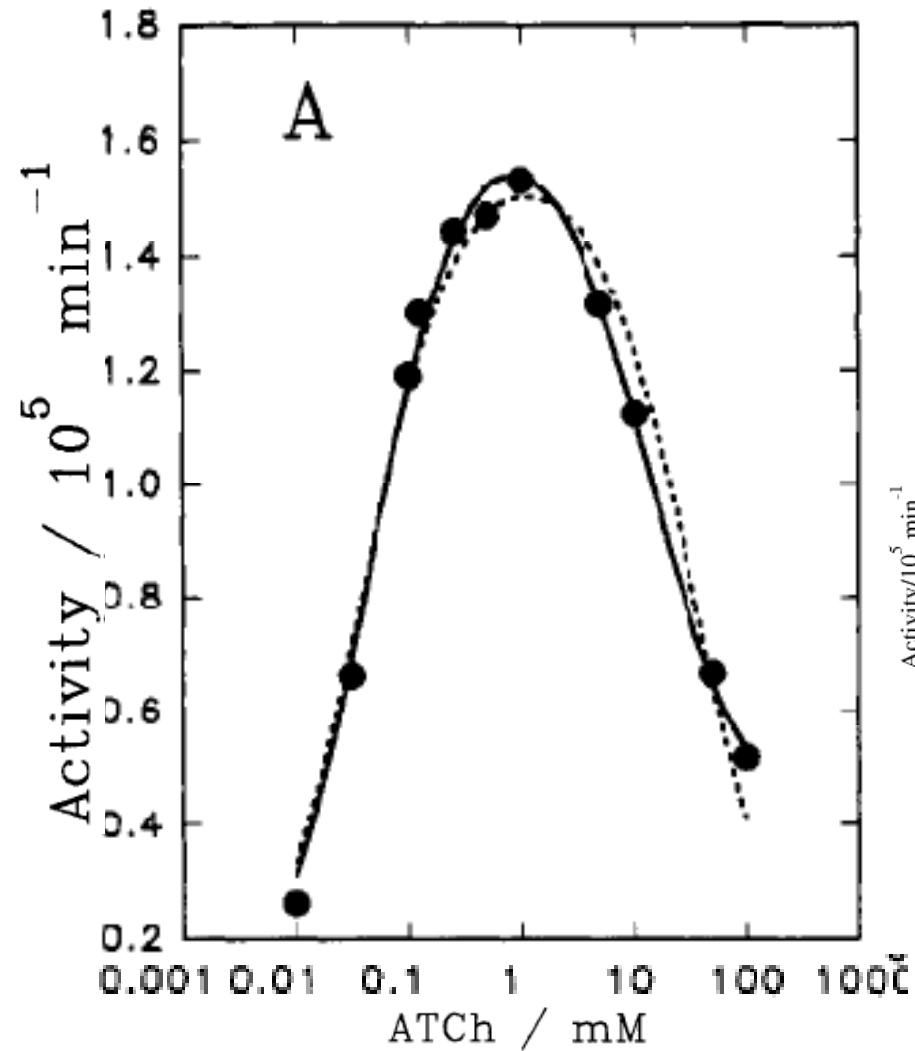


By John Heuser and Louise Evans
University of California, San Francisco

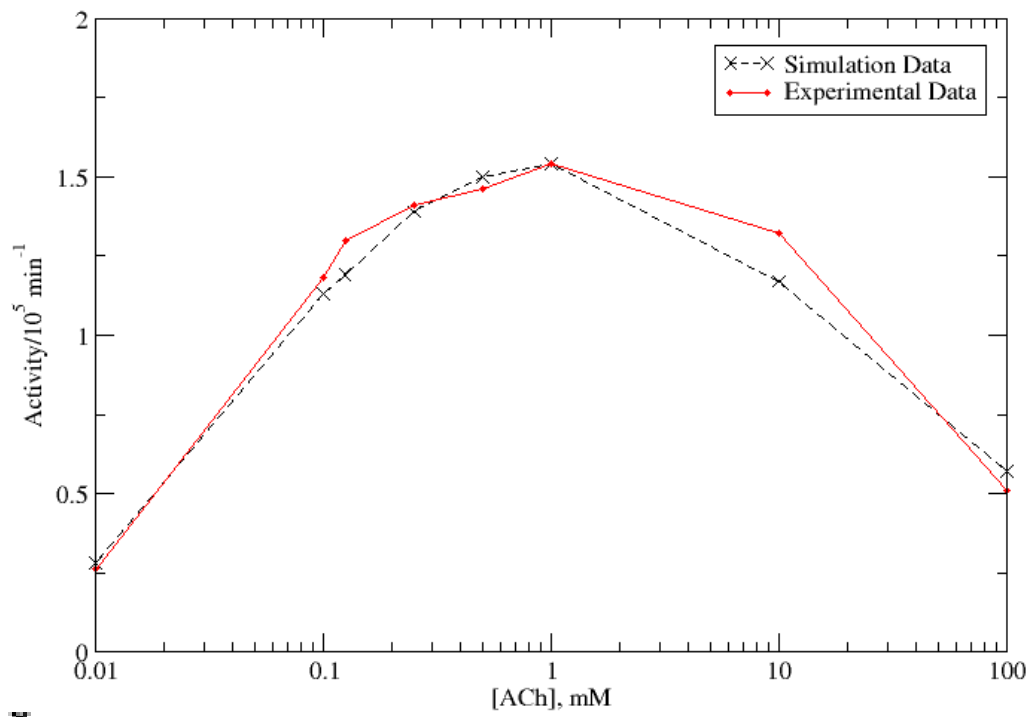
AChE Reaction Mechanism



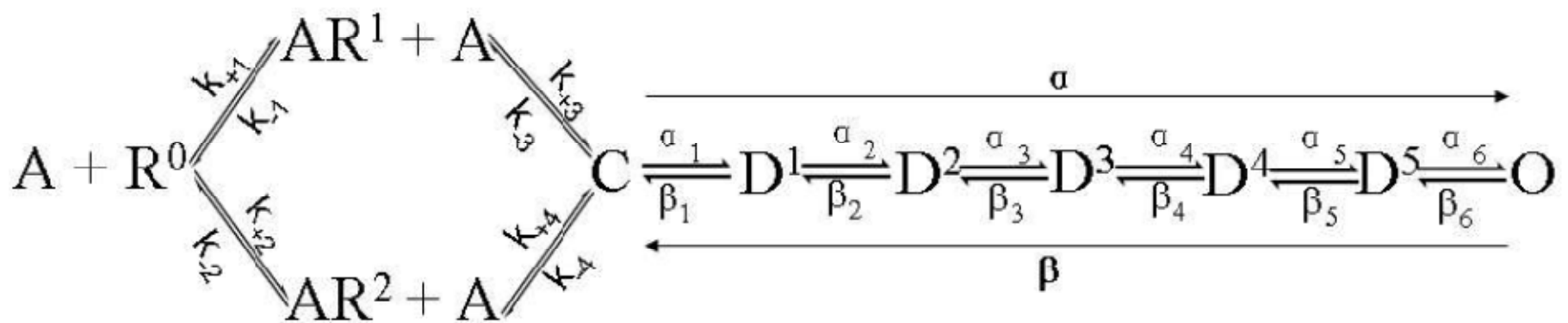
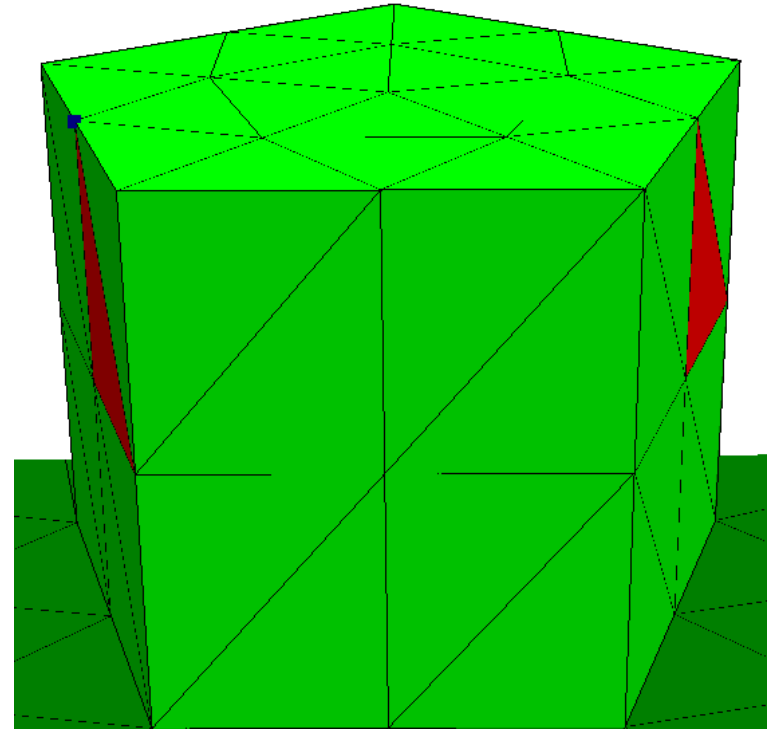
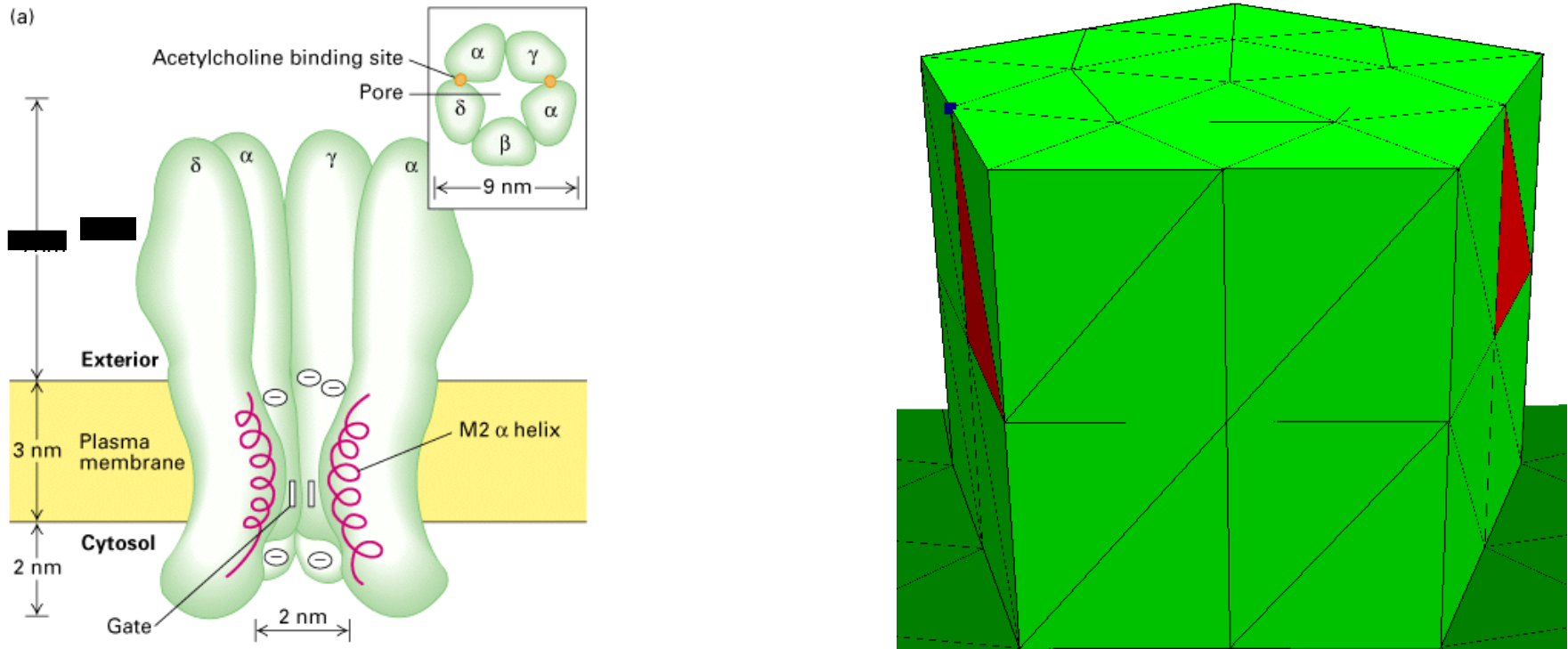
AChE Activity



$$v(i) = [AChE]_0 k_{cat} (\theta_1 + b\theta_3)$$



nAChR Reaction Model



nAChR Conformational Statistics

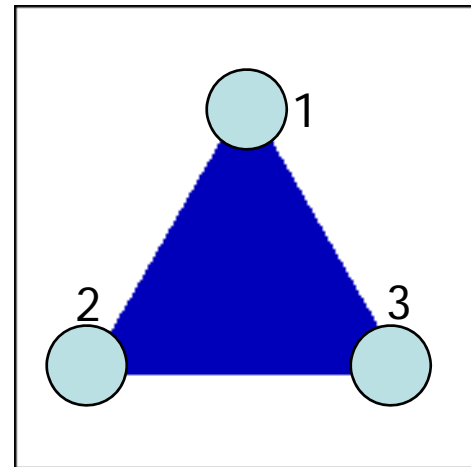
$$I(t) = \int_{\partial\Omega_{nAChR}^{act}} \frac{N_{nAChR}}{S_{\partial\Omega_{nAChR}^{act}}} (k_{bind}^+ p_{nAChR}(r, t | r_0, t_0) - k_{bind}^-) dS$$

$$N(t') = \int_0^{t'} I(t) dt$$

$N(t') \geq 2$, Diliganded

$1 \leq N(t') < 2$, Monoliganded

$0 \leq N(t') < 1$, Unliganded



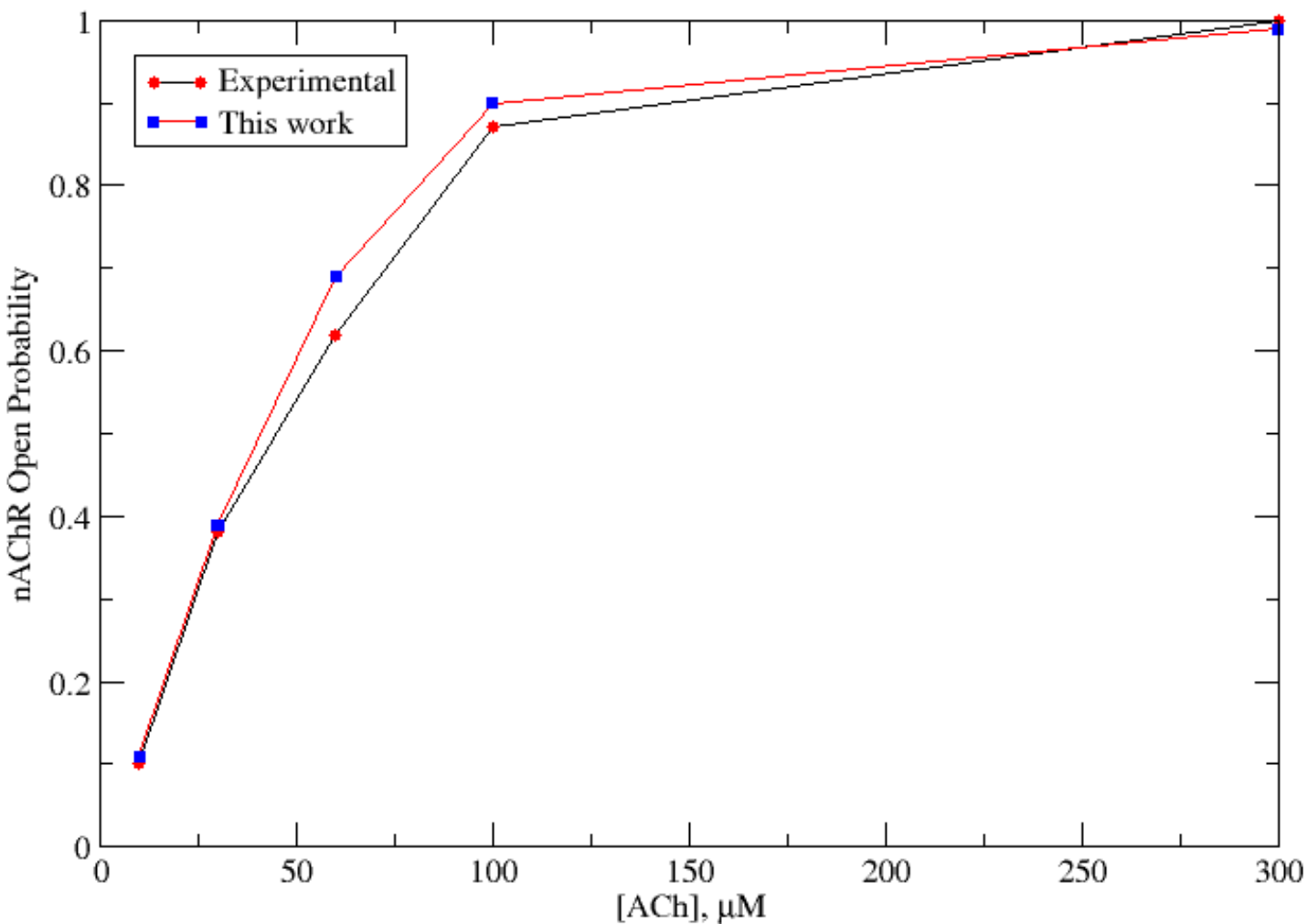
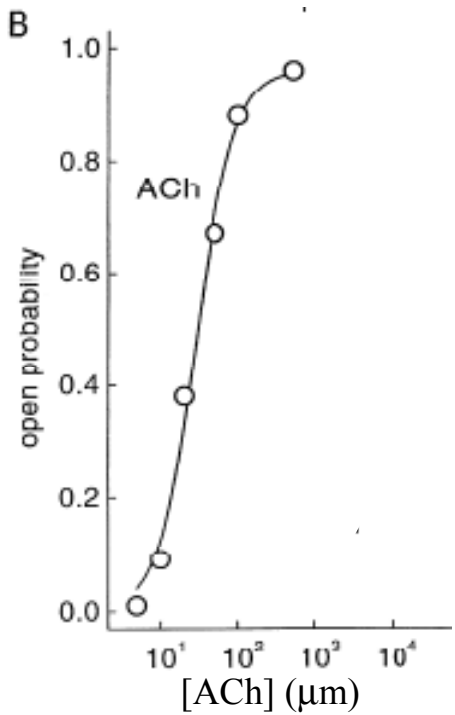
$$p(O)^I = \frac{\int_{\partial\Omega_{nAChR}^I} \phi_8 dS}{\int_{\partial\Omega_{nAChR}^I} 1 dS}$$

$$p(O)^H = \frac{\int_{\partial\Omega_{nAChR}^H} \phi_8 dS}{\int_{\partial\Omega_{nAChR}^H} 1 dS}$$

$$p(O) = \frac{p(O)^I + p(O)^H}{2}$$

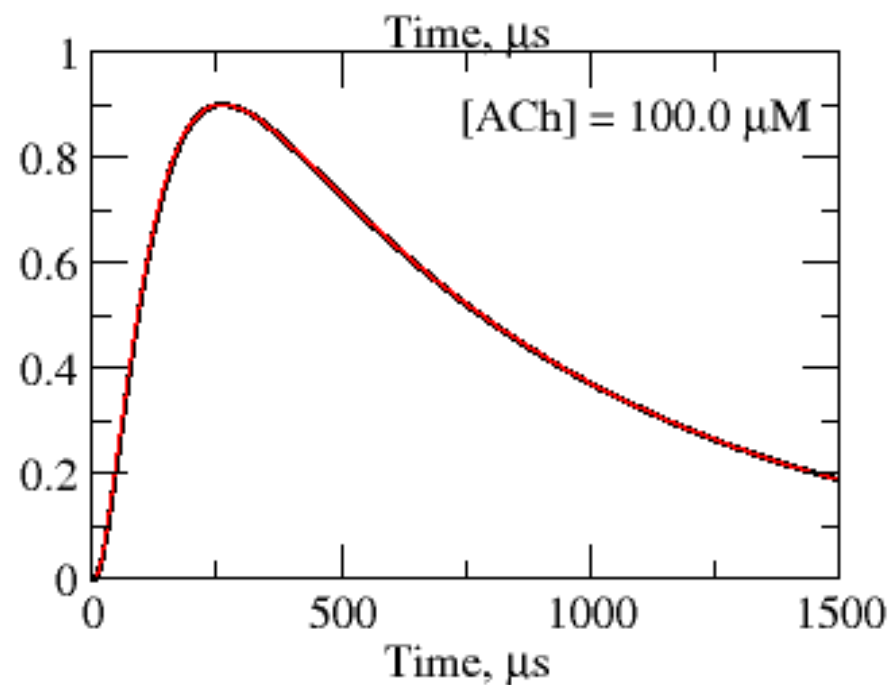
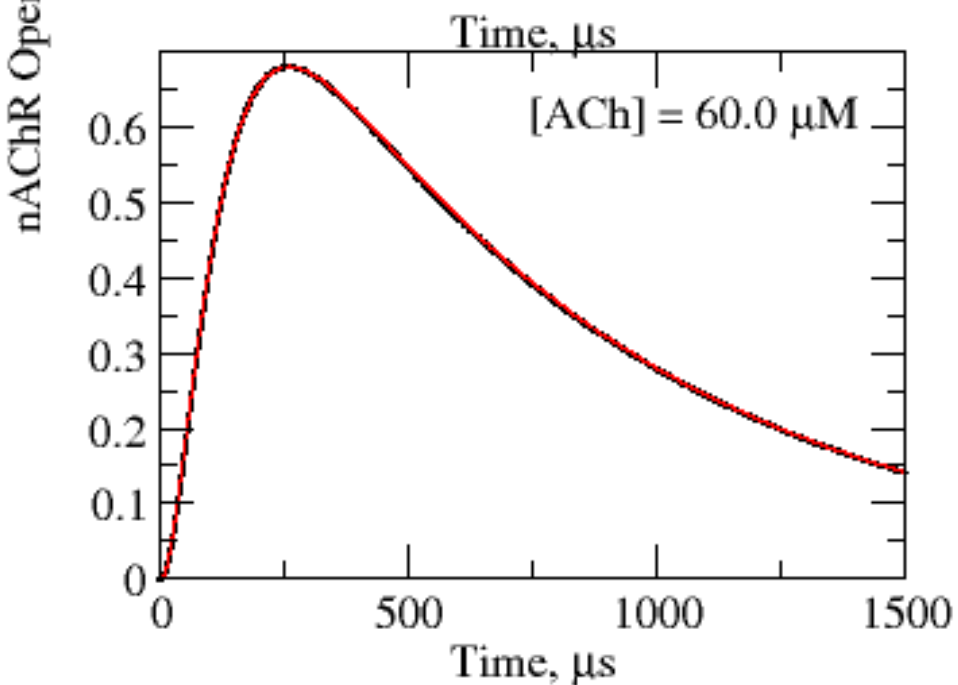
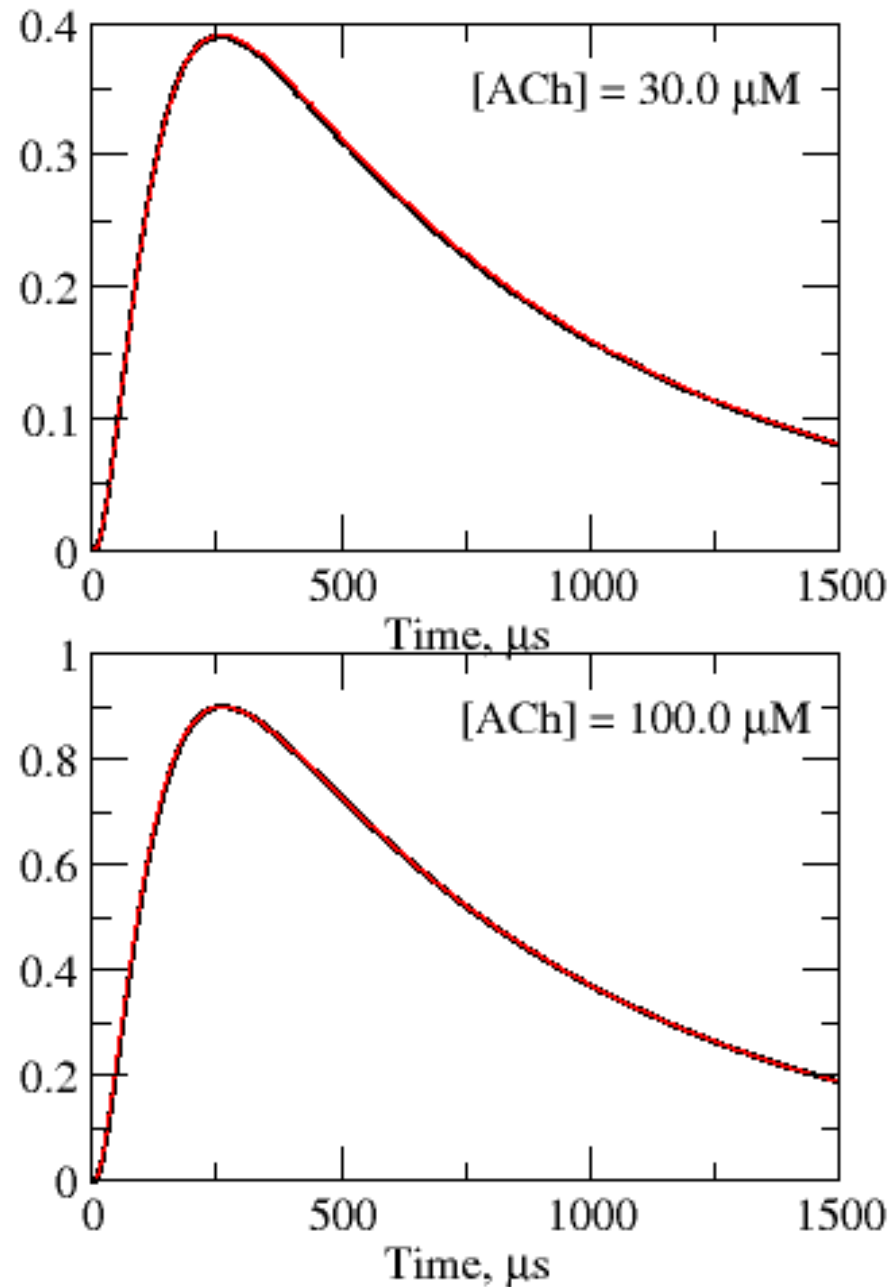
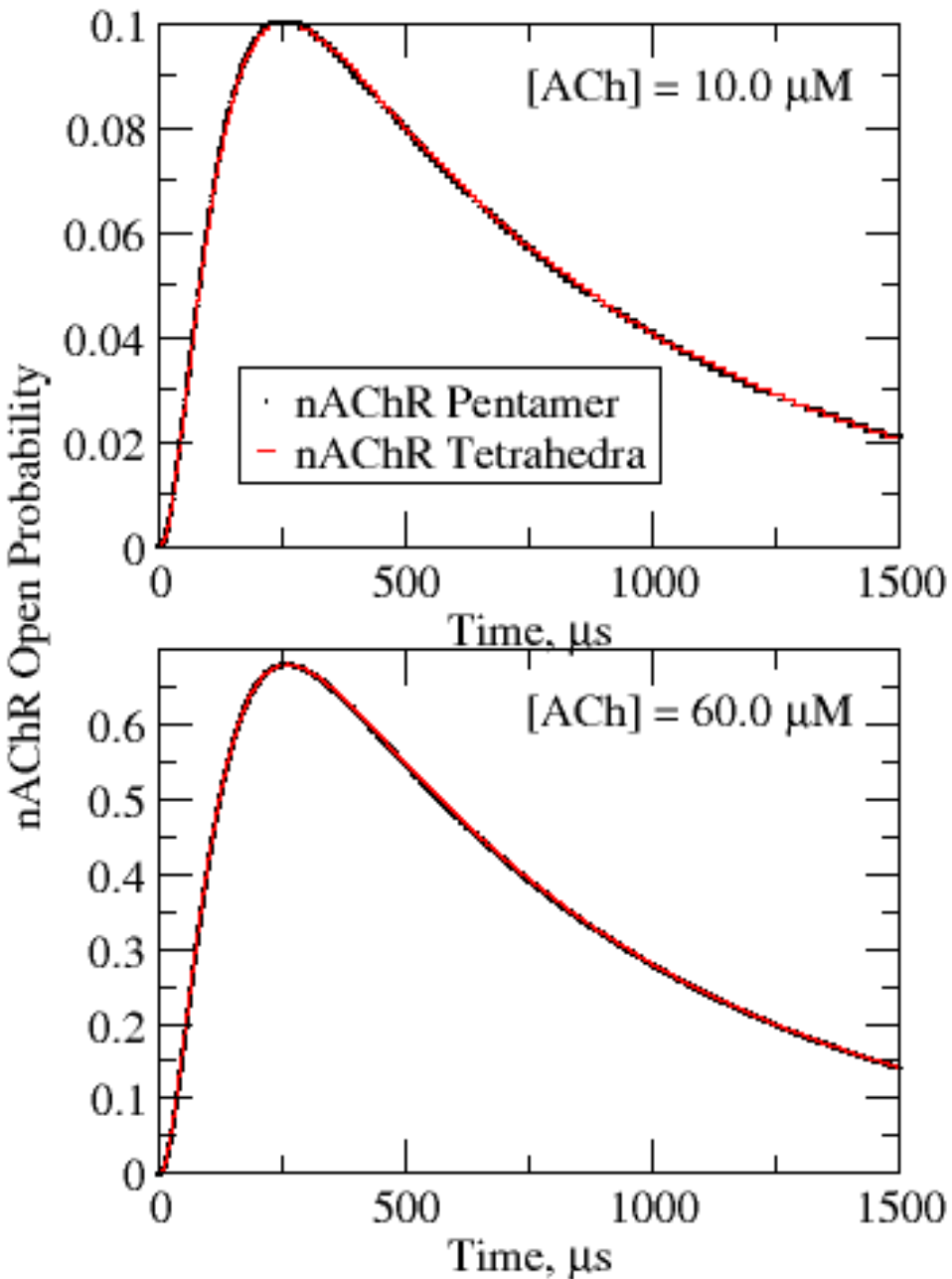
$$N(O) = N_{nAChR} p(O)$$

nAChR Activity

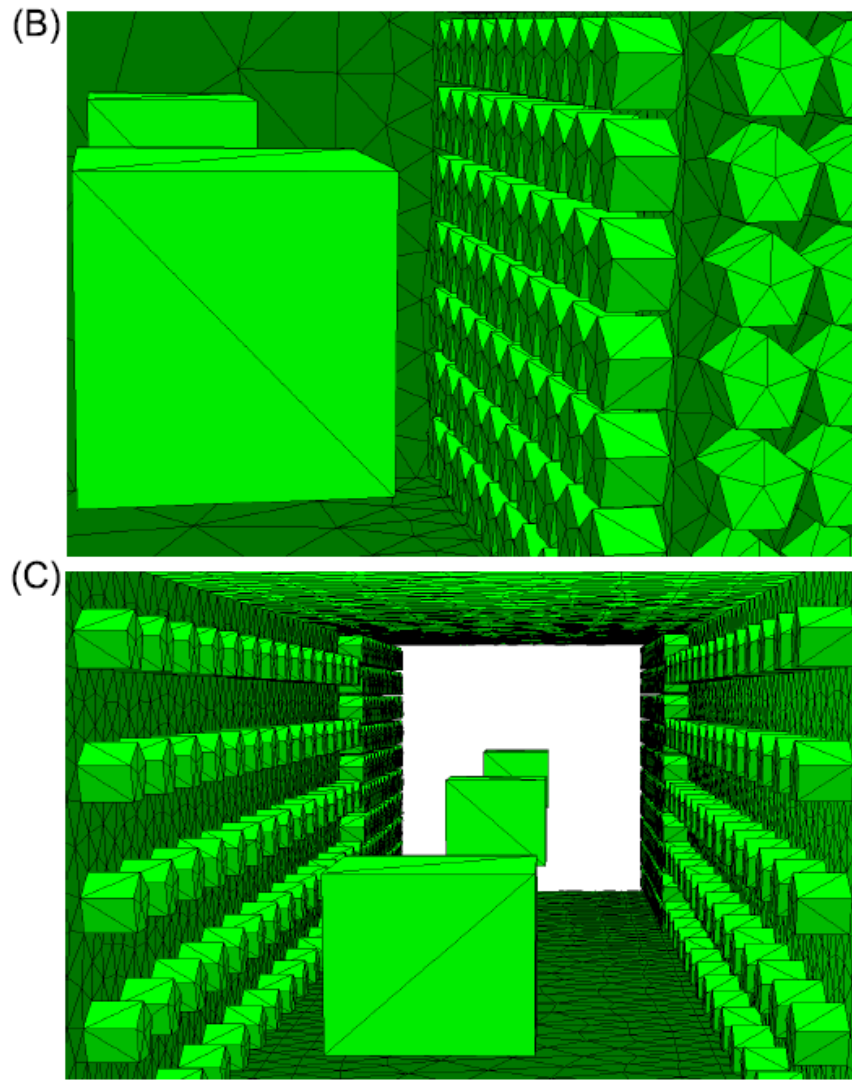
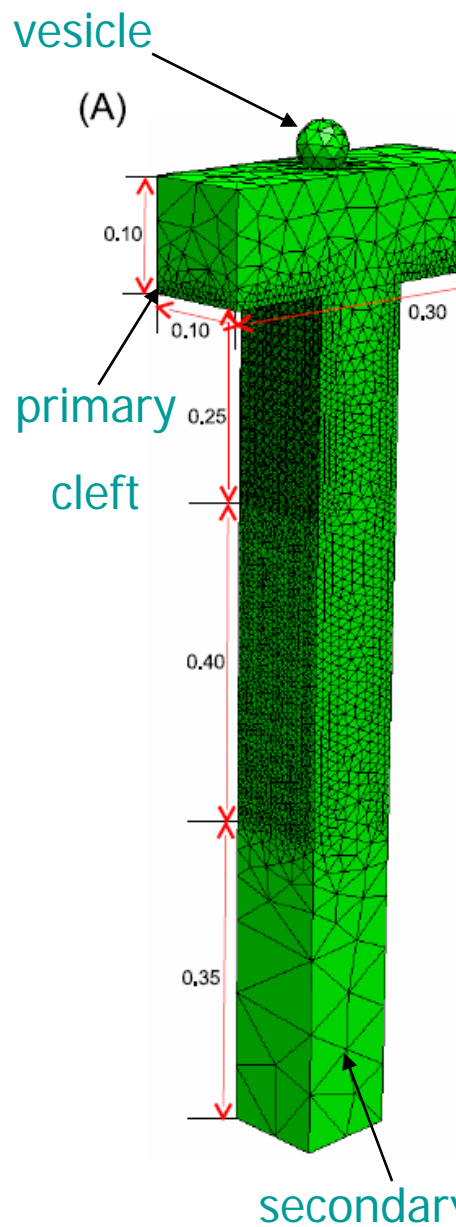


Br J Pharmacol 128:
1467-1476

nAChR Open Probabilities

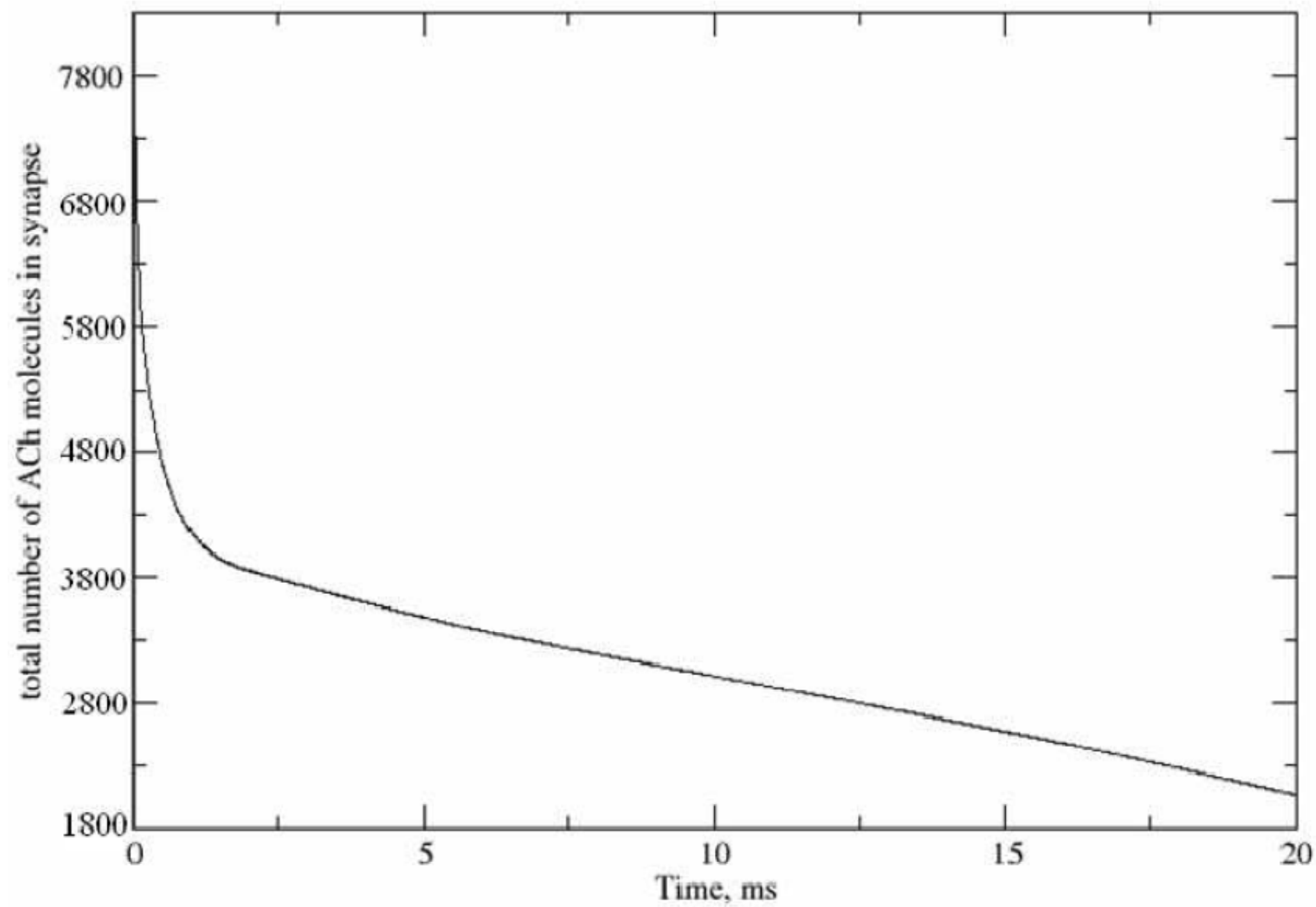


Assembly of Rectilinear NMJ

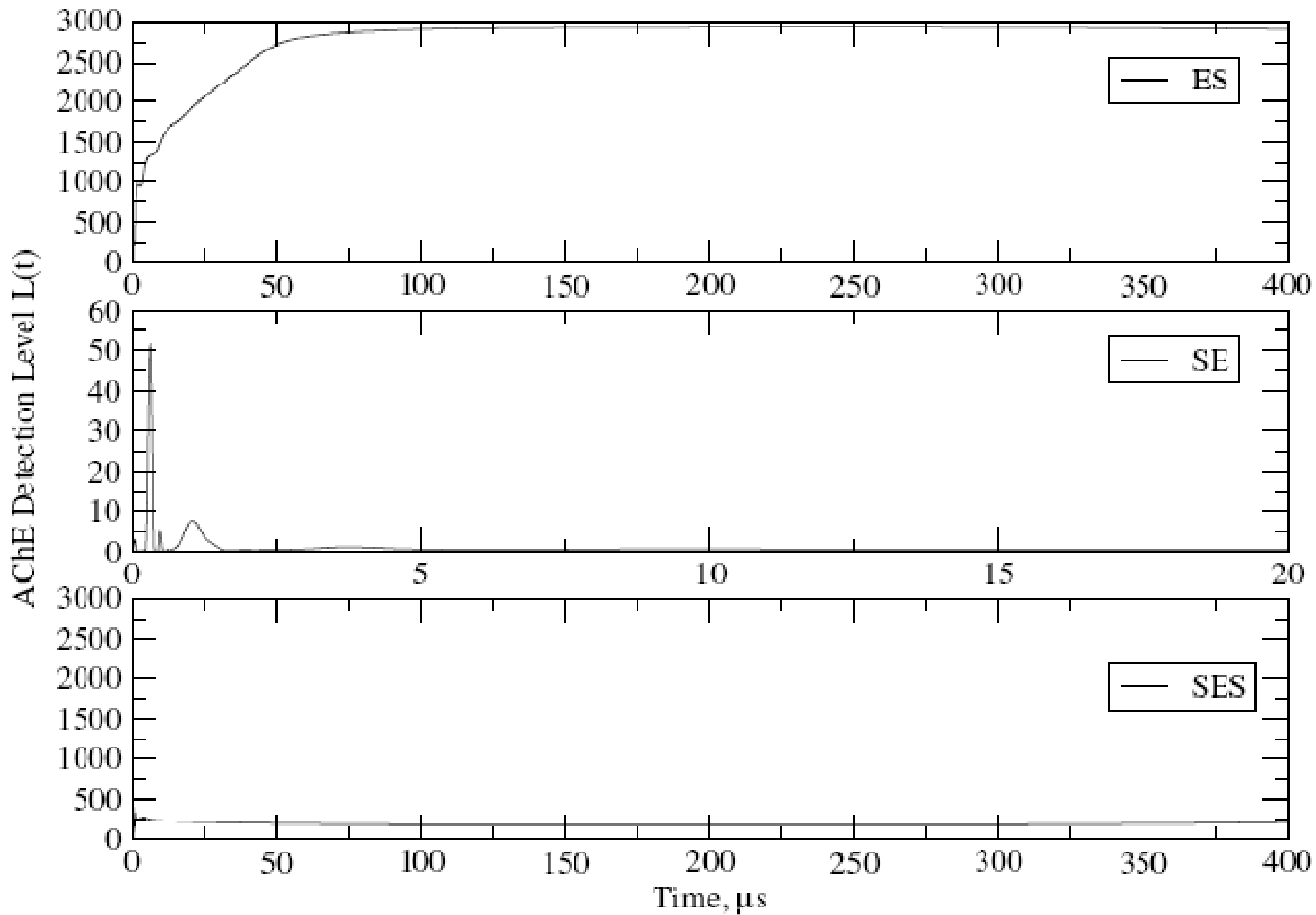


nAChR: 750
AChE: 8
ACh: 8,474

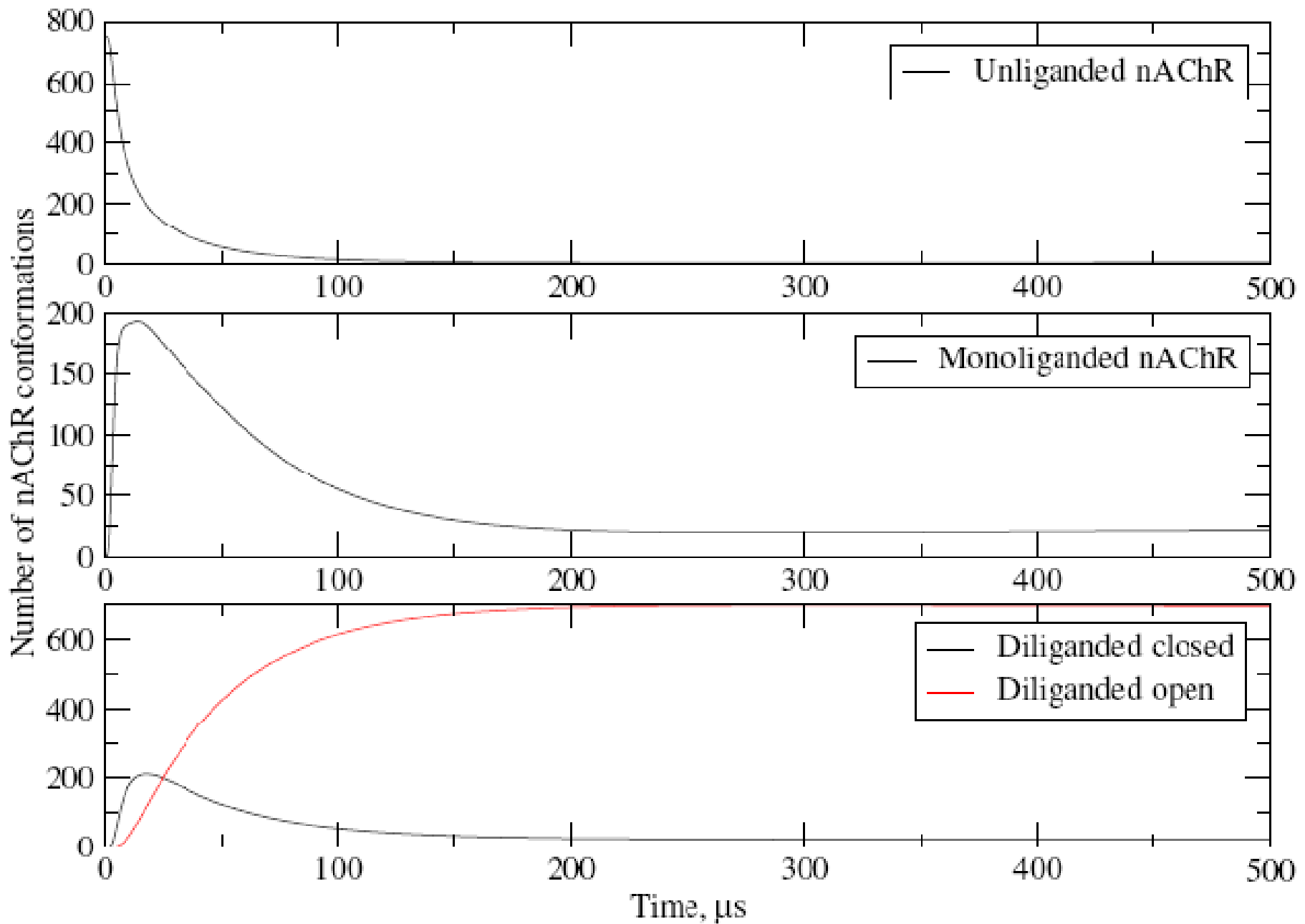
ACh Decay



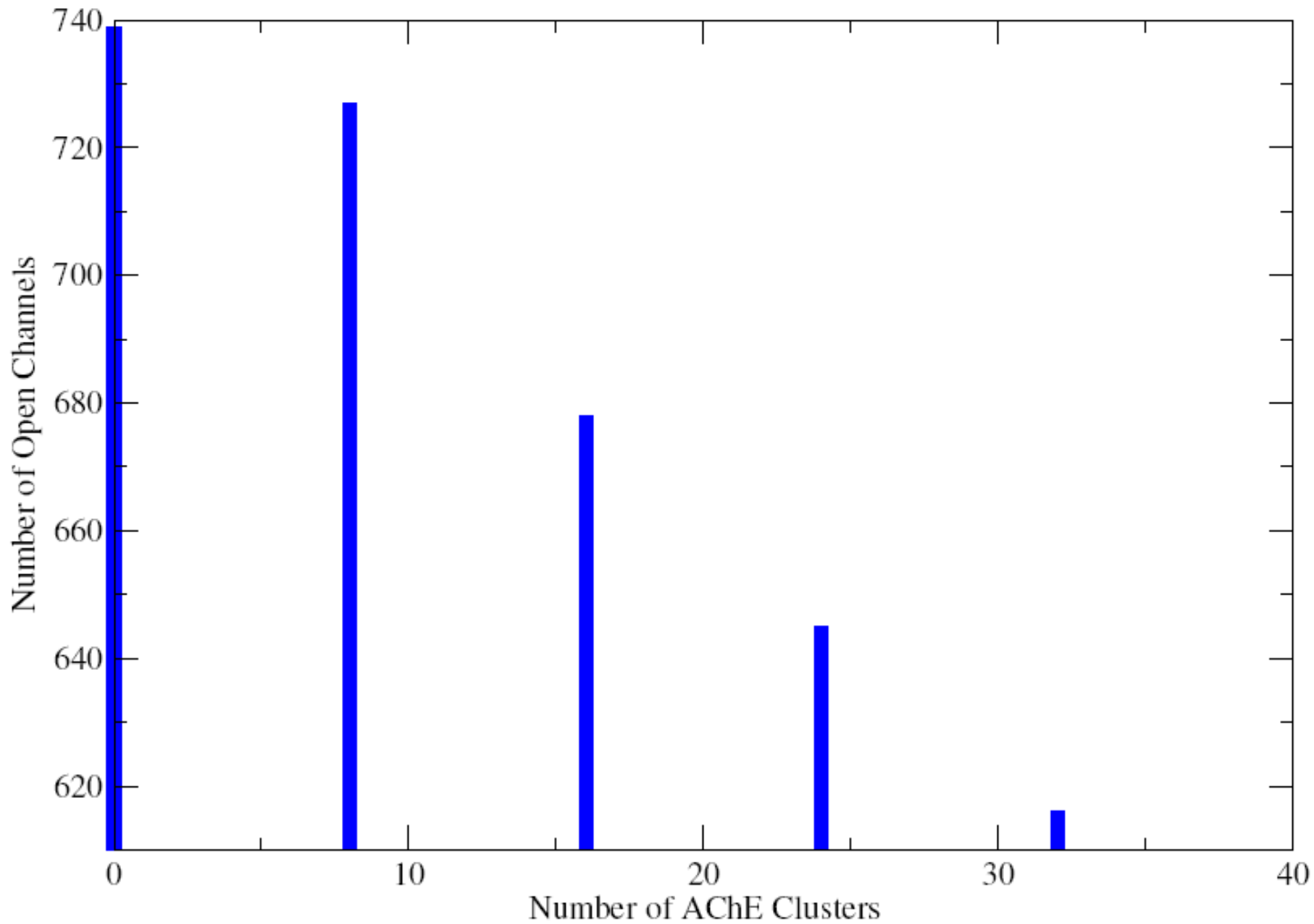
AChE Intermediates



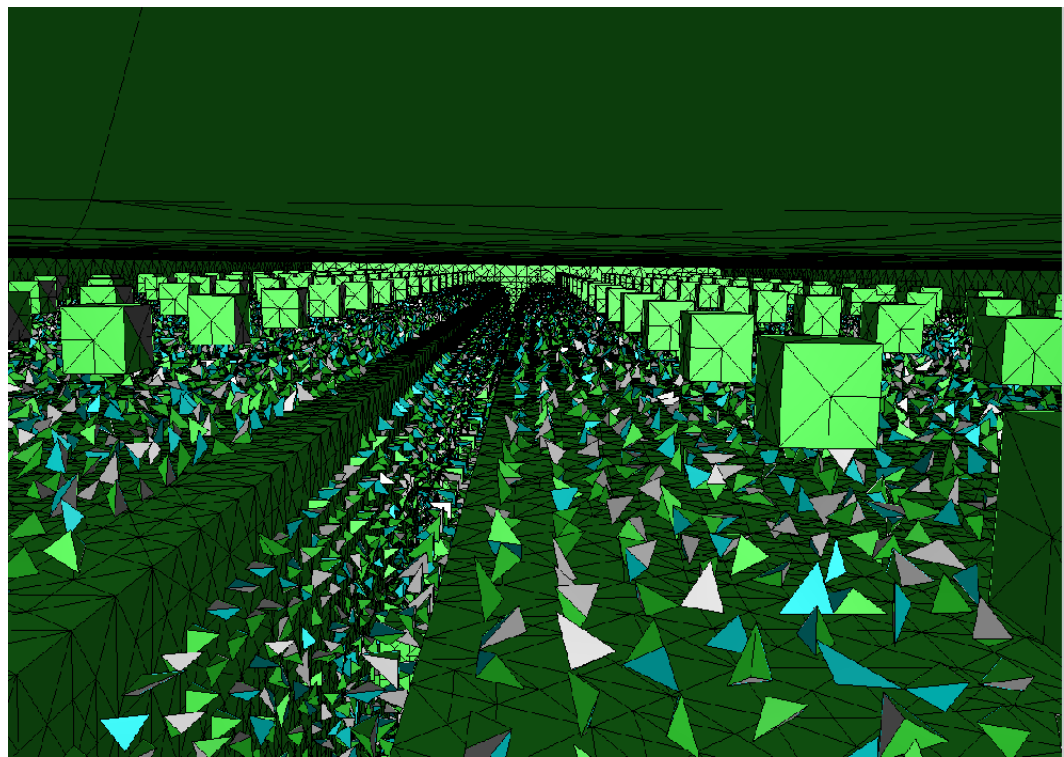
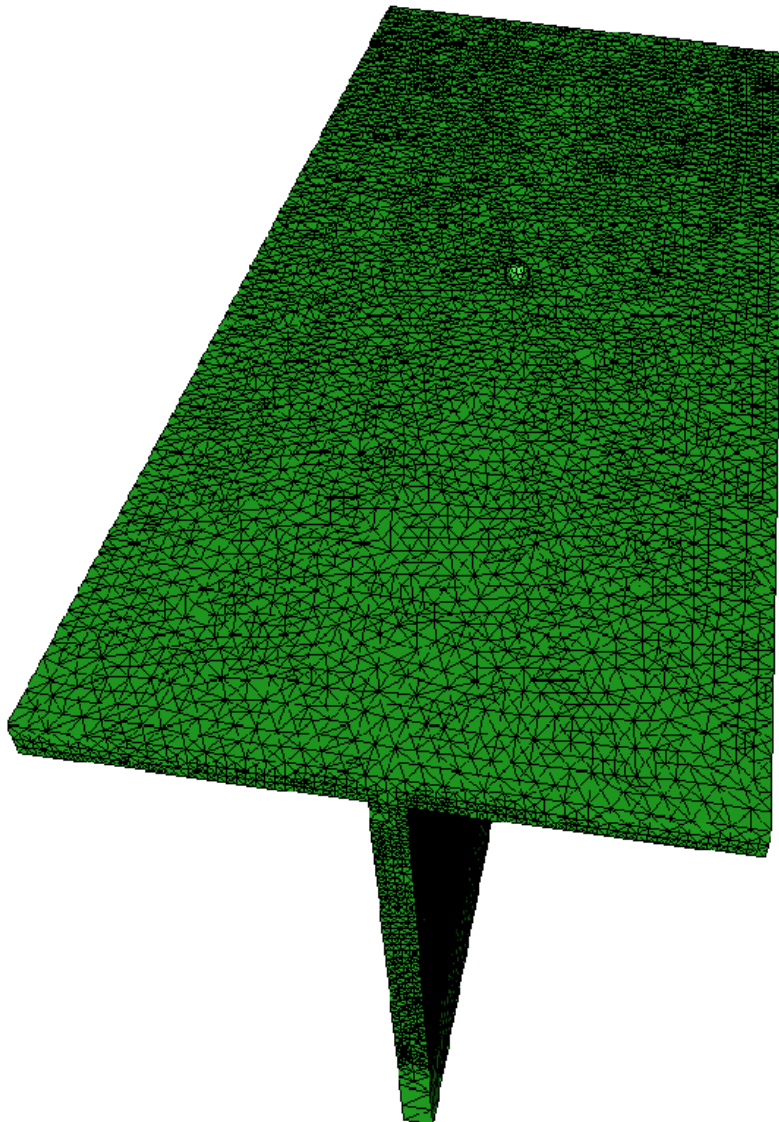
nAChR States



Open Channel Number vs. AChE Amount



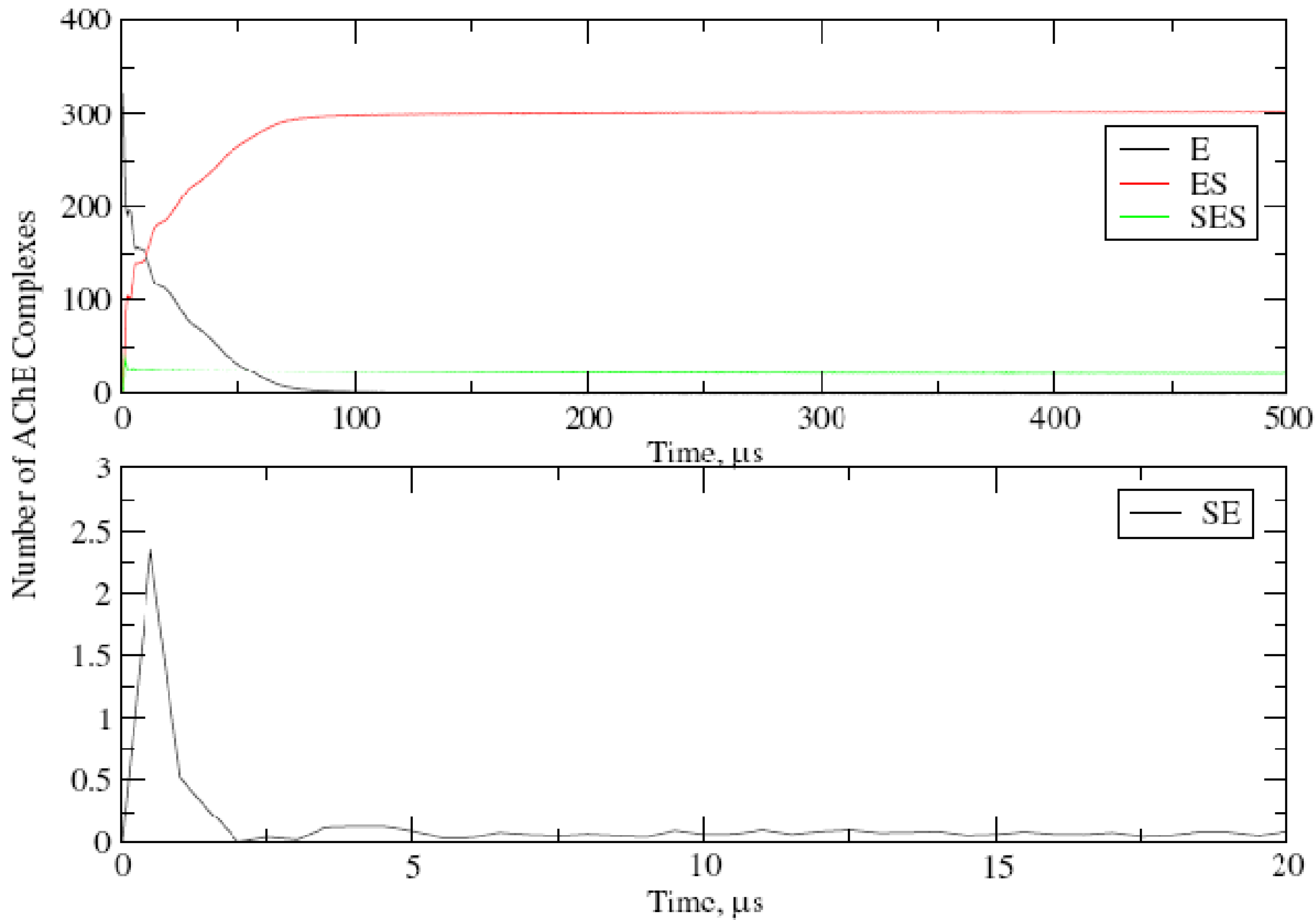
Larger NMJ Model



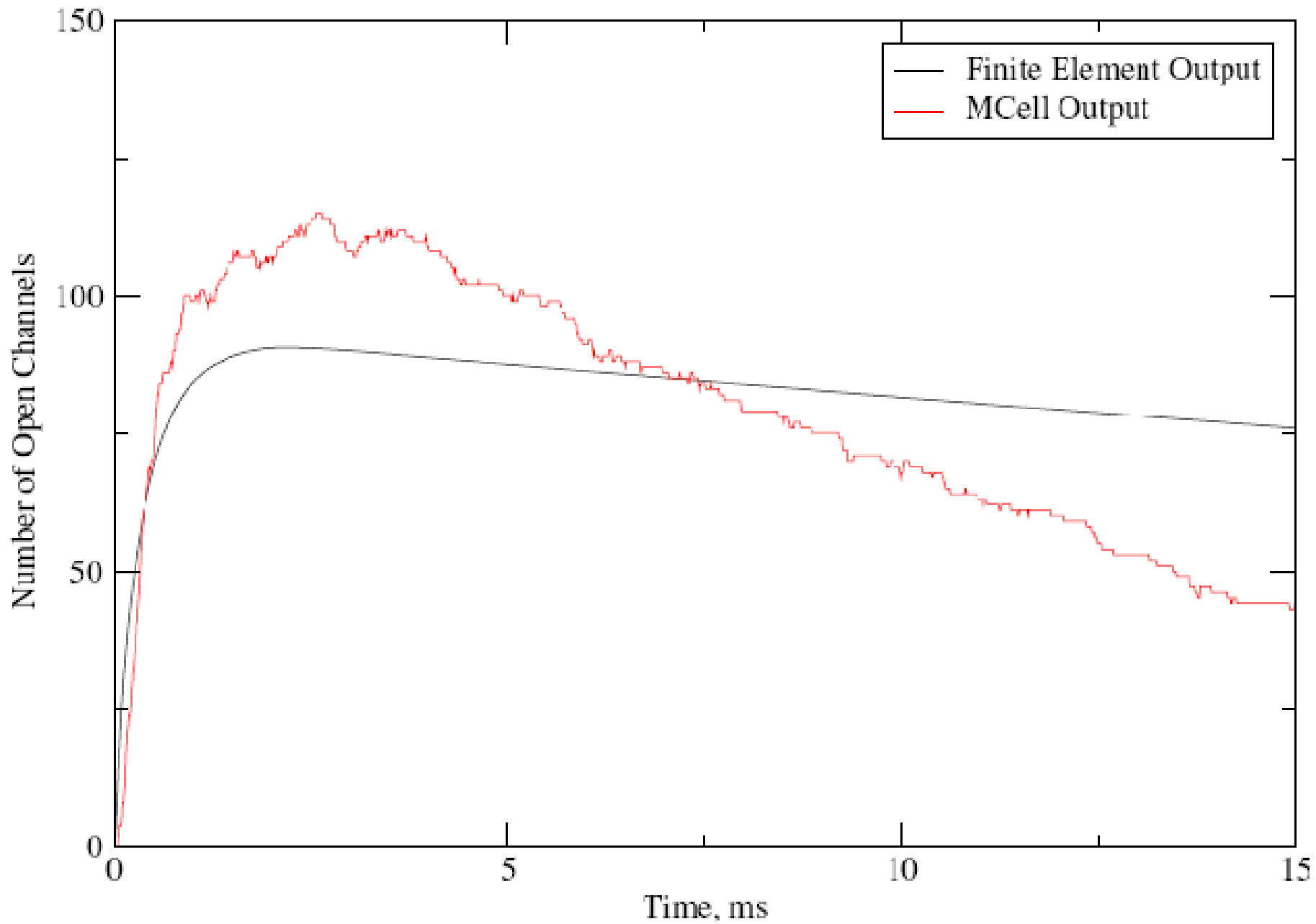
AChE Clusters: 323

nAChR: 29462

AChE Intermediates



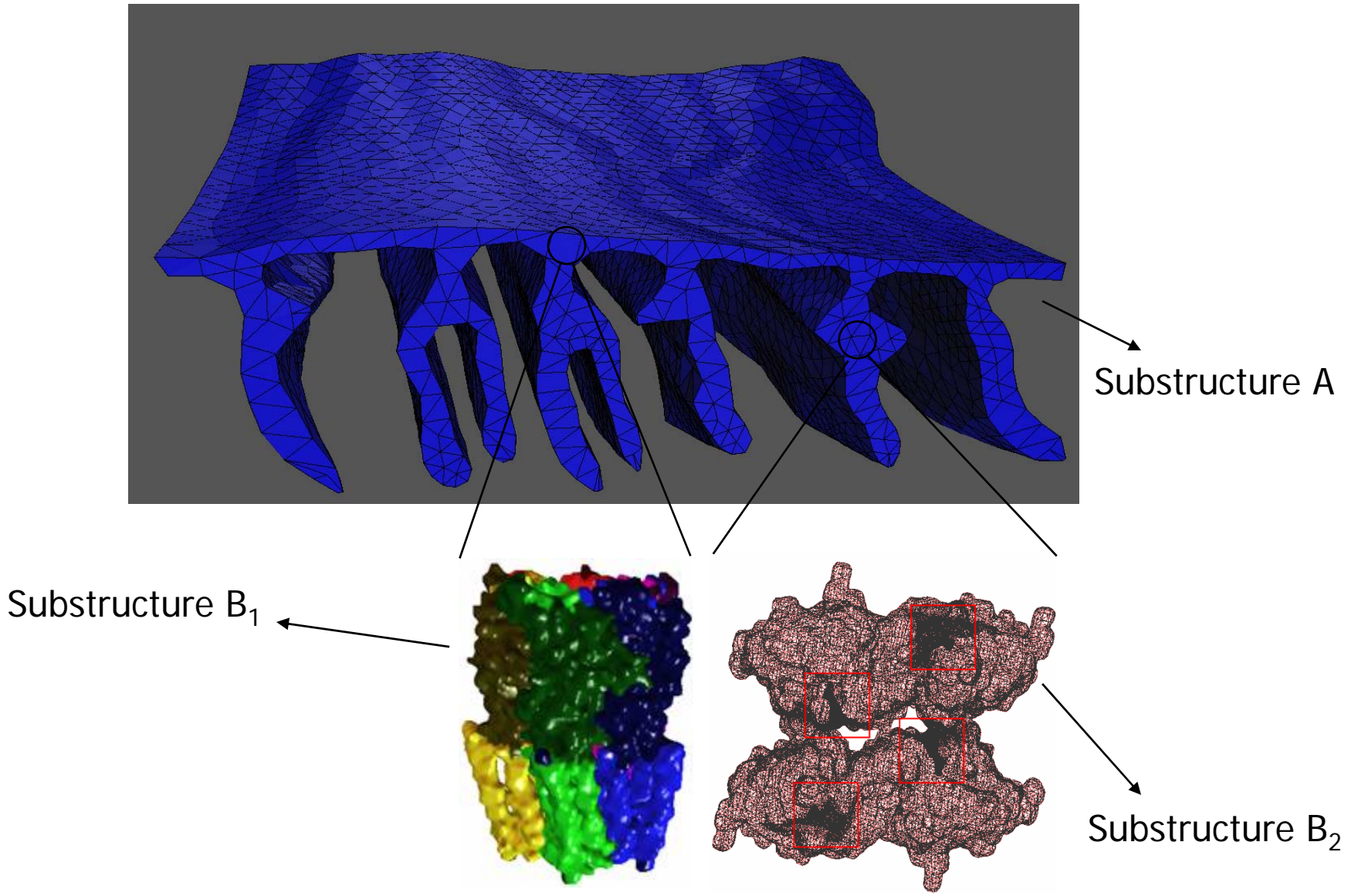
Open Channel Number



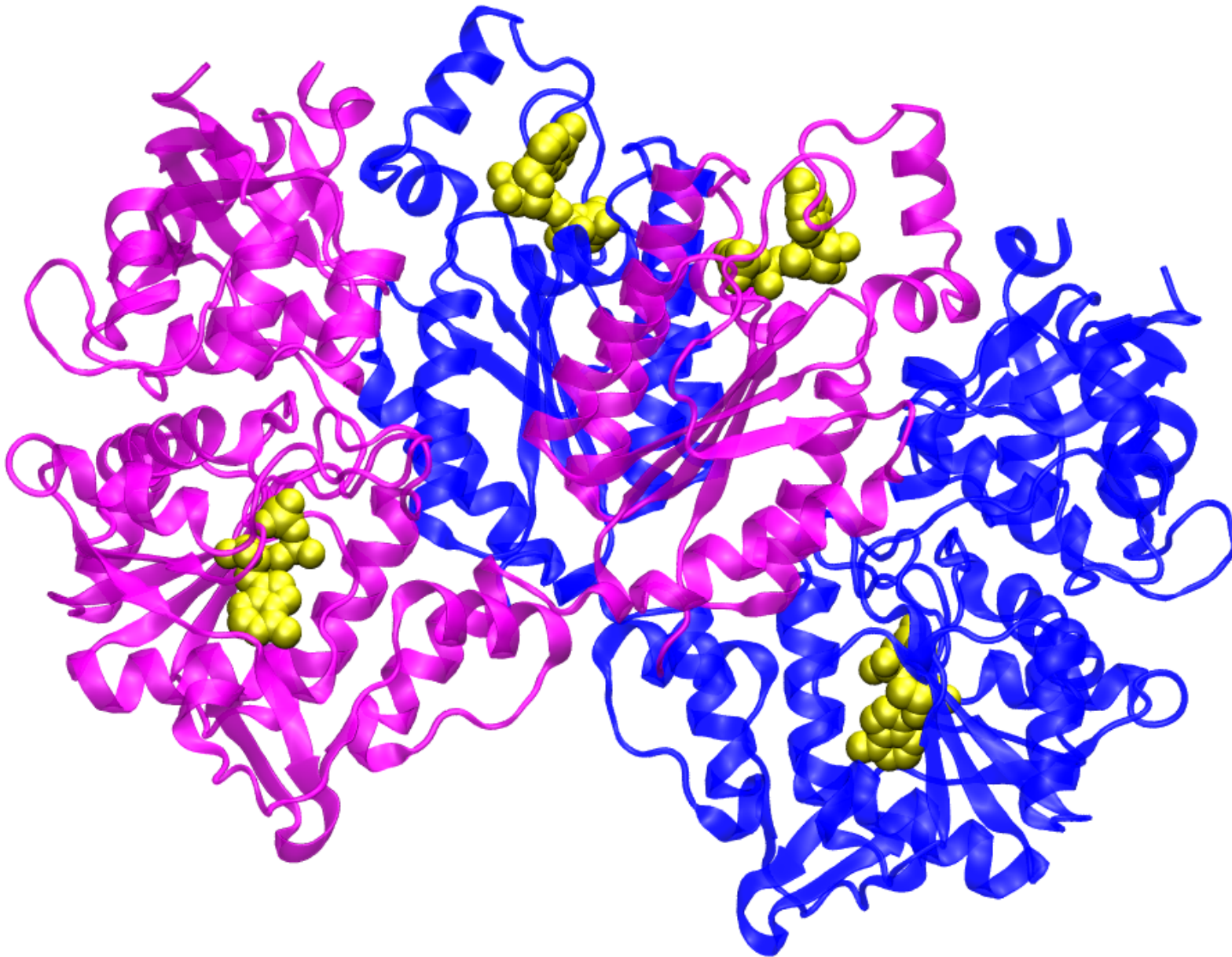
Neuromuscular Transmission

- The nAChR conformations are relatively insensitive to AChE densities or AChE inhibitor (More evidence in the future)
- Properties of neuromuscular junction designed to assure that every presynaptic action potential results in a postsynaptic one (i.e. 1:1 transmission)
- The NMJ is a site of considerable clinical importance

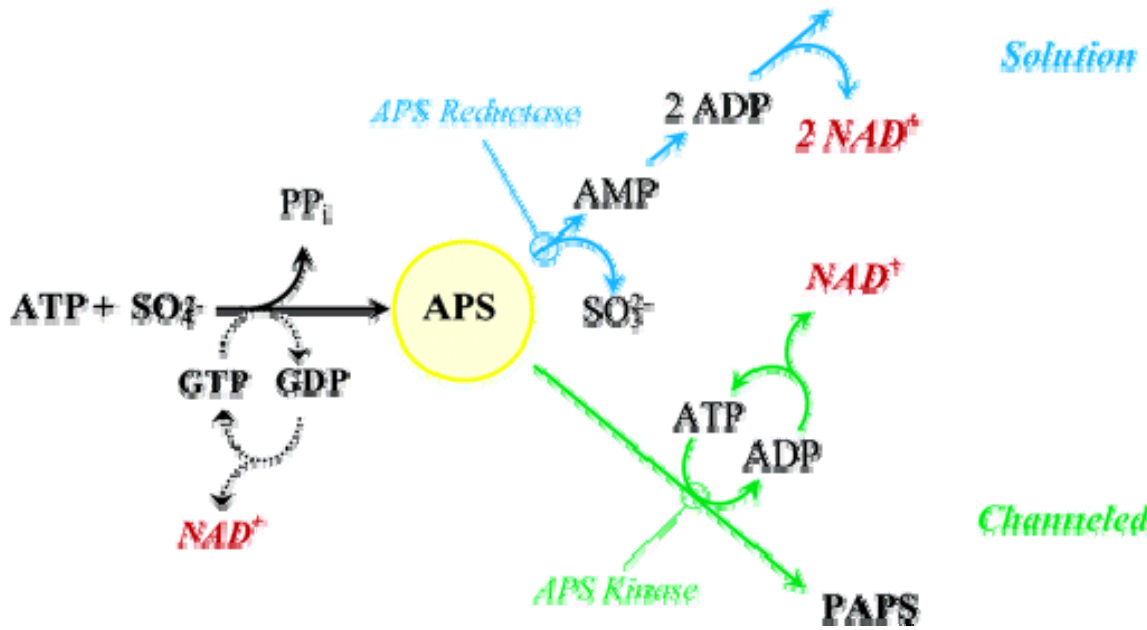
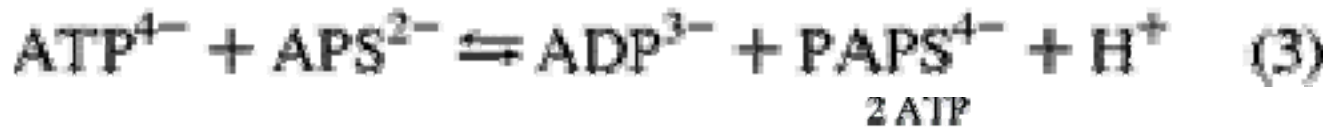
Future Direction

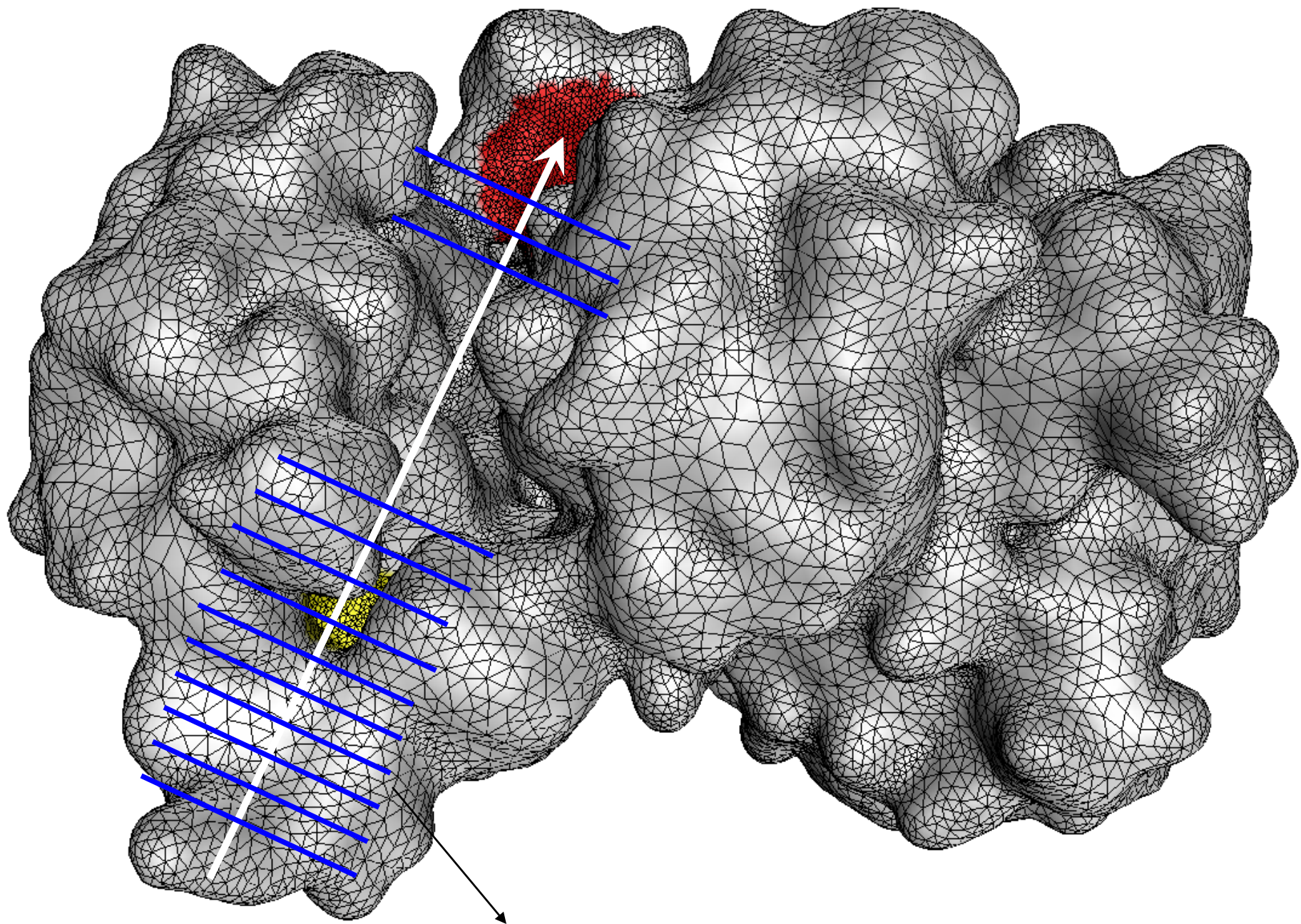


Channeling in Sulfate Activating Complexes



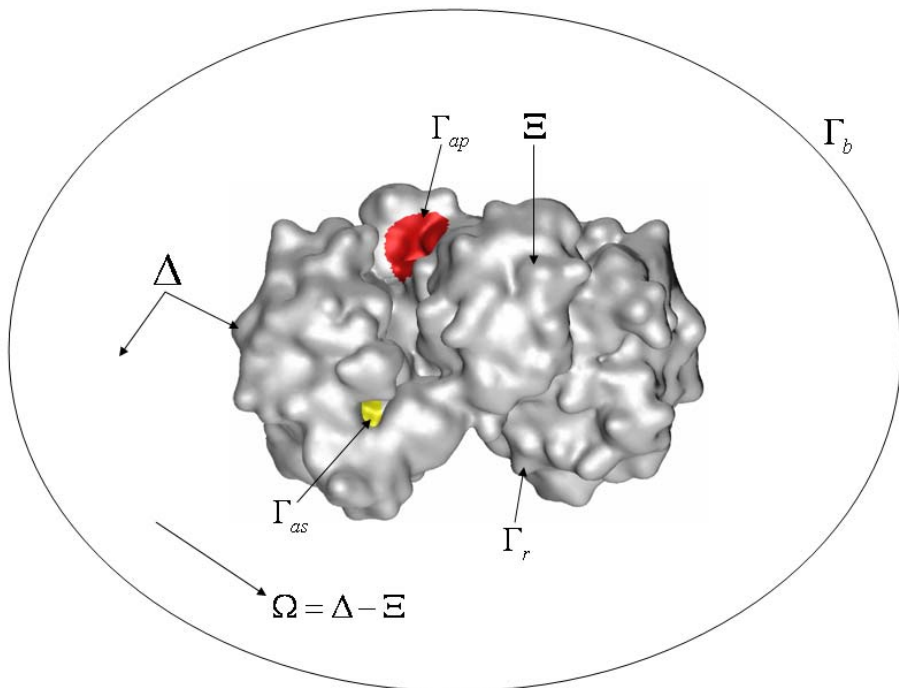
Reactions in the SAC





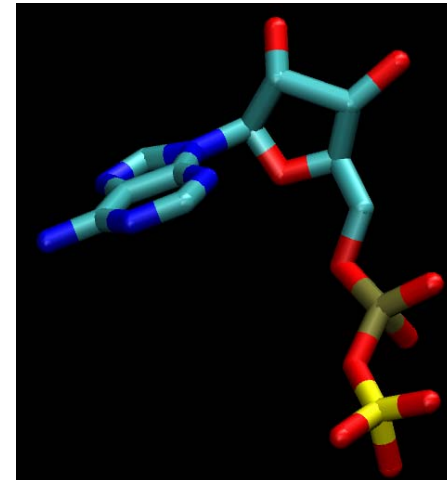
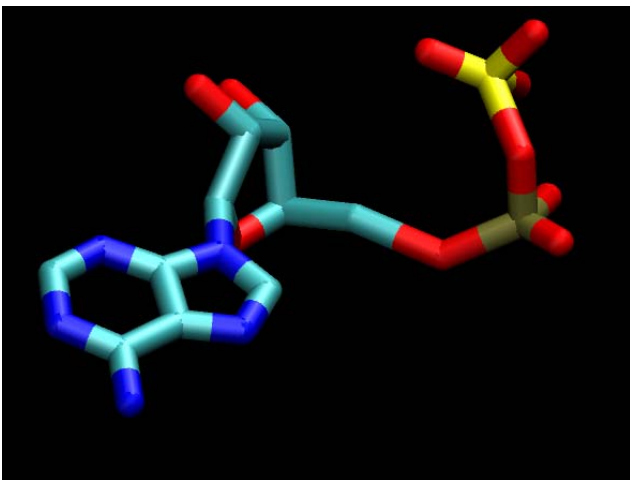
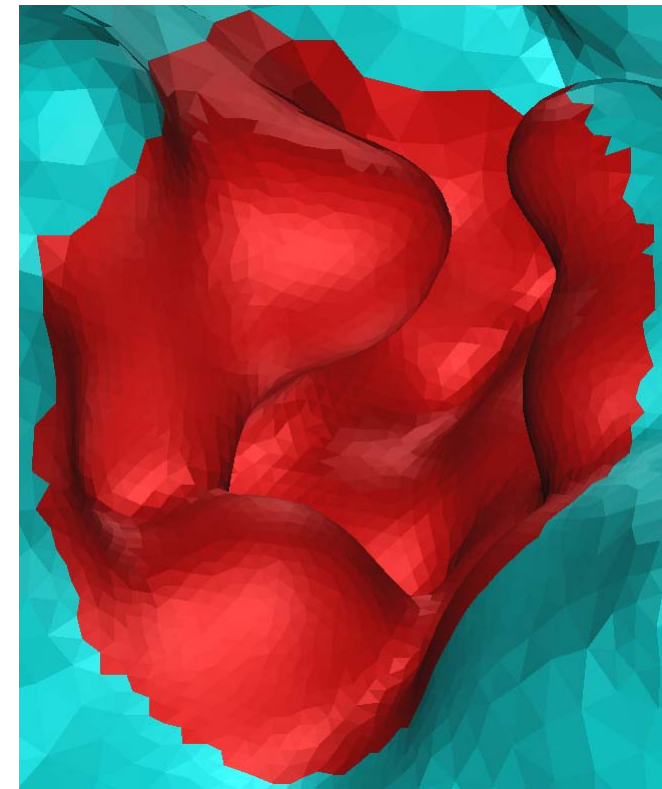
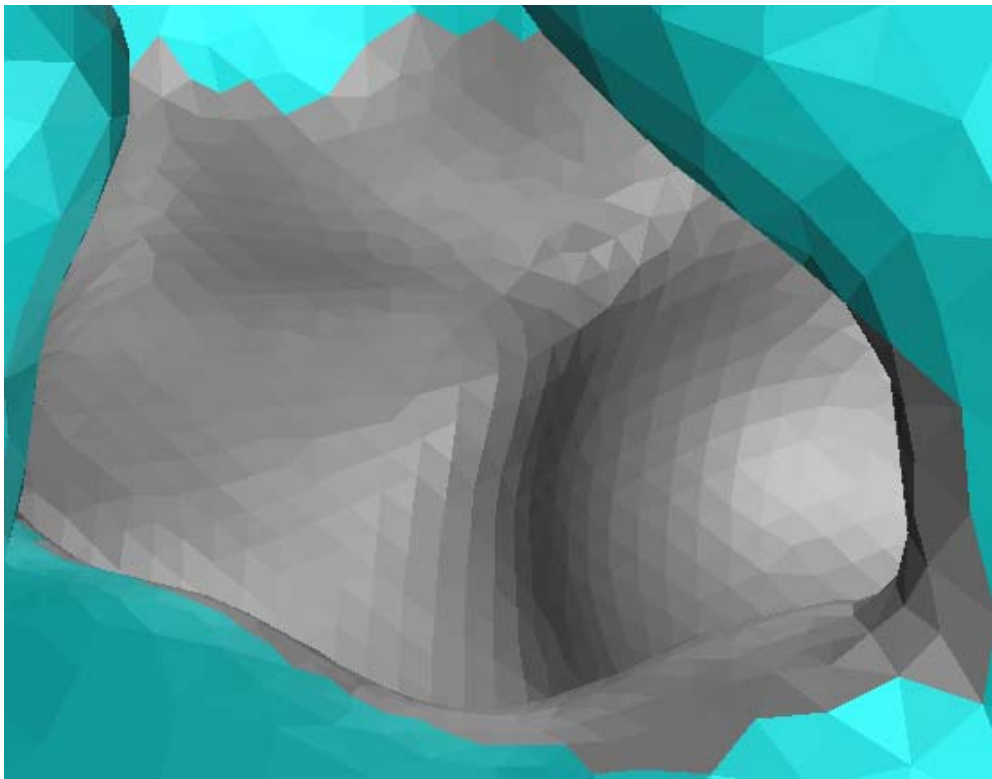
80 sections to divide the channel

Diffusional Channeling: Continuum Modeling



- Δ -- whole domain
- Ξ -- biomolecular domain
- Ω -- free space in Δ
- Γ_{ap} – reactive boundary I
- Γ_{as} – reactive boundary II
- Γ_r – reflective boundary
- Γ_b – boundary for Δ

The active sites of the SAC



Reactions in both active sites

Experimental conditions: SAC (19 nM), ATP (2.0mM, 13K_m), SO₄²⁻ (6.0mM, 6.0K_m), MgCl₂ (4.0mM), Hepes (50mM, PH8.0)

ATP sulfurylase active site:

$$[\text{SO}_4^{2-}] > [\text{ATP}] \gg [\text{SAC}] ,$$

$$\frac{d[\text{APS}]}{dt} = k_{\text{cat}}^{\text{as}} [\text{SAC}_{\text{tot}}]$$

APS kinase active site:

$$[\text{ATP}] \gg [\text{APS}], K_M + [\text{APS}] \approx K_M, \text{ first-order reaction}$$

$$-\frac{d[\text{APS}]}{dt} = k_{\text{cat}}^{\text{ap}} [\text{SAC}_{\text{tot}}][\text{APS}] / K_M^{\text{ap}}$$

The features of the reactions

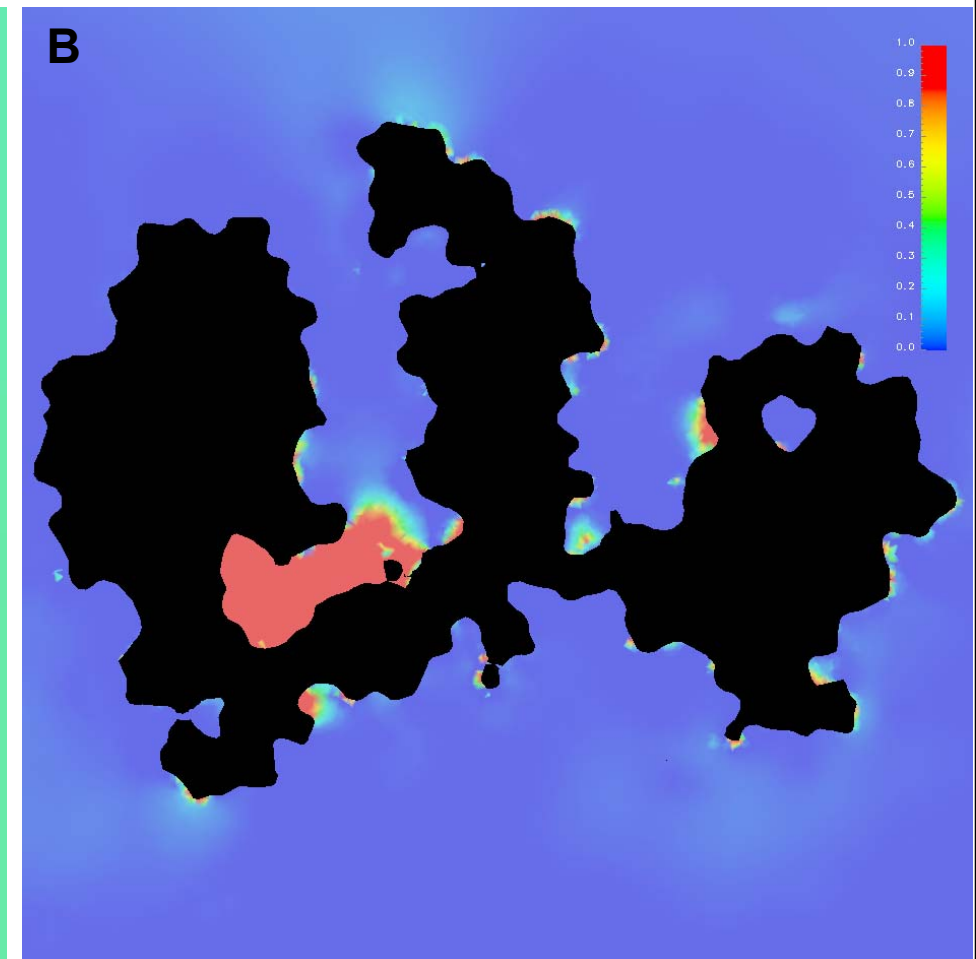
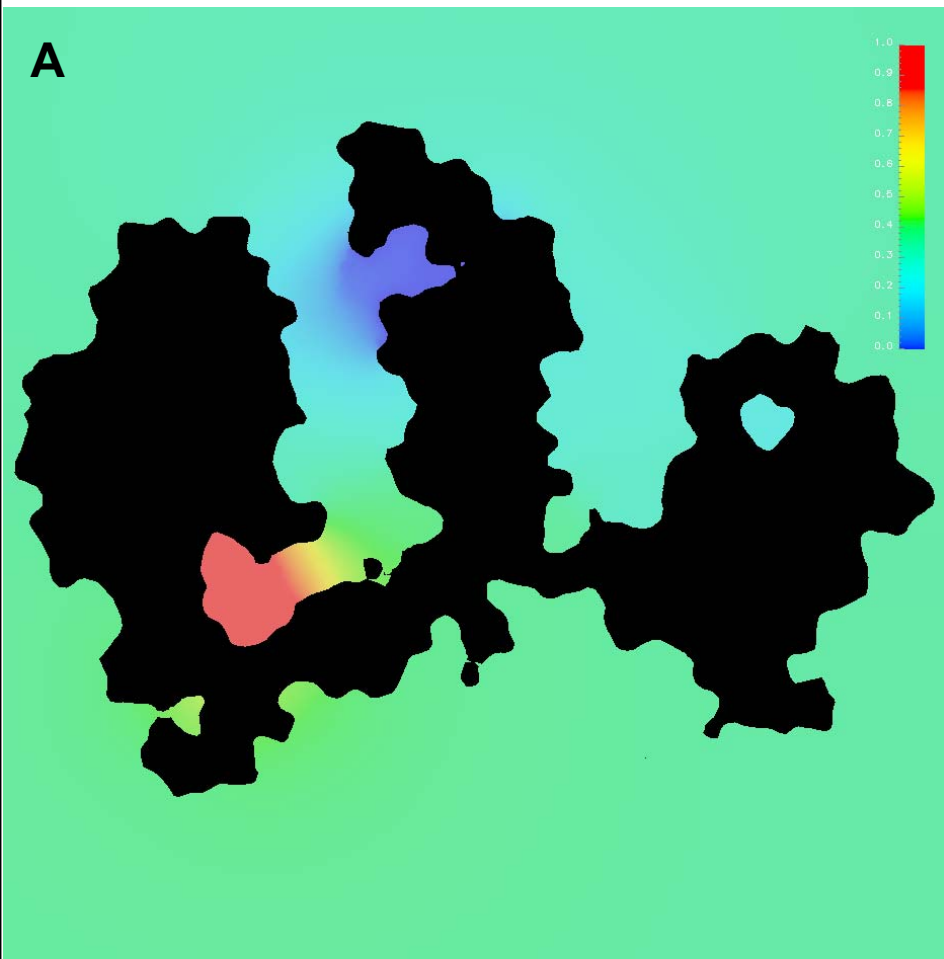
- Suppose the diffusion coefficient of APS²⁻ is similar with the ATP⁴⁻ in cytoplasm, i.e. 15000.0 Å²/μs
- Ionic strength is set at 0.040M according to experimental environment.
- Electrostatic potential is calculated using APBS 5.0.

Smoluchowski Diffusion Equation

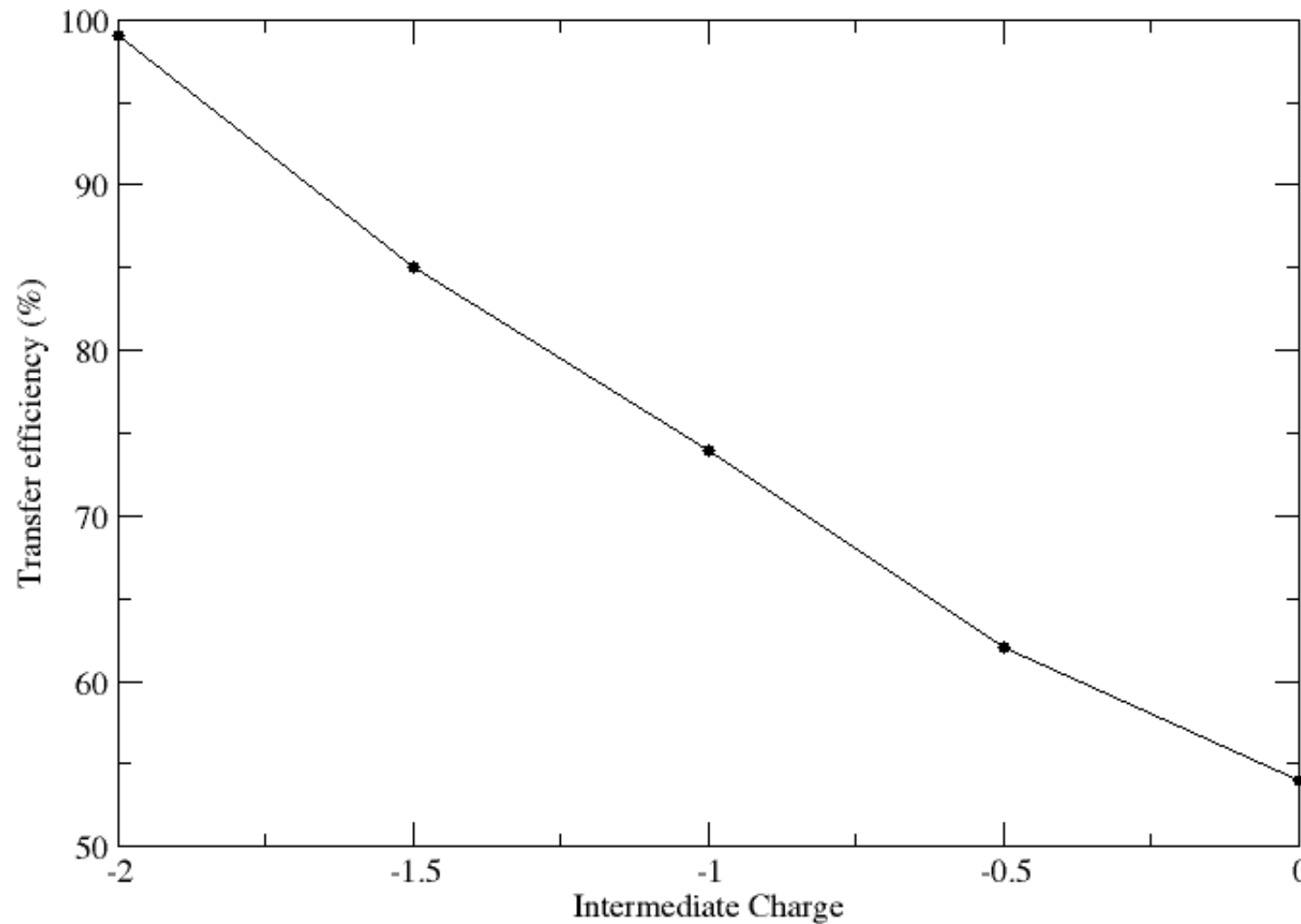
$$\begin{aligned} \frac{\partial p(\vec{r}, t | \vec{r}_0, t_0)}{\partial t} &= \nabla \cdot J p(\vec{r}, t | \vec{r}_0, t_0) \\ &= \nabla \cdot D e^{-\beta U(\vec{r})} \nabla e^{\beta U(\vec{r})} p(\vec{r}, t | \vec{r}_0, t_0) \\ \left. \begin{array}{l} \vec{n} \cdot \vec{J} p(\vec{r}) = 0 \text{ for } \vec{r} \in \Gamma_r \bigcup \Gamma_b \\ \vec{n} \cdot D \nabla p(\vec{r}) = \alpha(\vec{r}) p(\vec{r}) \text{ for } \vec{r} \in \Gamma_{ap} \\ \vec{n} \cdot D \nabla p(\vec{r}) = \beta(\vec{r}) \text{ for } \vec{r} \in \Gamma_{as} \end{array} \right\} \end{aligned}$$

$$\int_{\Gamma_{as}} n \cdot D \nabla p ds + \int_{\Gamma_{ap}} n \cdot D \nabla p ds = 0$$

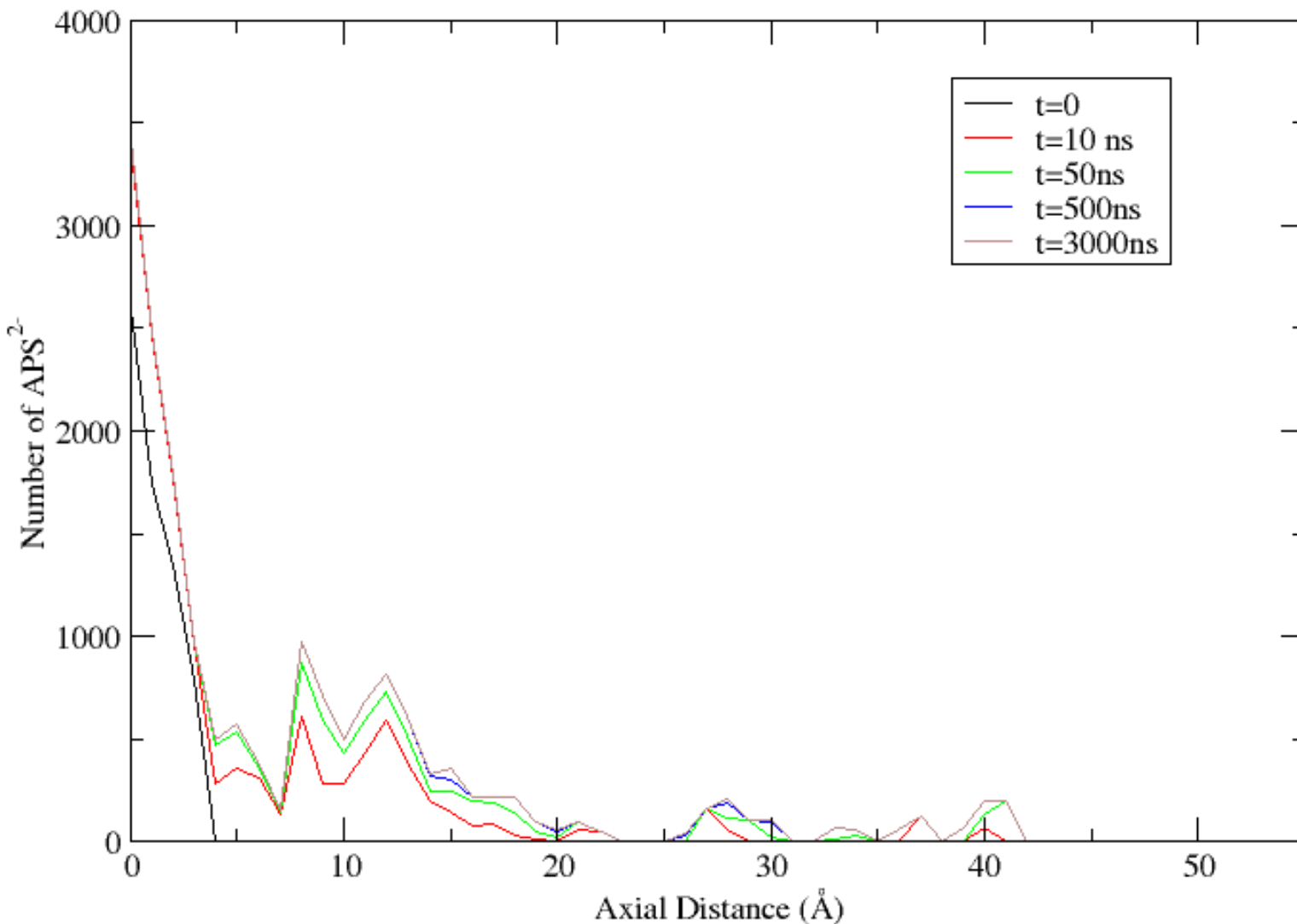
[APS] distribution under the steady state



APS transfer efficiency with different intermediate charge



APS²⁻ distribution in the channel at different simulation time



Coarse Grained Brownian Dynamics

- Each residue is represented by its C_α . APS is described with three beads.
- Protein coordinates are fixed, and APS is flexible.
- CGBD will stop once APS reacts in the active site of APS kinase (selected random numbers).
- 500 reacted cases were analyzed with different random numbers.

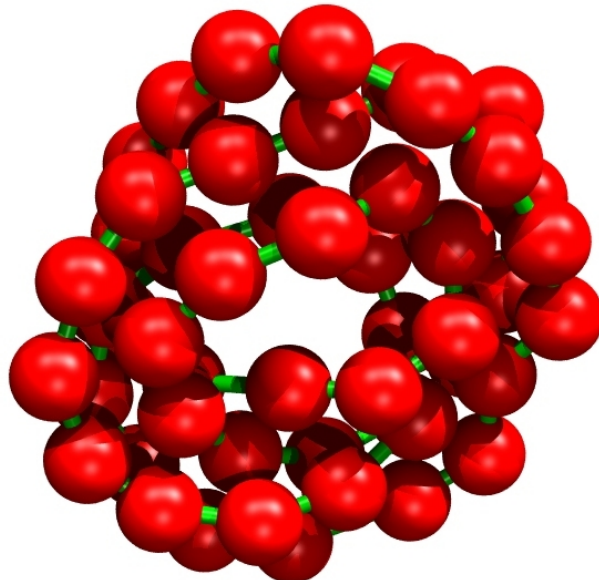
Coarse Grained Brownian Dynamics

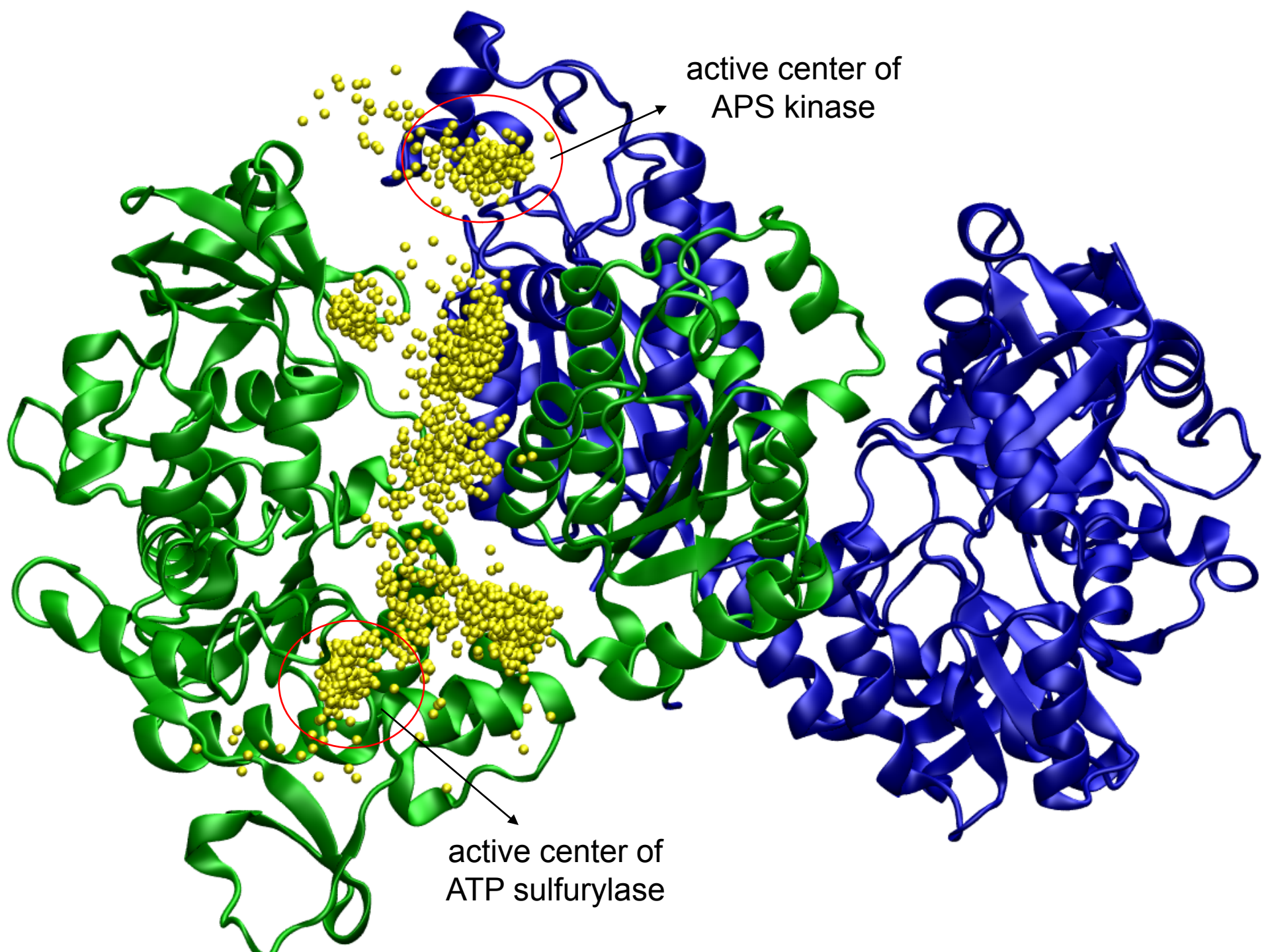
In the simulations, we solve the Langevin equation

$$m_i \frac{dv_i}{dt} = -m_i \gamma_i v_i + F_i^R + q_i E_i + F_i^S$$

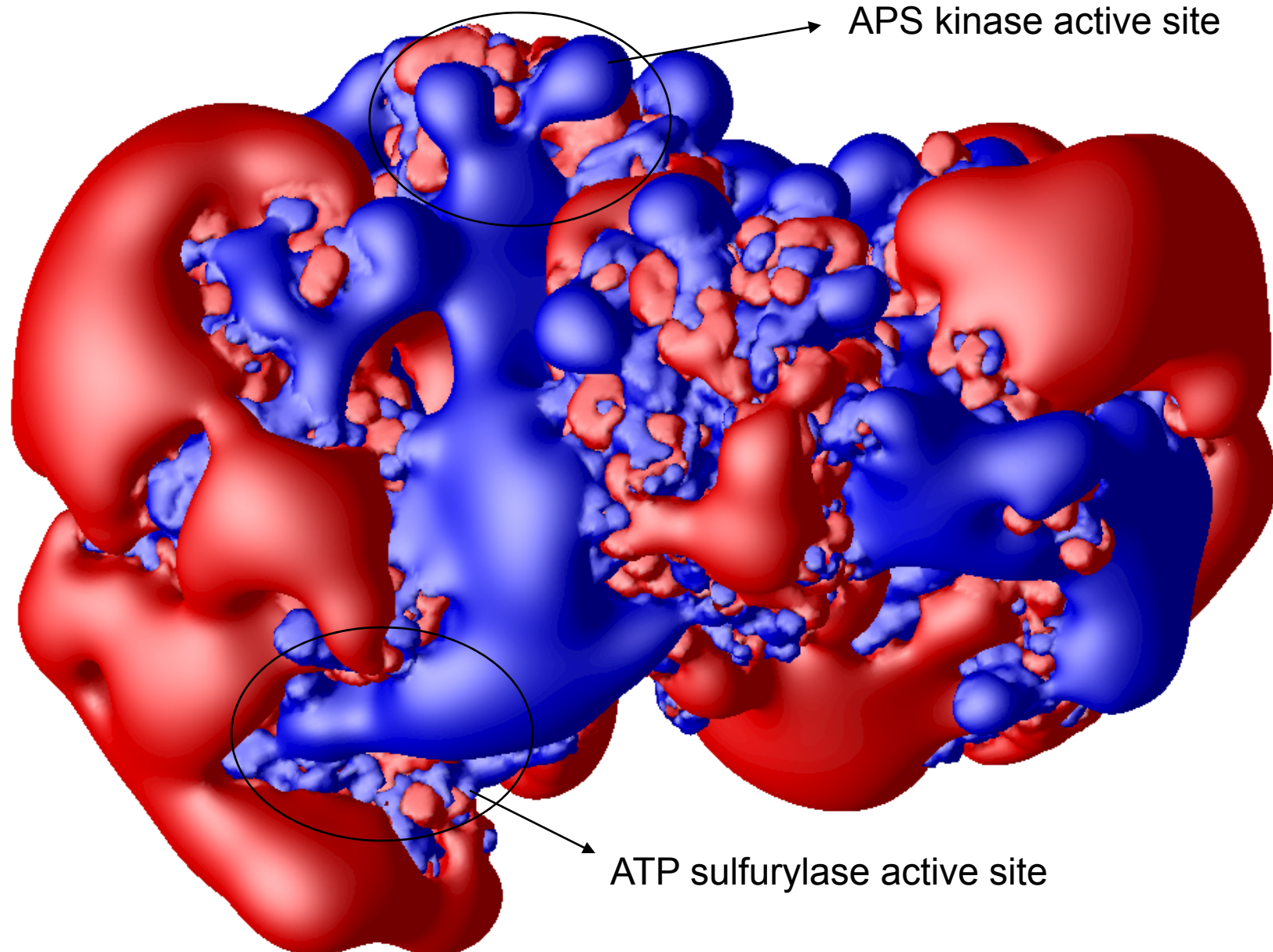
Where m_i , v_i , $m_i \gamma_i$, and q_i are the mass, velocity, friction coefficient, and charge on an ion with index i , whereas

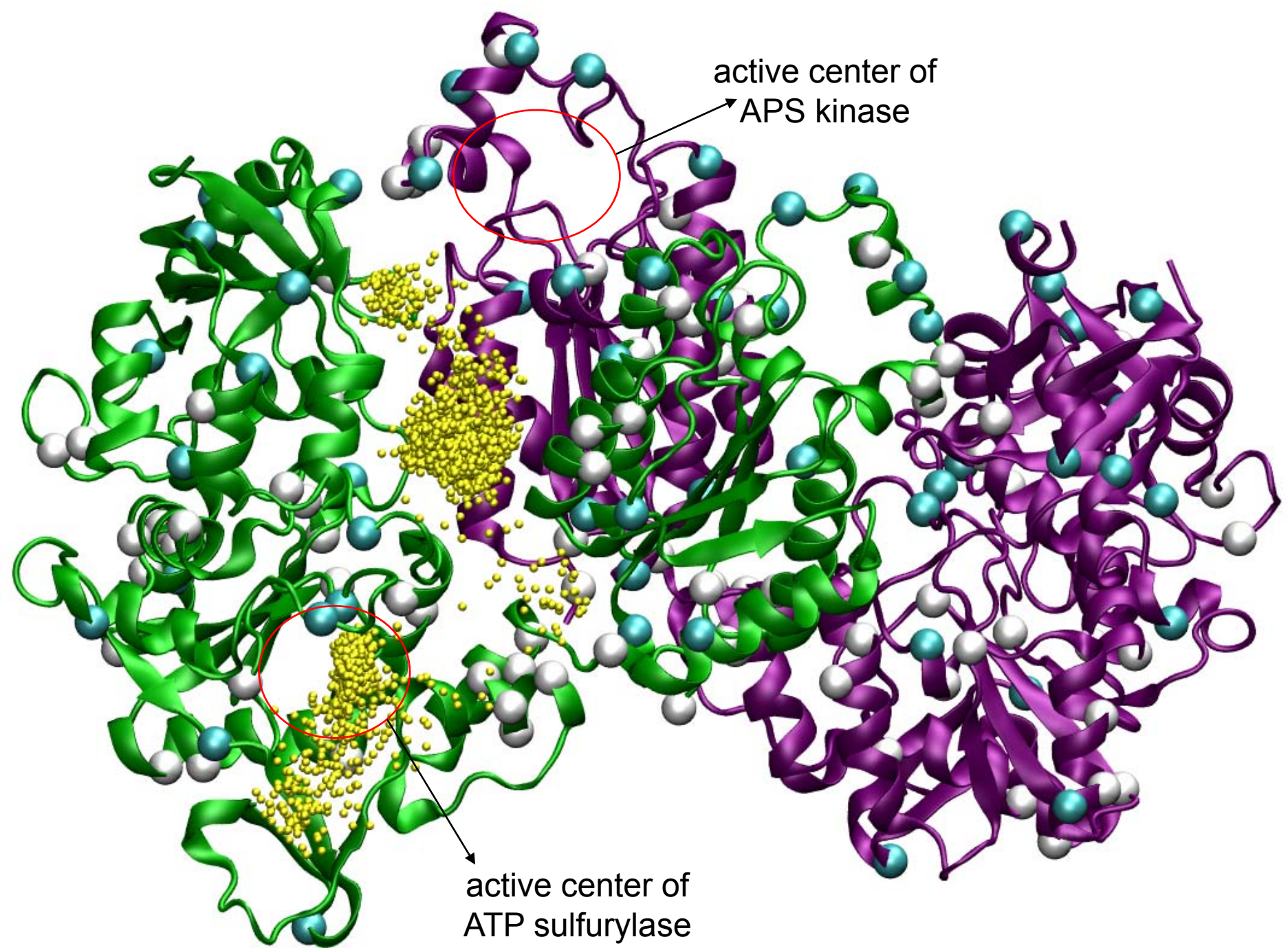
F_i^R , E_i , and F_i^S are the random stochastic force, systematic electric field, and short range forces experienced by the ion, respectively.



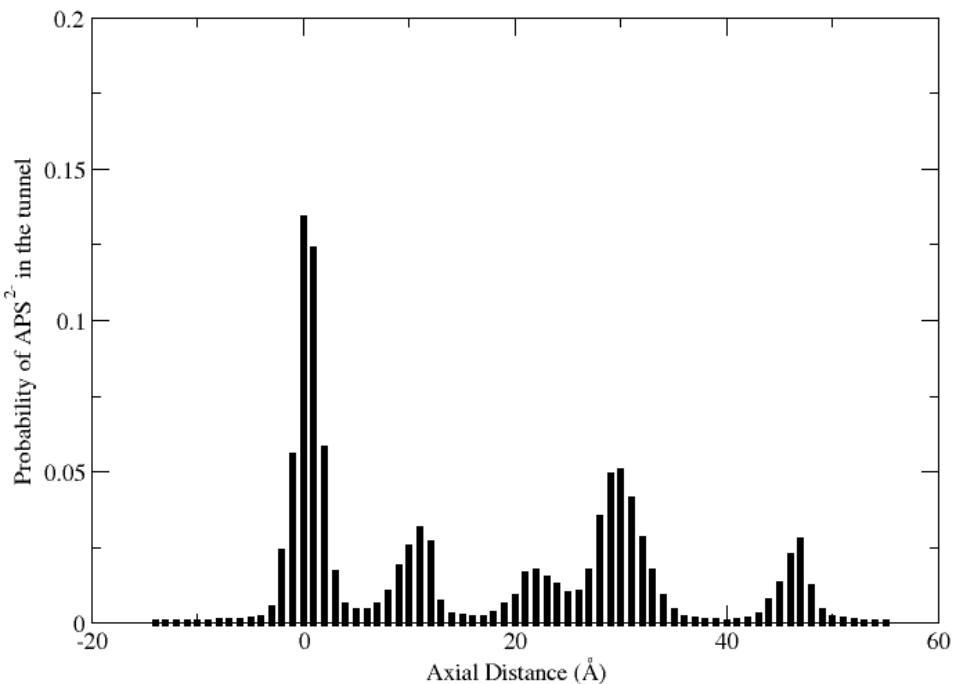


Electrostatic potential on the protein surface

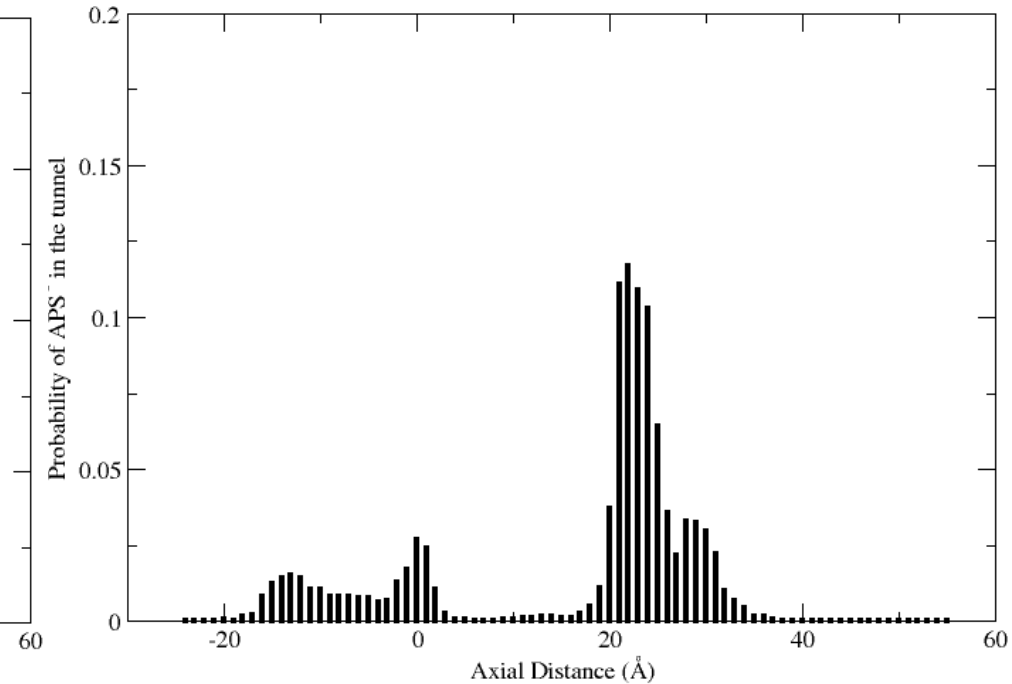




APS probability in the channel



APS^{2-}



APS^0

Poisson-Nernst-Planck Solver

$$\nabla \cdot (\epsilon \nabla \phi(\vec{R})) + \kappa^2 \sinh(\phi(\vec{R})) = \sum_i q_i \delta(\vec{R} - \vec{R}_i) + \sum_j q_j p_j(\vec{R}; t) \quad (1)$$

$$\frac{\partial p_j(\vec{R}; t)}{\partial t} = -\vec{\nabla} \cdot \vec{J}_j(\vec{R}; t) \quad (2)$$

where the particle flux is defined as:

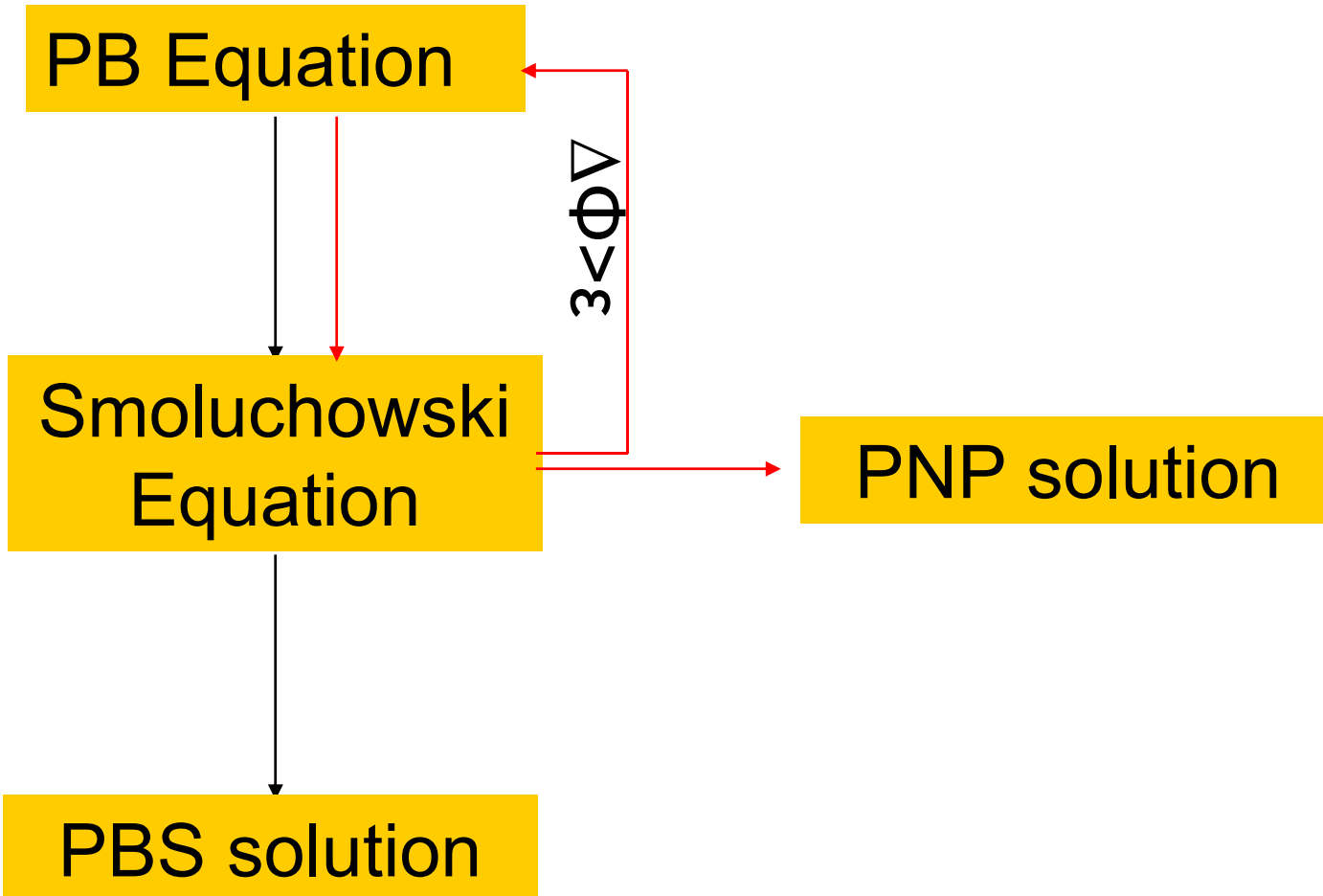
$$\begin{aligned} \vec{J}_j(\vec{R}; t) &= D_j(\vec{R}) [\vec{\nabla} p_j(\vec{R}; t) + \beta \vec{\nabla} \phi(\vec{R}) p_j(\vec{R}; t)] \\ &= D_j(\vec{R}) e^{-\beta q_j \phi(\vec{R})} \nabla e^{\beta q_j \phi(\vec{R})} p_j(\vec{R}; t) \end{aligned} \quad (3)$$

Diffusion controlled rate constant: $k(t) = p_{j \text{bulk}}^{-1} \int_{\Gamma_a} n(\vec{R}) \cdot \vec{j}(\vec{R}; t) dS$

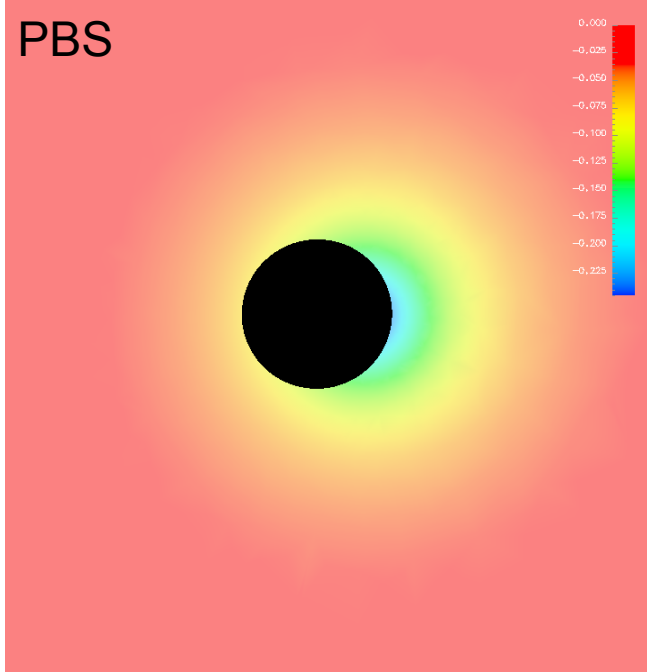
Local free energy density: $g(p_j(\vec{R}; t)) = p_j(\vec{R}; t) (\phi(\vec{R}) + \beta^{-1} \ln \frac{p_j(\vec{R}; t)}{p_j^{\text{bulk}}})$

Local entropy density: $s_j(\vec{R}; t) = -k_B p_j(\vec{R}; t) \ln \frac{p_j(\vec{R}; t)}{p_j^{\text{bulk}}}$

Poisson-Nernst-Planck Solver

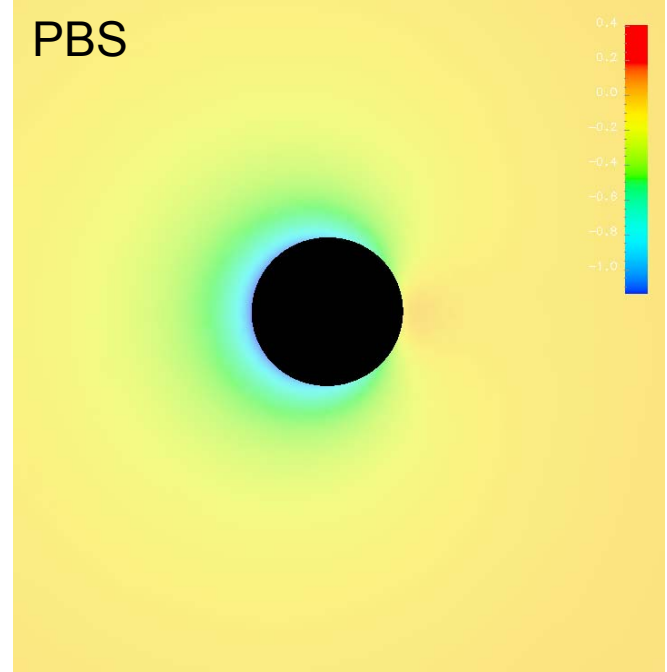


PBS



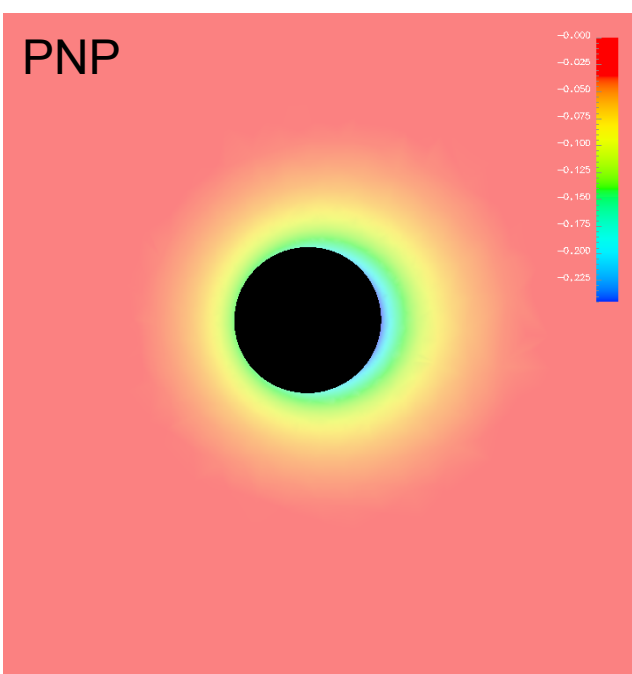
Free Energy

PBS



Entropy

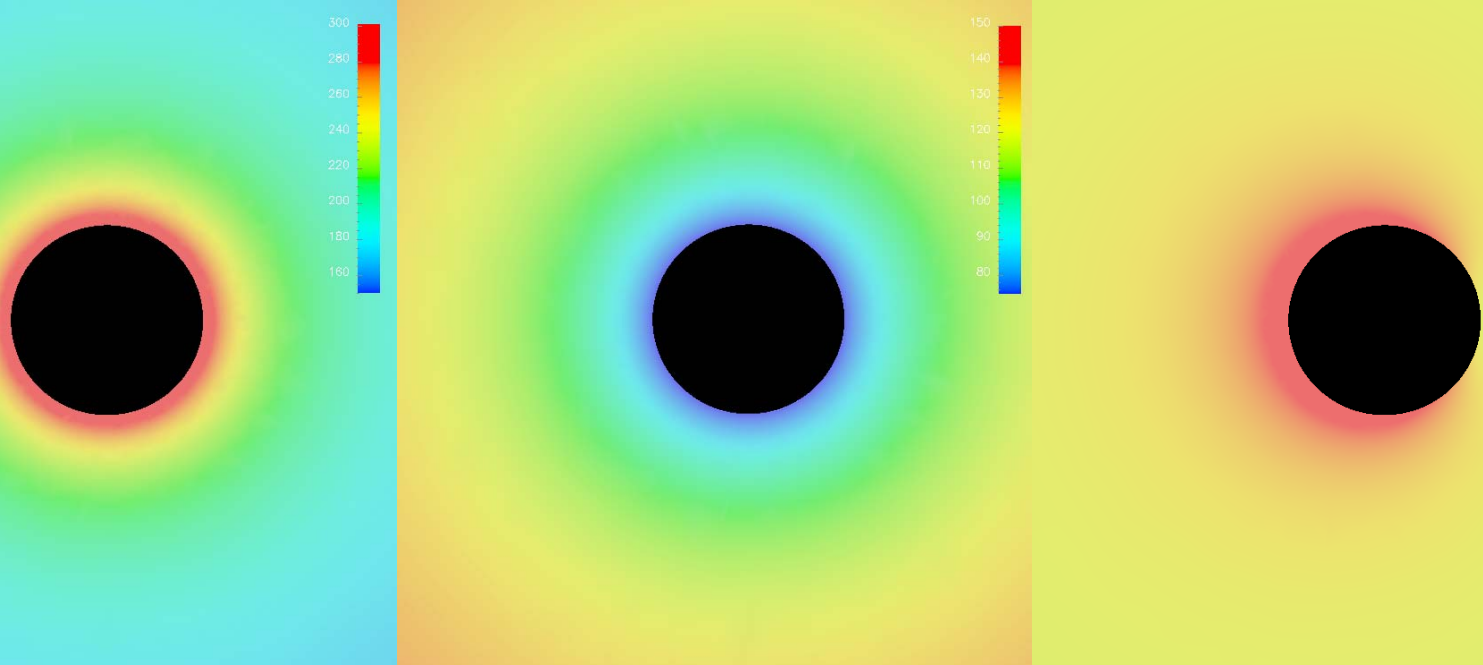
PNP



PNP



PBS

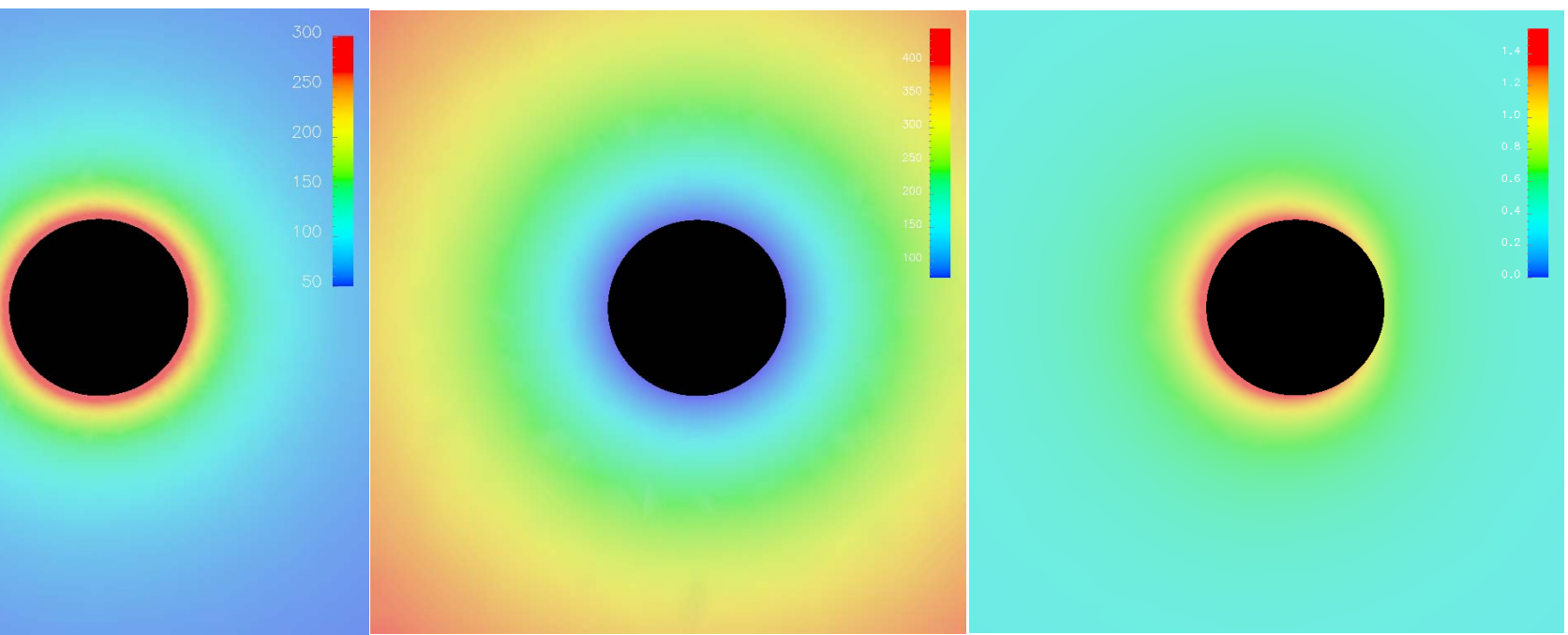


Na^+

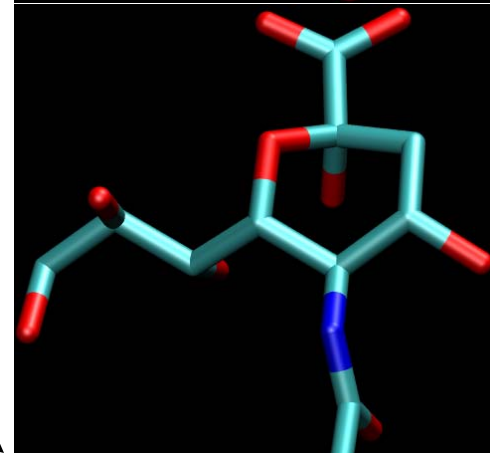
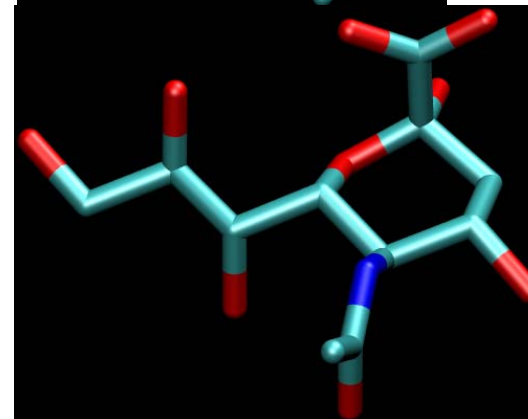
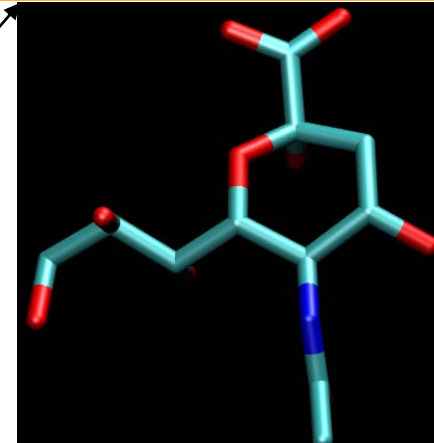
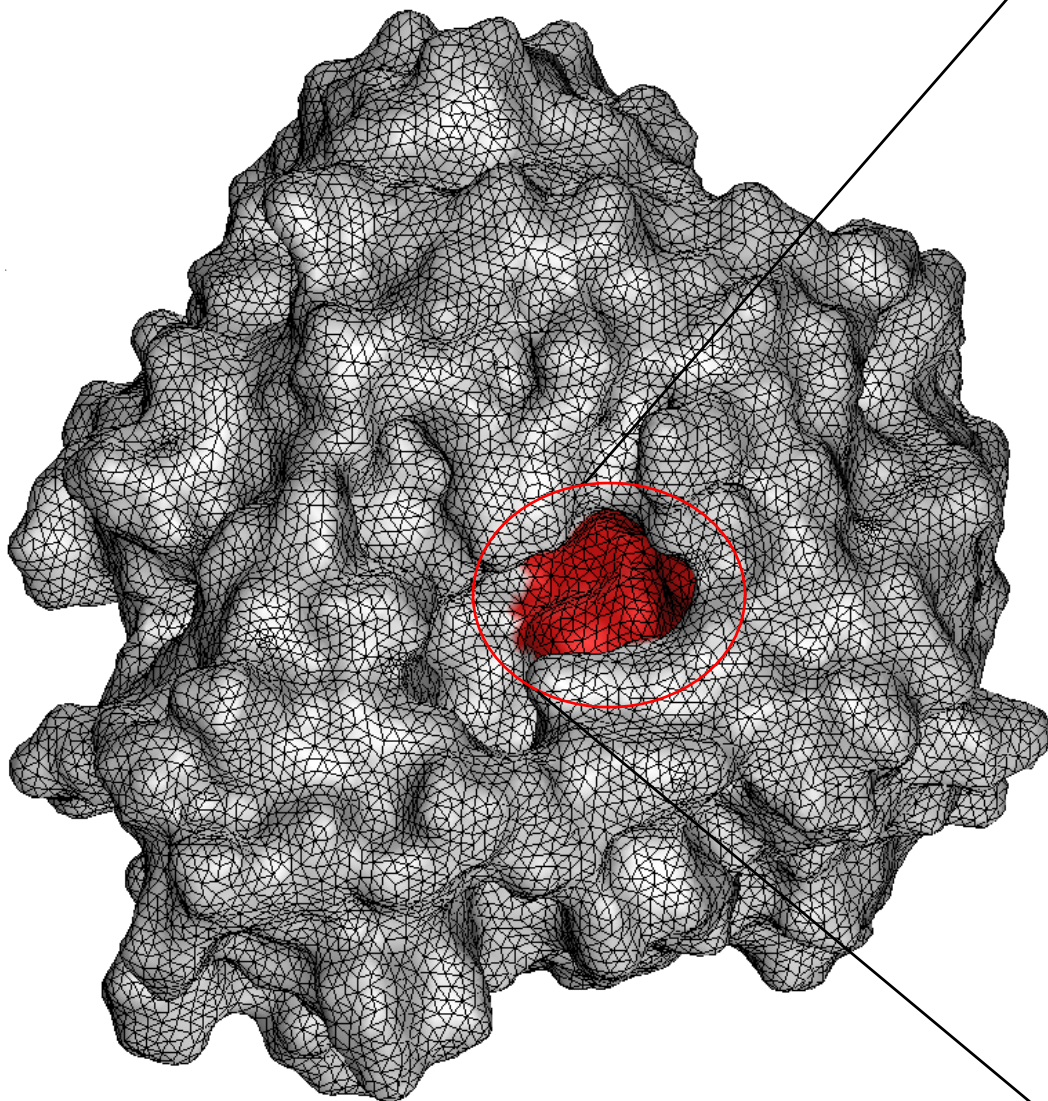
Cl^-

$+1\text{ e}$

PNP



Drug diffusion in Avian Influenza Neuraminidase

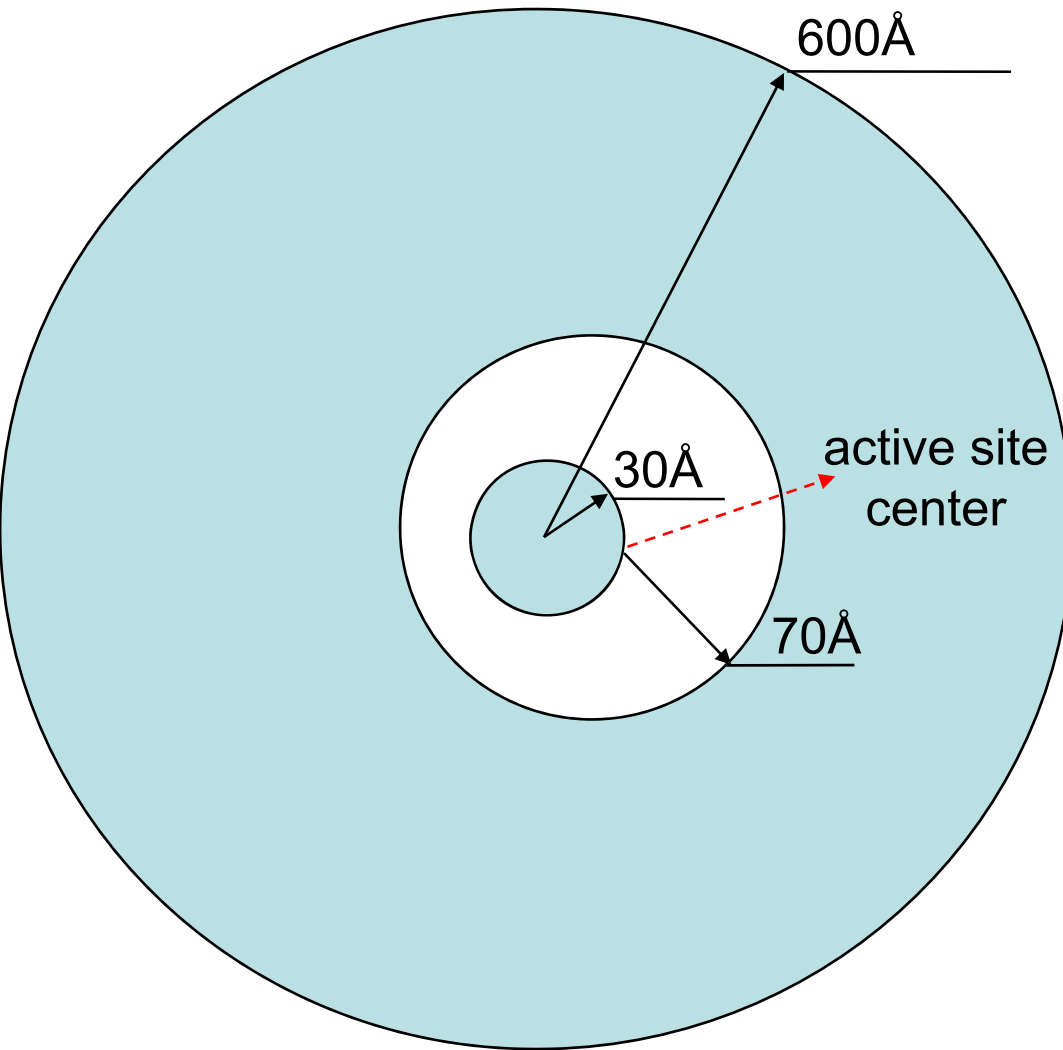


Problems and new projects...

	rate(PBS)	rate(PNP)	experimental
wild-type open	18.1	14.6	2.52
wild-type closed	23.1	19.1	2.52
3CL0	11.9	8.17	0.24
3CKZ	12.4	7.32	0.35
3CL2	16.5	11.8	1.1

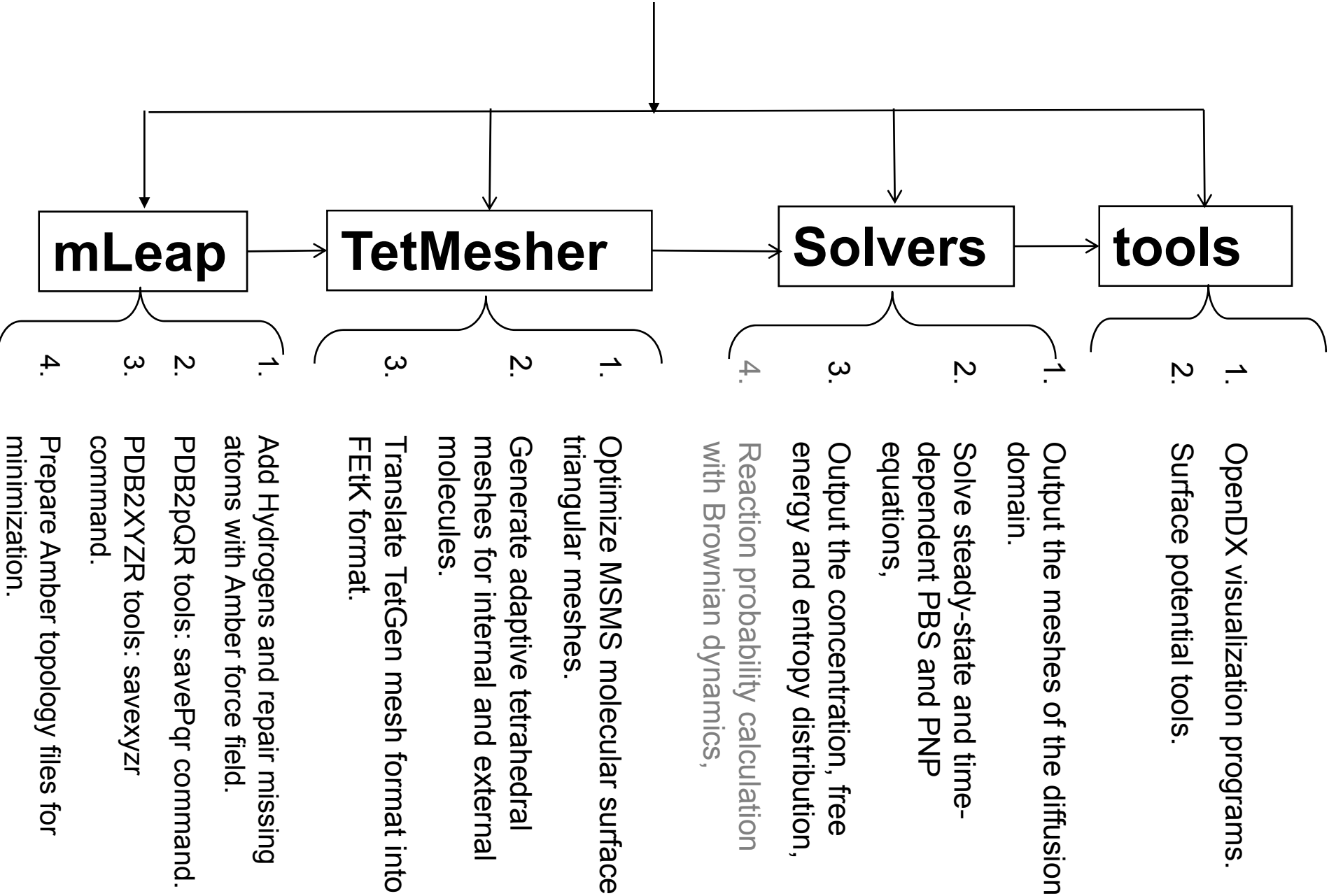
- 1.The reaction rate is the drug binding to the wild-type and mutated influenza virus neuraminidase.
The rate constant unit is $\mu\text{M}^{-1}\text{s}^{-1}$.
- 2.Continuum modeling predicts one order higher kinetic parameters than the experiment.

Numerical limitations and challenges



1. For a protein with 30 Å radius, Brownian dynamics region need at least 70 Å. The concentration of diffusion ions is approximately equal on the interface with 3% relative error.
2. The radius of the Brownian dynamics region is determined after the PBS or PNP steady state.
3. The “real” diffusion rate constant is
$$k = k_{\text{cont}} \beta$$
where k_{cont} is the rate constant predicted by continuum modeling and β is the reaction probability predicted by Brownian dynamics.

the SMOL package



Additional reading materials

1. <http://en.wikipedia.org/wiki/Diffusion>
2. Berg, H C. *Random Walks in Biology*. Princeton: Princeton Univ. Press, 1993
3. advanced diffusion materials:
<http://www.ks.uiuc.edu/Services/Class/PHYS498NSM/>
4. Adaptive Multilevel Finite Element Solution of the Poisson-Boltzmann Equation I: Algorithms and Examples. *J. Comput. Chem.*, 21 (2000), pp. 1319-1342.
5. Finite Element Solution of the Steady-State Smoluchowski Equation for Rate Constant Calculations. *Biophysical Journal*, 86 (2004), pp. 2017-2029.
6. Continuum Diffusion Reaction Rate Calculations of Wild-Type and Mutant Mouse Acetylcholinesterase: Adaptive Finite Element Analysis. *Biophysical Journal*, 87 (2004), pp.1558-1566.
7. Tetrameric Mouse Acetylcholinesterase: Continuum Diffusion Rate Calculations by Solving the Steady-State Smoluchowski Equation Using Finite Element Methods. *Biophysical Journal*, 88 (2005), pp. 1659-1665.